Evolution of Anti-HIV Envelope-specific Antibody Concentration and Antibody-dependent Functionality in HIV Primary Infection Before and after ART Initiation

Lauren Amanda Nagel
Division of Experimental Medicine
McGill University, Montreal
April 2020

A thesis submitted to McGill University in partial fulfillment of the requirements of the degree of Master of Science

Table of Contents

Abbreviations

Ab: antibody
ADCC: antibody dependent cellular cytotoxicity
ADCD: antibody dependent complement deposition
ADCP: antibody dependent cellular phagocytosis
ADCT: antibody dependent cellular trogocytosis
AIDS: acquired immune deficiency syndrome
APC: antigen presenting cell
APOBEC3: Apolipoprotein B mRNA-editing enzyme, catalytic polypeptide-like type 3
ART: antiretroviral therapy
AUC: area under the curve
bNAb: broadly neutralizing antibody
BSA: bovine serum albumin
CD4i: CD4 induced
CDC: Centers for Disease Control and Prevention
cDNA: complementary DNA
CEM.NKr.CCR5: CCR5 positive natural killer cell resistant CEM
CNS: central nervous system
DMSO: dimethyl sulfoxide
DPI: days post-infection
ds: double stranded
EDTA: ethylenediaminetetraacetic acid
ELISA: enzyme linked immunosorbent assay
Env: envelope
FAb: antigen-binding fragment
FACS: fluorescence associated cell sorter
FBS: fetal bovine serum
Fc: fragment crystallizable
FcDF: Fc-dependent function
FcR: Fc receptor
GIT: gastrointestinal tract
HIV: human immunodeficiency virus
HSA: heat stable antigen
HTLV: human T-lymphotropic retrovirus
siCEM cells: sorted NL4-3.IRES.HSA HIV infected CEM.NKr.CCR5 cells
IFN: interferon
Ig: immunoglobulin
IgX: immunoglobulin isotype
IN: integrase
INI: integrase inhibitor
IRES: internal ribosome entry site
kb: kilobase
KIR: killer-cell immunoglobulin-like receptor
LD: Live/Dead® Fixable Violet dye
LTR: long terminal repeat
MA: matrix protein
MAC: membrane attack complex
MFI: mean fluorescence intensity

MHC-II: class II major histocompatibility complex
mL: millilitre
mM: millimolar
mRNA: messenger RNA
MSM: men who have sex with men
nAb: neutralizing Ab
NC: nucleocapsid
NK: natural killer
nnAb: non-neutralizing antibody
NRTI: nucleoside reverse transcriptase inhibitor
NNRTI: non-nucleoside reverse transcriptase inhibitor
^{o}C: degrees Celsius
PAMP: pathogen associated molecular pattern
PBMC: peripheral blood mononuclear cell
PBS: phosphate buffered saline
PCR: polymerase chain reaction
PFA: paraformaldehyde
PI: primary infection
PI: protease inhibitor
PIC: pre-integration complex
PK: proteinase K
PR: protease
PrEP: pre-exposure prophylaxis
PRRs: pattern recognition receptors
PS: phosphatidylserine
QVOA: quantitative viral outgrowth assay
RNA: ribonucleic acid
rpm: rotations per minute
RT: room temperature
RTr: reverse transcriptase
SAMHD1: SAM and HD Domain Containing Deoxynucleoside Triphosphate Triphosphohydrolase 1
SIV: simian immunodeficiency virus
ss: single stranded
TCR: T cell receptor
Th: T helper
TILDA: Tat/rev Induced Limiting Dilution Assay
TLR: toll-like receptor
TMB: tetramethylbenzidine
TP: time point
TRIM5: Tripartite Motif Containing 5
UNAIDS: *The Joint United Nations Programme on HIV/AIDS*
USA: United States of America
VIH: le virus de l'immunodéficience humaine
Vpr: viral protein R
µg: microgram
µL: microlitre
uniCEM: uninfected CEM cell
WHO: World health organization

Abstract

When the Fc portion of antibody (Ab) molecules binds to Fc Receptors (FcR) on an array of innate immune cells, signals are transmitted that modulate their function. Fc-dependent functions (FcDFs) include antibody dependent (AD) cellular cytotoxicity (ADCC), AD cellular trogocytosis (ADCT), AD cellular phagocytosis (ADCP), and AD complement deposition (ADCD). The only vaccine trial to date demonstrating significant (31.2%) protection against HIV-1 infection was the RV144 trial that identified anti-Env Abs and Fc-dependent ADCC as correlates of protection. At present, anti-retroviral therapy (ART) remains the standard of care for HIV infection though only 62% of HIV-1 infected people worldwide are receiving ART. While the timing of the appearance of HIV-specific Abs in acute infection has been defined, less is known about the effect of starting ART at various times during acute infection on the evolution of FcDF responses. Plasma samples from subjects in the Montreal HIV Primary Infection cohort were collected at time points up to 34 months post-treatment. A plate-based enzyme-linked immunosorbent assay (ELISA) was used to quantify total immunoglobulin G (IgG) and HIV Envelope (Env) gp120-specific Ab levels in the plasma samples of untreated and treated subjects. The samples' anti-Env Ab concentrations were quantified using a new cell-based quantitative assay that employs uninfected CEM (uniCEM) cells and sorted Env-expressing HIV infected CEM.NKR.CCR5 (siCEM) cells. Our siCEM cell model expresses HIV Nef and Vpu and hence downregulates CD4, allowing for accurate quantification of the binding of anti-Env Abs in a model exemplifying Env's conformation in genuinely infected cells. Subject samples were also used to quantify and characterize four FcDFs including ADCC, ADCT, ADCP, and ADCD. siCEM cells were the target for the ADCC, ADCT, and ADCD assays while gp120 coated beads were used as the target in the ADCP assay. In untreated subjects there was an increase in Ab concentration over time that was significantly different from "0" for total IgG, anti-gp120, and anti-Env Abs. There was a 46.1x higher concentration of anti-gp120 Abs on average than anti-Env Abs in subject plasma. This ratio was enhanced in treated subjects compared to untreated subjects and in those treated <90 DPI compared to those treated > 90 DPI. The activity of all four FcDFs increased with days post-infection (DPI), with statistically significant increases in ADCC and ADCP. Differences in Ab concentration and FcDF activity were observed between subjects who initiated treatment less than vs. greater than 90 DPI. Anti-gp120 and anti-Env Ab concentrations declined with a significantly steeper slope

of decline in the late compared to early treatment group. At treatment initiation, there was a significantly higher concentration of anti-Env Abs as well as higher ADCT and ADCP activity in the late compared to the early treatment group. Correlation analyses demonstrated stronger correlations between anti-Env Ab concentration than anti-gp120 Ab concentration with the functional assays. The work described in my thesis contributes to our understanding of Fc-mediated immune activity. This work may inform strategies on the ideal time to initiate ART that balance allowing development of persistent anti-HIV immune responses before starting ART, while still controlling the size of the HIV reservoir.

Abrégé

La liaison du segment Fc d'un anticorps (Ab) à son récepteur Fc (FcR) exprimé par les cellules immunitaires innées, transmet un signal à ces cellules capable de moduler leurs fonctions. Les fonctions dépendantes du segment Fc d'un anticorps (FcDF) incluent la cytotoxicité cellulaire anticorps-dépendante (AD) (ADCC), la trogocytose cellulaire AD (ADCT), la phagocytose cellulaire AD (ADCP) et le dépôt de complément AD (ADCD). A ce jour, un seul essai clinique vaccinal a démontré une protection significative (31,2%) contre l'infection par le VIH-1, nommément le RV144. Cet essai a permis d'identifier les Abs anti-Env et l'ADCC comme corrélats de protection. Bien que la thérapie antirétrovirale (ART) soit la norme actuelle de soins pour l'infection VIH, seulement 62% des personnes infectées par le virus en bénéficie.

Alors que la cinétique d'apparition des Abs anti-VIH est connue, peu de données sont encore disponibles concernant l'impact d'une ART sur l'évolution des réponses FcDF, lorsque celle-ci est initiée au début ou plus tard dans la phase aigüe de l'infection. Des échantillons de plasma appartenant à la cohorte Montreal Primary Infection ont été prélevés chez des patients non traités ou jusqu'à 34 mois après traitement. Des tests immuno-enzymatique (ELISA) classiques ont été utilisé pour quantifier les concentrations d'immunoglobuline G (IgG) totales et spécifiques de la protéine gp120 de l'enveloppe du VIH (Env) dans ces échantillons. Les concentrations d'IgG anti-Env ont également été mesurées par cytometry de flux à l'aide d'un nouveau test quantitatif utilisant des cellules CEM.NKR.CCR5 qui expriment toutes la protéine Env (siCEM) après avoir été infectées *in vitro* par le VIH. Ce modèle permet de quantifier précisément les IgG anti-Env dans la mesure ou les siCEM expriment aussi les protéines Nef et Vpu du VIH qui bloquent l'expression membranaire du CD4 et permettent ainsi à Env d'adopter une conformation tridimensionnelle telle qu'elle est observée sur des cellules réellement infectées *in vivo*. Des échantillons ont également été utilisés pour quantifier et caractériser quatre FcDF incluant l'ADCC, l'ADCT, l'ADCP et l'ADCD. Les mêmes siCEM ont servi de cible pour les tests ADCC, ADCT et ADCD tandis que les billes recouvertes de gp120 ont été utilisées comme cible dans le test ADCP.

Nos résultats montrent une augmentation significative des concentrations plasmatiques d'IgG totales, anti-gp120 et anti-Env avec le temps chez les sujets non traités. La concentration plasmatique d'IgG anti-gp120 est en moyenne 46 fois plus élevée que la concentration d'IgG anti-Env. L'activité des quatre FcDF augmente avec les jours suivant l'infection (DPI), et ce de

manière statistiquement significative pour l'ADCC et l'ADCP. Chez les patients traités, on distingue un impact différent du traitement sur les concentrations plasmatiques d'IgG et les activités FcDF selon le moment ou le traitement a été initié. En effet, à l'initiation du traitement, les plasmas de patients traités au-delà de 90 jours après infection montrent une concentration en IgG anti-Env et une activité ADCT et ADCP significativement plus importante que ceux traités avant 90 jours. Après traitement, les concentrations en IgG anti-gp120 et anti-Env diminuent toutefois de façon significativement plus importante dans le groupe de patients traités après 90 jours d'infection. Par ailleurs, les analyses de corrélation démontrent des corrélations plus fortes entre les tests fonctionnels et la concentration plasmatiques d'IgG anti-Env, qu'avec la concentration plasmatique d'IgG anti-gp120.

Le travail réalisé pendant ma thèse contribue à la compréhension de l'activité immunitaire médiée par le segment Fc des IgG. En outre, ce travail nous informe potentiellement sur le moment idéal pour commencer une ART. Un période de temps qui doit être suffisamment longue pour permettre le développement de réponses immunitaires anti-VIH persistantes capables de contrôler le VIH, avant d'initier une ART qui va limiter le développement de ces réponses.

Acknowledgements

First and foremost I would like to thank and acknowledge my supervisor, Dr. Nicole Bernard, for taking me on and helping me to grow as a scientist. Through Dr. Bernard I learned valuable skills such as teamwork, project management, how to properly critique a paper, and how to be more concise. I feel very fortunate to have had the chance to work on such an interesting project, made possible by Dr. Bernard's vision and hard work.

I would also like to acknowledge Sanket Kant who took the time to teach me almost all of the experiments performed in this thesis. I truly appreciate him taking time away from his own work in order to train me, teaching strict protocols that taught me how to do good science.

I must also thank Alexa Del Corpo, Tsoarello Mabanga, Franck Dupuy and Louise Gilbert for the training and wisdom they provided during my degree. Alexa trained me in my first ELISAs and sent me various resources to help me better understand the techniques and approaches we used. Tara also helped me learn my first ELISAs, showed me the ropes of the lab, and performed countless tasks that helped the lab run smoothly and allowed me to complete my experiments. Franck trained me in the newer assays such as ADCC and HIV reservoir quantification, and was also the recipient of many of my questions, answering them all with a seemingly endless supply of knowledge. Louise trained me and helped me complete experiments, taught me her refined techniques, and graciously allowed me to practice my French. Thank you all for your terrific help.

I would also like to acknowledge Dr. Jean-Pierre Routy for his experience and resources provided for my work. Dr. Routy's HIV Primary Infection Cohort is the reason my project was possible and remains an invaluable tool for the field of HIV research. Additionally, I would like to thank the members of my thesis committee, Dr. David Labbé, Dr. Momar Ndao, Dr. Petronela Ancuta and Dr. Nicolas Chomont for their thoughtful questions and suggestions.

I would like to thank the individuals enrolled in the Primary Infection Cohort who generously give their time and samples for the greater good. I will always admire their foresight and unselfishness.

Finally, I would like to thank my family for their unconditional support throughout my education. I have always felt encouraged by their interest in my research and guided by their advice as I found my path. Thank you for everything, Mom, Dad, Jamie, Joanna and Tara.

Contribution of Authors

Unless otherwise stated, the primary author was responsible for writing the entirety of this thesis. However, assistance was obtained with editing, experiments and with presentation of these results. The data presented in this thesis comes from two primary sources, my own experimental work and that of a previous Masters' student named Chris Leeks. The samples of the 99 subjects enrolled in the Primary Infection Cohort used in the study were split approximately evenly between Chris and myself and we each performed the total IgG and anti-gp120 Ab quantifications, ADCC, ADCT, ADCP, and ADCD assays on our own portion of the samples. I performed the HIV infected cell-based assay and the integrated HIV reservoir quantification on samples from both Chris and I's subject list. Finally, Dr. Bernard was involved at every stage of my project and thesis writing, providing invaluable feedback and editing the various versions.

Chapter 1: Literature Review

1.1 Discovery and Characterization of HIV/AIDS

The identification of Human Immunodeficiency Virus (HIV)/Acquired Immunodeficiency Syndrome (AIDS) in 1983 coincided with the first findings on human retroviruses. The events surrounding the discovery of HIV/AIDS as well as its history since the first transmission events to humans are outlined here.

Origins of HIV

The first known case of HIV dates back to 1959, isolated from an adult Bantu male living in the Belgian Congo (now the Democratic Republic of Congo) (Zhu et al., 1998). Genotypic analysis of the viral sequence suggests that the transmission event from primates to humans that caused the worldwide HIV epidemic likely occurred in the early 20th century, as the last common ancestor of the pandemic strain can be dated to 1931 (Korber et al., 2000). HIV spread from the Congo through to Western Africa and the United States of America (USA) as early as 1968, though it only gained recognition as a public health concern in the early 1980s (Worobey et al., 2008; Garry et al., 1988). Two major types of HIV exist, HIV-1, responsible for the global transmission described above, and HIV-2, which is less pathogenic and largely sequestered to West Africa (Dufoort et al., 1988; Guyader, 1987). HIV-1 was discovered to have been transmitted from *Pan troglodytes* chimpanzees to humans while HIV-2 was passed on by *Cercoecebus atys* sooty mangabeys (Gao et al., 1999; Hirsch et al., 1989). HIV-1 viruses have been further divided into four groups based on four zoonotic transmission events from primates to humans, notably not all having been derived from chimpanzees. Group M, for Major, is the most common virus group responsible for the global HIV epidemic and derives from chimpanzees. Group O, for Outlier, has been found in about 100,000 individuals located in West Africa. There have been less than twenty infections with Group N, meaning Non-M/ Non-O, in the Cameroon region, and finally Group P, for Pending further cases, has been isolated from one Cameroonian woman (De Leys et al., 1990; Simon et al., 1998; Plantier et al., 2009). Group N is hypothesized to be descendent of a chimpanzee virus whereas group P is likely derived from a transmission event from gorillas, with group O most closely resembling group P (Mourez et al., 2013). HIV-1 M is the virus group responsible for the

worldwide spread and at present it can be classified into nine unique subtypes, A-D, F-H, J, and K, based on geographic-genetic divergences. For the purposes of this thesis, subtype B is most relevant, predominant in North America where our experimental cohort exists, as well as in Western Europe (Magiorkinis et al., 2016). The transmission timeline described above was not calculated until after the virus took the world stage, beginning with its discovery in the USA in 1981. For simplicity, throughout the remainder of this thesis, "HIV" refers to HIV-1 group M unless otherwise indicated.

Identification of the HIV Virus

In 1981, the Centre for Disease Control and Prevention (CDC) made public their discovery of five cases of *Pneumocystis carinii* pneumonia (now known as *Pneumocystis jerovesi* pneumonia) in five young homosexual men in the USA, a rare finding in such a young and typically healthy population (CDC, 1981a). The same year, 26 cases of Kaposi's sarcoma were reported in homosexual men in New York and California, again, a typically "uncommonly reported malignancy in the United States" (CDC, 1981b). The cause of these unlikely illnesses was unknown. Around this same time that the first human retroviruses were being discovered, and researchers hypothesized that they may be the cause of the disease showing up in these men that would later be known as HIV-AIDS. Two years later at the Pasteur Institute in Paris, using techniques designed for identification of retroviruses in non-human animals, Luc Montagnier's team discovered reverse transcriptase activity in the cell culture supernatant of an HIV-infected patient, thus discovering an AIDS-related retrovirus (Barre-Sinoussi et al., 1983). The following year, Robert Gallo's group at the National Cancer Institute in Maryland isolated the virus in a total of 48 subjects that had "pre-AIDS" or AIDS, thus establishing a causal relationship between the retrovirus and the immunodeficiency syndrome (Gallo et al., 1984). Samples at laboratories throughout the world continued testing positive for HIV, demonstrating that the infection was already widespread with hypotheses of a likely origin in Africa. For several years the virus was known under various names including human T-lymphotropic retrovirus (HTLV), lymphadenopathy-associated virus, AIDS-associated retrovirus, etc., until a group of scientists suggested the name HIV in 1986 (Case, 1986).

HIV and AIDS

As more was learned about HIV following its discovery, it became evident that the virus caused a decline in $CD4^+$ T cells leading to the development of AIDS (Shearer et al., 1986) . In addition to $CD4^+$ T cells, any immune cell with a CD4 receptor, such as dendritic cells, monocytes, and macrophages, could become infected with HIV (Müller et al., 1986). It was then learned that the T cell depletion was caused not only by the killing of HIV-infected cells, but also by cytolytic activity aimed at uninfected $CD4^+$ T cells carrying gp120 shed from neighbouring infected cells (Siliciano et al., 1988). In all, this was a disease that was wreaking havoc on the immune system from all sides. The early effects of HIV infection take place during the acute phase, which lasts from about two weeks post-infection to several weeks or months later. During this phase, up to 90% of HIV infected people will experience flu-like symptoms such as fever, headache, malaise, lymphadenopathy, and general aches and pains (Robb et al., 2016). These symptoms tend to disappear after a few weeks and can be followed by years of asymptomatic infection. After this point, the progress of the infection can be characterised by the number of $CD4^+$ T cells in circulation, with any cell count below 200 cells/mm^3 as defining AIDS (CDC, 1993). At this stage, with T-cell mediated cellular immunity effectively lost, the subject becomes highly susceptible to opportunistic infections such as *Pneumocystis jerovesi* pneumonia, cryptococcal meningitis, Kaposi's sarcoma and others that can ultimately lead to death (Pitchenik et al., 1983). In the absence of treatment, most HIV-infected people eventually succumb to the disease. Transmissibility of HIV is directly proportional to the plasma viral load, with a 2.4 times increased risk of transmission for every $\log_{10}$ increase in viral load (Quinn et al., 2000). Viral load peaks shortly after infection, so many HIV-infected subjects are at maximum risk of transmitting the disease before they may even know they are infected. The virus is transmitted through exchange of bodily fluids, such as via vaginal or anal sexual contact, exposure to HIV-infected blood through needles or transfusion, and from mother to child prenatally, perinatally or through breast feeding (Lifson et al., 1988).

1.2 Virology

HIV compromises the immune system of the host by infecting $CD4_+$ immune cells with its virion, using the host cell's replication machinery as a means to replicate its own genome (Maartens et al., 2014). The details of these processes are outlined below.

Virion Structure

The structure of the HIV virion is that of a classic retrovirus, an enveloped particle of approximately 100nm diameter coated in envelope surface protein, encompassing two ribonucleic acid (RNA) copies of its genome and the proteins required for its replication (Figure 1) (Musumeci et al., 2015). The HIV RNA is positive sense, belongs to the lentivirus genus and is a member of the retroviridae family (Moore and Hu, 2009; German Advisory Committee Blood, 2016). The HIV genome itself is approximately 9.8kb in length and composed of nine genes that are differentially spliced into several unique proteins (Muesing et al., 1985; Wain-Hobson et al., 1985). Beginning at the surface, embedded in the lipid bilayer is the protein gp41, covalently attached to the extracellular protein gp120. Together a trimer of gp41 and gp120 constitute the Env protein, of which there are up to 72 units on the virion surface (Gelderblom, 1991). The lipid bilayer is derived from host cells and is interiorly lined by a spherical layer of matrix protein (MA) which protects the inner capsid made of the p24 core antigen. Approximately 1500 p24 protein monomers assemble

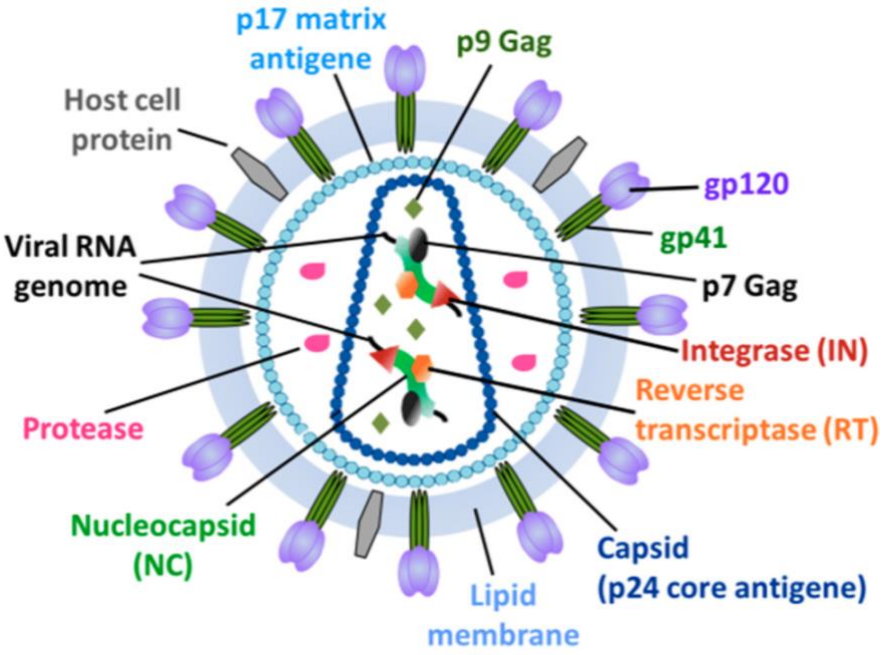

Figure 1: Structure of the HIV Virion. A lipid membrane forms the outer shell of the virion, embedded with Env protein consisting of gp120-gp41 trimers responsible for binding target cells. Within the membrane, MA protein provides a layer of support around the p24 capsid containing two copies of viral RNA, bound by NC with IN and RTr needed for copying the viral genome. *Image reproduced from "G-Quadruplex Forming Oligonucleotides as Anti-HIV Agents". Musumeci, D.; Riccardi, C.; Montesarchio, D., Molecules, 2015, 20, 17511-17532 with open access permission under the Creative Commons Attribution License.*

into hexamers and pentamers that form the cone-shaped capsid structure encapsulating the HIV genetic material and replication proteins (Campbell and Hope, 2015). Within the capsid are two strands of ssRNA, reverse transcriptase (RTr), protease (PR) integrase (IN), and several accessory proteins. Nucleocapsid (NC), the product of gene p7, binds to the ssRNA inside the capsid to assemble the nucleoprotein/RNA complex and later chaperones the reverse transcription and integration of the HIV RNA (Thomas and Gorelick, 2008).

Target Cell Entry

HIV infection begins at the surface with key interactions between Envelope (Env) protein and the CD4 receptor of target cells. Env is the product of the *env* gene, which is transcribed and translated into the gp160 protein and subsequently cleaved into the subunits gp120 and gp41 that constitute the membrane-bound machinery (Robey et al., 1985; Veronese et al., 1985). Three gp41-gp120 units operate as a covalently-bound trimer to form the functional surface protein (Zhang et al., 2001). When Env protein on the surface of a virion comes into contact with the CD4 receptor, gp120's CD4 binding site (CD4bs) interacts with the receptor, inducing a conformational change that allows the binding of CD4's co-receptor, generally CCR5, to gp120 (Eckert et al., 2001). This

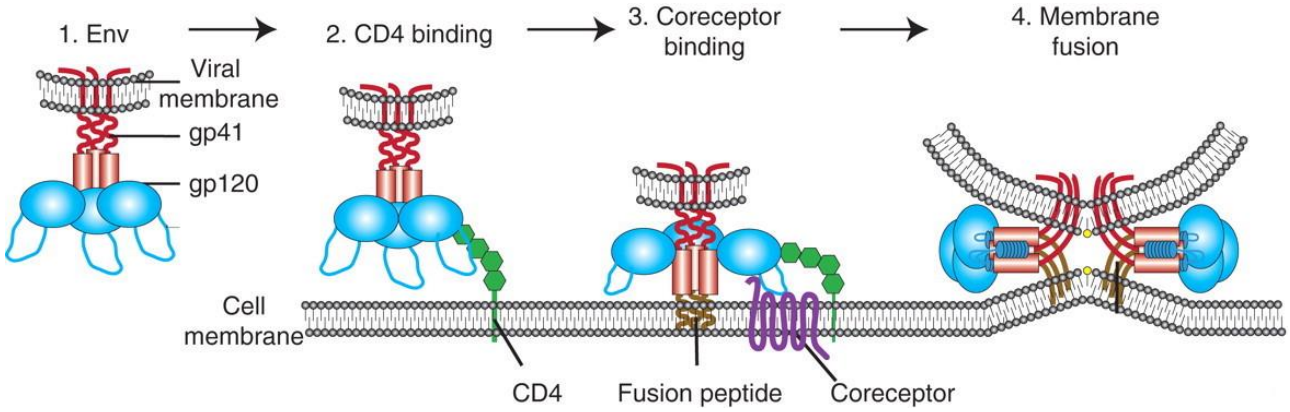

Figure 2: HIV Entry into Target Cells. When a virion encounters a target cell, gp120 surface protein interacts with the CD4 protein, initiating a conformational change that brings the virion into closer proximity with the cell so that gp120 can also interact with the co-receptor. gp41 fusion peptide then infiltrates the target cell membrane, initiating a reaction that causes the fusion of the two membranes and entry of the HIV capsid into the cytoplasm. *Image reproduced from "HIV: Cell Binding and Entry", Wilen, C.B., Tilton, J.C., Doms, R.W., Cold Spring Harbor Perspectives in Medicine, 2012, Copyright Cold Spring Harbor Laboratory Press.*

interaction induces another conformational change in Env, allowing gp41 to insert its fusion peptide into the target cell membrane and drawing the membranes together, initiating a fusion

reaction (Figure 2) (Wilen et al., 2012). While the viral material enters the cell, the plasma membranes merge and the Env proteins at the virion surface become a component of the host cell's own plasma membrane. The HIV protein capsid enters the target cell cytoplasm where it is taken up by an endosome and a change in the pH induces the breakdown of the capsid and release of its contents into the cytoplasm (Stein et al., 1987). Over the course of infection, the HIV Env protein can undergo mutations that allow it to use the CXCR4 co-receptor in addition to CCR5. This shift in usage generally occurs at later stages of infection and is associated with a rapid decline in $CD4^+$ T cells and progression to AIDS (Tersmette et al., 1989) . After this series of events, the HIV RNA and proteins are free in the host cell cytoplasm and ready to be used for HIV replication. An additional feature of HIV is that it is a lentivirus, a subclass of retroviruses that are characterized by long incubation periods leading to chronic and deadly diseases (Yaniz-Galende and Hajjar, 2014) . Lentiviruses are unique in that they integrate into the host DNA in both dividing and non-dividing cells, so this process of target cell infiltration can occur in both active and resting cells.

HIV Replication

As a retrovirus, HIV uses RNA RTr to transcribe its RNA into complementary DNA (cDNA) for incorporation into a host genome, leading to its transcription and translation during host replication (Barré-Sinoussi, 1996). After binding the single stranded RNA (ssRNA) in the cytoplasm, RTr recruits host nucleotides to build a cDNA strand bound to the original HIV RNA (Sousa et al., 1993). The double strand then passes through the enzyme again, replacing the RNA with DNA nucleotides to form a double stranded DNA molecule, while the RNA is degraded enzymatically by RNase H (Beilhartz and Götte, 2010; Figiel, 2017). This series of steps is chaperoned by the NC molecule, which facilitates the annealing of complementary bases, maintains interactions between proteins, and later packages the RNA genome, among other functions. (Tsuchihashi and Brown, 1994; Accola et al., 2000; Berkowitz et al., 1996). Due to a lack of proofreading, the RTr enzyme has a very high error rate so the HIV sequence mutates rapidly, allowing it to evade immune attack or drug treatments (Preston et al., 1988). This genetic multiplicity is reflected by the diversity of viruses isolated from HIV-infected individuals, resulting from the mutation rate that is five to six orders of magnitude higher than for most mammalian genes (Goodenow et al., 1989; Korber, 2000). The dsDNA is transported to the nucleus within the pre-integration complex (PIC), composed of the IN and MA proteins and viral protein R (Vpr) (Bowerman et al., 1989;

Farnet and Bushman, 1997). At this stage, some strands self-ligate to become 2-long terminal repeat (2-LTR) circles that cannot be transcribed, while others remain as linear fragments. Within the nucleus, the host cell protein LEDGF/p75 binds the HIV DNA and brings it to the host DNA for integration, inserting the strand preferentially at a transcription unit (Maertens et al., 2003; Mitchell et al., 2004). Integration at transcriptionally-active sites is key for virus replication as infected T cells have a half-life of only 1.6 days before they succumb to the infection or are destroyed by the cellular immune system (Perelson, 1996). After integration, host RNA polymerase may transcribe the HIV DNA and the resulting mRNA is sent out of the nucleus into the cytoplasm where it is translated into protein by a ribosome. Transcribed HIV proteins concentrate at the plasma membrane of the cell where Gag polyprotein directs the protein-protein interactions necessary for the formation of Env-coated spherical particles, which bud off as new virions able to infect new targets (Sundquist and Kräusslich, 2012) . In the newly formed viral particle, proteolysis is required to convert the immature virion to a mature infectious one. PR is responsible for cleaving five sites within Gag and five within the Gag-Pro-Pol polyproteins that lead to production of the proteins required for the mature virion. This cleavage also leads to downstream changes in the immature virion, including assembly of the capsid, stabilisation of the RNA genome, and preparation for target cell entry (Sundquist and Kräusslich, 2012). After fulfilment of the maturation process led by Gag and PR, the virion is complete and capable of infecting new $CD4^+$ T cells.

Stages of HIV Infection

The progression of HIV infection can be defined by the levels of virus present in the body and by the body's immune response. Broadly speaking, the disease course can be divided into acute infection, chronic infection, and AIDS, distinguished by the viral load and $CD4^+$ T cell count. Acute infection is characterized by a very high viral load, peaking at over 6 log10 copies/mL two weeks from infection and subsequently declining to a set point about one month later (Robb et al., 2016). Viral load is a strong predictor of disease progression, superior to $CD4^+$ T cell count (Mellors et al., 1996). During this same six week period, the $CD4^+$ T cell count undergoes a steep decline, followed by a slight recovery, though not to pre-infection levels (Brenchley et al., 2004). Both the viral load increase and $CD4^+$ T cell decline are magnified in the gastrointestinal tract (GIT) where there is a pronounced decline in T cells, specifically type 17 T helper (Th17) cells,

which are especially susceptible to HIV infection (Figure 3) (Brenchley et al., 2006; Cecchinato et al., 2008). Chronic phase infection occurs after this acute period when viral load has reached a set point and $CD4^+$ T cells decline at a level of approximately 50 cells/mm^3 per year until AIDS is diagnosed (Henrard et al., 1995; Patrikar et al., 2014). For the next ten years or so, the HIV infected person undergoes a period of asymptomatic infection during which viral load increases gradually

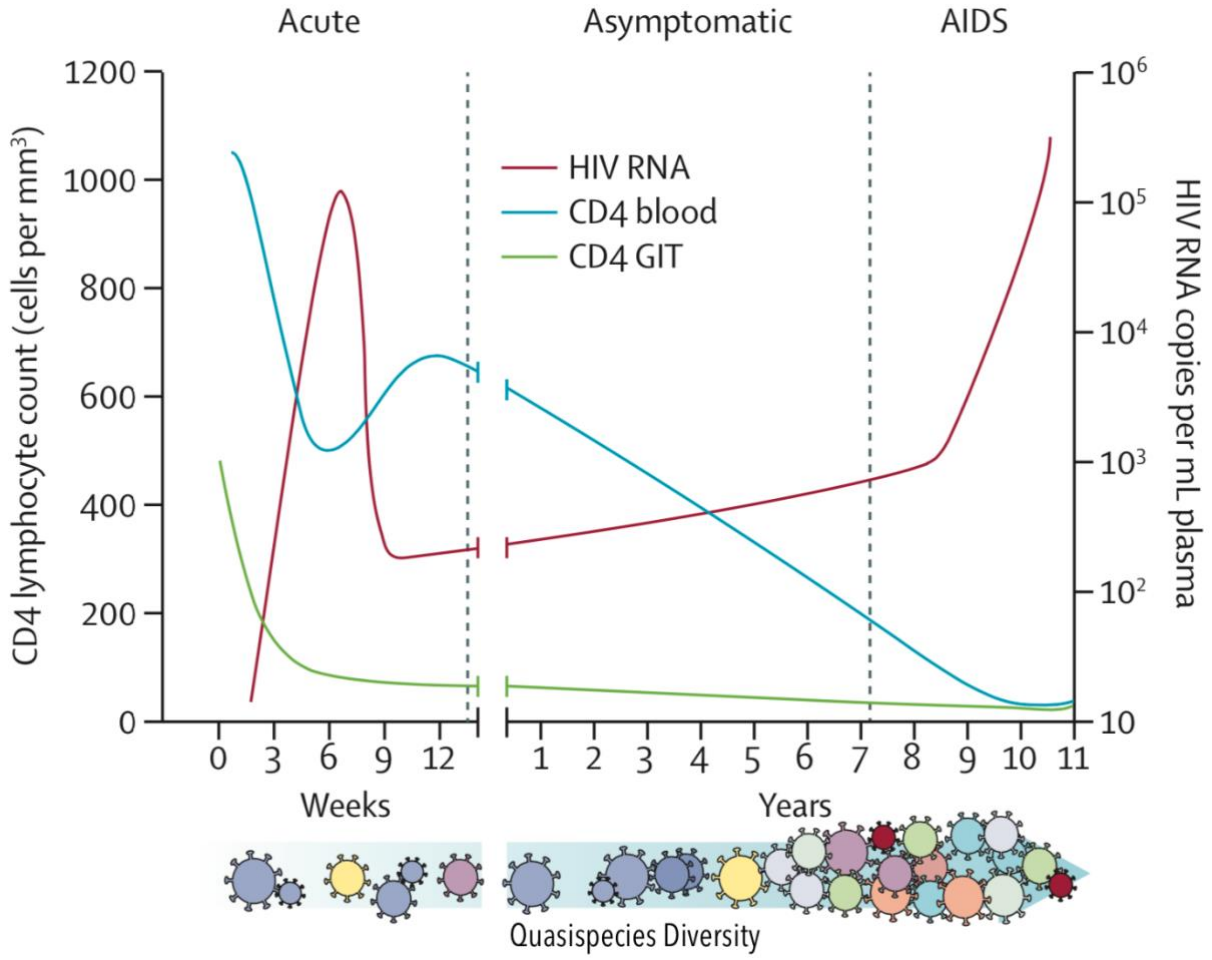

Figure 3: CD4 Count, Viral Load Dynamics and Quasispecies Diversity. Shortly after HIV infection, during the acute phase, $CD4^+$ T cell counts decline steeply in the blood and in the GIT. After this initial decline, $CD4^+$ T cell levels recover somewhat in the blood but do not recover in the GIT. Correspondingly, during the first weeks after infection, there is a steep increase and peak in viral load (HIV RNA), which declines to a level about 2 logs lower post-peak. During the asymptomatic phase viral RNA continues to gradually increase over time while CD4 count declines until the onset of AIDS several years later when the $CD4^+$ T cell blood count drops below 200 cells/mm^3. At this point viral load increases steeply as does the diversity of HIV quasispecies, which had increased gradually to that time. *Image reproduced from "HIV infection: epidemiology, pathogenesis, treatment, and prevention", The Lancet, Vol 384, Issue 9948, Gary Maartens, Connie Celum, Sharon R. Lewin, 258-271, Copyright (2014), with permission from Elsevier.*

while $CD4^+$ T cell count slowly declines. The progression to the disease stage know as AIDS is defined by a $CD4^+$ T cell count of less than 200 cells/mm^3, diagnosis of an AIDS-defining opportunistic infection, and accompanied by a rapid increase in viral load and HIV quasispecies diversity (CDC, 1993; Goodenow et al., 1989). AIDS-defining opportunistic infections include *Pneumocystis jerovesi* pneumonia, cryptococcal meningitis, Kaposi's sarcoma and others that can ultimately be the cause of death (Pitchenik et al., 1983). Another system has been devised to classify the stages of acute HIV infection, called the Fiebig stages, carrying the additional benefit of allowing estimation of the date of infection (Fiebig et al., 2003). The earliest stage of infection, called the eclipse phase, lasts an average of ten days beginning at the date of infection and is characterized by undetectable viral RNA in plasma by a polymerase chain reaction (PCR) test. During this period, the virus is replicating in the mucosa, submucosa and draining lymphoreticular tissues so cannot yet be detected in the blood (Cohen et al., 2011). The following five days or so are called Fiebig stage 1 where viral RNA becomes detectable, followed by progression into stage 2 whereby p24 protein is detectable by Enzyme-linked Immunosorbent Assay (ELISA). In stages 3, 4, and 5, HIV-1 specific antibodies (Abs) become detectable by ELISA and Western blot up to one month post-infection. The final mark, Fiebig stage 6, occurs when p31 protein becomes detectable by Western Blot, about one hundred days post-infection (DPI) (Fiebig et al., 2003; McMichael et al., 2009). If samples are taken within the first month post-infection, a fairly accurate date of infection can be derived from the results of the various tests. It has become clear that HIV is able to rapidly establish an irreversible infection before it is even detected, highlighting the importance of effective screening and prevention methods.

1.3 HIV Reservoir

The HIV Reservoir may be defined as a cell type or anatomical site in which a replication-competent form of virus exists in spite of antiretroviral therapy (ART) suppression (Vanhamel et al., 2019). These evasive cells present the final challenge in the battle of eradicating the virus from the body.

Defining the HIV Reservoir

The leading treatment regimens for HIV infection, ARTs, interfere with various stages of the HIV replication cycle, eliminating activated HIV-infected cells. There exists a population of latently infected memory T cells that are not targeted by ART or the immune system because the virus in these resting cells is not actively replicating in compartments easily accessed by ART or immune responses. These latently infected cells are called the HIV reservoir (Finzi et al., 1997). The reservoir is established in $CD4_+$ T cells by 3 days after infection, at least in simian immunodeficiency virus infected rhesus macaques (Whitney et al., 2014). This is much earlier than our ability to detect infection and thus too late to prevent permanent establishment of infection (Chun et al., 1998; Kulpa and Chomont, 2015). The majority of the reservoir is composed of memory $CD4_+$ T cells in the blood though the exhaustive definition of the HIV reservoir is debated (Chomont et al., 2009). Some argue that the HIV reservoir includes infected cells that continue replicating at low levels during treatment in so-called HIV "sanctuaries", areas of the body such as the central nervous system (CNS) that allow only limited infiltration of ART (Letendre et al., 2008). In these sites, the lack of ART medication allows HIV infected cells such as microglia and macrophages to continue replicating and producing low levels of virus (Ko et al., 2019), leading to a debate as to whether these fit into the same category as latently infected $CD4_+$ T cells in other compartments. Furthermore, due to the variety of cell types and sites harbouring viral DNA despite treatment, some prefer to refer to this group of persistently infected cells, in the plural form, as the HIV reservoir"s". Another question of qualification for the reservoir includes the virus' replication competency. Viral DNA may be integrated into a cell's genome, but this does not guarantee that the DNA retains the ability to be transcribed and translated into a replication-competent virus. The current state-of-the-art techniques for quantifying the HIV reservoir differ in their methods of measuring "replication-competent" HIV DNA. Some focus on measuring integrated HIV DNA, others on HIV RNA transcripts, or cells with the ability to infect other cells upon activation (Vandergeeten et al., 2014; Procopio et al., 2015; Laird et al., 2013). For the purposes of this thesis, the HIV reservoir will be defined as a cell type or anatomical site in which a replication-competent form of virus exists in spite of ART suppression (Vanhamel et al., 2019). A major obstacle to the detection of the HIV reservoir is its extremely small size, as several leading tests measure no more than 24 latently infected cells per million $CD4_+$ T cells, a challenging quantification to obtain and defend (Procopio et al., 2015; Hosmane et al., 2017). The total size of the reservoir has been

estimated at 1 x 10^6 cells, with findings showing that only about 1% of $CD4^+$ T cells carry intact provirus (Chun et al., 1997; Siliciano et al., 2003). While small in number, the half-life of memory $CD4^+$ T cells is estimated to be 44 months, indicating that the time required to clear the entire reservoir from the body would be approximately 73 years (Finzi et al., 1999). Eradicating the HIV reservoir is thus a priority for future treatments as natural clearance of the virus will not occur within the lifespan of most HIV-infected people. The principal takeaway from our knowledge of the HIV reservoir is that it is the reason behind our inability to completely clear the virus from the body despite otherwise very effective treatments.

Techniques for Quantifying the HIV Reservoir

A number of techniques exist that estimate the size of the latent HIV reservoir, though none claim to be more than that, an estimate. Current leading methods either overestimate the size of the reservoir by including un-integrated and non-replication-competent virus while other assays underestimate the size of the reservoir due to their inability to activate all the resting cells harbouring virus from latency.

Several techniques may be used in combination to determine a range rather than single value for the reservoir, a sort of compromise that acknowledges the shortcomings of the assays. Common leading techniques that greatly overestimate the size of the reservoir are ones that rely on quantitative polymerase chain reaction or qPCR. These are widely used due to issues relating to feasibility and the ease with which qPCR assays can be carried out (Ibàñez et al., 1999). Additionally, they requires a low sample volume so in addition to quantifying the blood-based reservoir they can also be run on samples of cerebrospinal fluid from the CNS and lymph fluid (Kamat et al., 2007; Hey-Nguyen et al., 2017). qPCR-based techniques may quantify one of several HIV DNA templates, two common options being total and integrated HIV DNA. Total DNA qPCR assays use a forward and reverse primer which both target the 5' long-terminal repeat (LTR) region of HIV DNA and thus include all sequences present in a sample regardless of integration status or replication competence. Integrated HIV DNA assays use a forward primer for HIV's 5' LTR and a reverse primer for the human genome element Alu, thus only including sequences that have been integrated into the host cell genome (Vandergeeten et al., 2014). Research has shown that total HIV DNA levels decline after the initiation of ART while integrated HIV DNA levels stay constant. Thus, it can be argued that integrated HIV DNA is a better measure of the persistent

reservoir (Ibàñez et al., 1999). However, integration into the host genome does not guarantee the production of virus capable of infecting neighbouring cells, the ultimate concern surrounding the existence of the reservoir and the reason ART cannot be ceased. Thus, the qPCR techniques overestimates the size of the replication-competent HIV reservoir. In contrast to qPCR, a technique that underestimates the size of the viral reservoir and which is commonly considered the "gold standard" for HIV reservoir quantification strategies is the quantitative viral outgrowth assay (QVOA). The QVOA technique measures the ability of infected $CD4^+$ T cells to produce infectious virus after latency reversal, as measured by the production of p24 protein by uninfected cells cultured with the supernatant of the re-activated cells (Laird et al., 2013). If the uninfected cells become infected after incubation with the supernatant, it is evidence that the re-activated cells were able to produce viral particles capable of infecting other cells. While this technique answers the question of replication competency, follow-up studies have shown that not all cells are reversed from latency during the assay's activation process, leading to reservoir estimates that may be 6-fold too low (Ho et al., 2013). Two assays that yield intermediate values between the PCR-based and QVOA assays are the Tat/rev Induced Limiting Dilution Assay (TILDA) and a flow cytometry based assay referred to as HIV-Flow, both developed by the Chomont lab at l'Université de Montréal (Procopio et al, 2015; Pardons et al., 2019). The TILDA assay detects transcripts for *tat*/*rev* and uses this as an indicator of cells harbouring inducible virus. To perform the assay, $CD4^+$ T cells are activated from latency with PMA and ionomycin and distributed in a PCR plate for amplification via a nested PCR with primers targeting the *tat*/*rev* transcripts. Performing this assay in a limiting dilution format provides an estimate of the proportion of activated cells that are induced to produce viral transcripts. The TILDA estimates the reservoir at roughly 4% of the size of that approximated by the integrated HIV DNA PCR assay. The HIV Flow assay is based on a similar concept but instead measures the amount of p24 protein produced by activated cells rather than viral transcripts. After stimulation with PMA and ionomycin, cells are stained with two anti-p24 Abs and cells with double positivity are identified using flow cytometry (Pardons et al., 2019). The use of two anti-p24 Abs reduces false-positive detection, as was observed in HIV-uninfected individuals when only one anti-p24 Ab was used. The HIV-Flow assay estimates the reservoir at roughly 0.8% of the size of the detectable integrated HIV DNA assay and approximately five

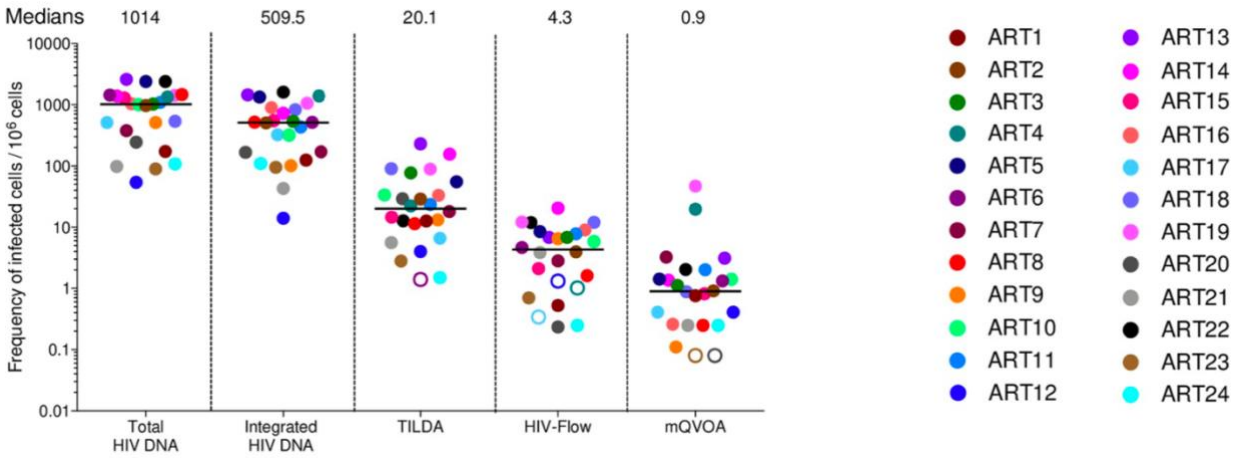

Figure 4: Assays for Quantifying the HIV Reservoir. Displayed are the reservoir quantification results for 24 ART-treated individuals using five different techniques. Left to right the assays are displayed from least to most sensitive, with decreasing frequencies of detected infected cells. The Total and Integrated HIV DNA assays overestimate the HIV reservoir while QVOA underestimates the reservoir. TILDA and HIV-Flow represent intermediate estimates though they still likely overestimate the size of the replication-competent reservoir. *Image reproduced from "Single-cell characterization and quantification of translation-competent viral reservoirs in treated and untreated HIV infection". Pardons, M., et al., PLoS Pathogens, 2019, 15(2), e1007619 with open access permission under the Creative Commons Attribution License.*

times larger than that identified by QVOA when run on the sample subject samples (Figure 4). This assay may still overestimate the size of the reservoir capable of propagating in the absence of treatment, as production of viral proteins does not equate to infectivity. Approximations made by these techniques suggest that an assay producing intermediate estimates between those of the PCR-based and QVOA assays, such as TILDA or HIV-Flow, likely produces the most accurate measurement of the size of the replication competent HIV reservoir. In the absence of a perfect assay, one possible strategy for providing an accurate estimate is to perform several assays and display reservoir values as a range rather than a single figure.

1.4 Host Responses

In the majority of HIV-infected individuals, the body's immune response is insufficient to clear the virus. Presented here is a discussion of the humoral responses that occur following infection as well as a discussion of subjects who manage to control their infection naturally.

Innate Immune Response

The initiation of the innate immune response to infection relies on the recognition of pathogen-associated molecular patterns (PAMPs) on HIV by pathogen-recognition receptors (PRRs) on host cells, which induce an array of innate reactions. Several potential PAMPs exist within the HIV virion, though only some have been confirmed experimentally, such as LTR-derived ssRNA, gp120, gp41, and structural proteins p17 and p24 (Heil et al., 2004; Gringhuis et al., 2010; Henrick et al., 2015). Several PRRs exist that recognize HIV PAMPs, including RIG-1-like receptors, cyclic GMP-AMP synthase, and Toll-like receptors (TLRs). In mucosal epithelial cells, TLRs trigger proinflammatory cytokine production resulting in the recruitment of innate immune cells to the site of virus infiltration (Nazli et al., 2013). As the viral load increases, a surge of inflammatory cytokine production occurs, initially produced by dendritic cells and later by multiple cell types, led by interferon-α and interleukin-15 (Stacey et al., 2009). While these inflammatory reactions contribute to the antiviral response, the resulting cytokine storm can also lead to excessive immune activation that may result in the further depletion of $CD4_+$ T cells. PRRs also serve to activate transcription factors such as NF-κB, which drive the production of restriction factors that limit HIV replication, including tetherin, SAM and HD Domain Containing Deoxynucleoside Triphosphate Triphosphohydrolase 1 (SAMHD1), Apolipoprotein B Editing Complex (APOBEC3), and Tripartite Motif Containing 5 (TRIM5) (Hotter et al., 2013; Simon et al., 2015). The wide range of activities mediated by PRRs aim to limit HIV spread in the earliest phases of acute infection, just days after HIV acquisition. Interestingly, the earliest detectable signal indicating an immune response to infection is the presence of acute phase reactants $alpha_1$-antitrypsin and serum amyloid A, both associated with inflammation, which become detectable in plasma three to five days post-acquisition in response to early pathogenesis (Kramer et al., 2010). A number of the cytokines produced during acute infection also act as activators of natural killer (NK) cells, which act directly on infected cells and indirectly in immune modulation (Stacey et at., 2009). NK cells possess the ability to directly kill infected $CD4_+$ T cells via secretion of perforin and granzyme B that leads to target cell lysis, thus reducing the infected cell population (Tomescu et al., 2007). During acute infection, the NK cell population expands rapidly and NK activity is correlated with the level of viral replication (Alter et al., 2007). They also act to modulate the strength of the immune response by regulating activated, virus-specific $CD8_+$ T cells (Waggoner

et al., 2012; Altfeld et al., 2015). Though NK cell-mediated killing reduces the population of HIV-infected cells, it also puts evolutionary pressure on the virus causing the development of escape mutants (Alter et al., 2011). In summary, the innate immune response to HIV infection is a highly coordinated reaction that employs many cell types and non-cell molecules to reduce the population of infected cells. Concurrently, the anti-viral responses encourage the formation of viral escape mutants, leading to a greater diversity of HIV quasispecies that are more difficult to eliminate.

Humoral Immune Response

While the innate immune response represents the body's first line of defense against HIV infection, active even before viral RNA is detectable in circulation, the humoral immune response is responsible for continued and specific anti-viral protection after seroconversion. The first detectable anti-HIV Ab responses come in the form of immune complexes approximately 18 DPI, present five days earlier than the first detectable free plasma Abs (Tomaras et al., 2008). The first free Abs, detectable at a median of 23 DPI, are anti-gp41 Abs, detectable in 90% of subjects in one cohort by 28 DPI. In the same group, anti-gp120 Abs emerged at a median of 38 DPI with greater variability of timing between subjects compared to the appearance of anti-gp41 Abs (Figure 5) (Tomaras et al., 2008). The first class of Abs binding gp41 were IgM Abs, detectable at a median time of 23 DPI, appearing sooner than IgG and IgA Abs in 41% of subjects and at the same time as anti-gp41 IgG and IgA in the other 59%. Ab concentration peaked for all three Ab classes around 30 DPI, and then proceeded to decline for IgM and IgA Abs whereas IgG levels plateaued or continued increasing gradually through day 40 post-infection (Tomaras et al., 2008). HIV structural component Abs targeting p24, p17, p31, etc. developed significantly later than those binding gp41, though still during acute infection. Two important subsets of Abs that emerge after the acute phase are neutralizing Abs (nAbs) and broadly neutralizing Abs (bnAbs), both capable of preventing the spread of HIV. NAbs act directly on the virus in a number of ways such as by interfering with virion binding and uptake into cells, preventing uncoating of the viral genome, and aggregating many virus particles (Weiss et al., 1986; Payne, 2017). While impressive, these nAbs generally appear no sooner than three months post-infection and are rapidly evaded by HIV due to its high mutation rate (Wei et al., 2003). In contrast, in about 10-20% of HIV infected people, Abs effective at neutralizing a broad range of HIV viruses emerge, called bnAbs (Gray et al., 2011; Landais et al., 2016). bnAbs by definition need only neutralize a few strains of HIV,

though some bnAbs such as 10-1074 can neutralize upwards of 60.5% of strains tested in a broad panel (Caskey et al., 2017). The use of bnAbs in experimental therapies has become a popular approach, though no bnAb-based treatments have passed the trial phase nor have they been successfully elicited in vaccine trials (Nishimura and Martin, 2017). Additional shortcomings of bnAbs are that they generally only appear years after disease acquisition and similarly to nAbs can

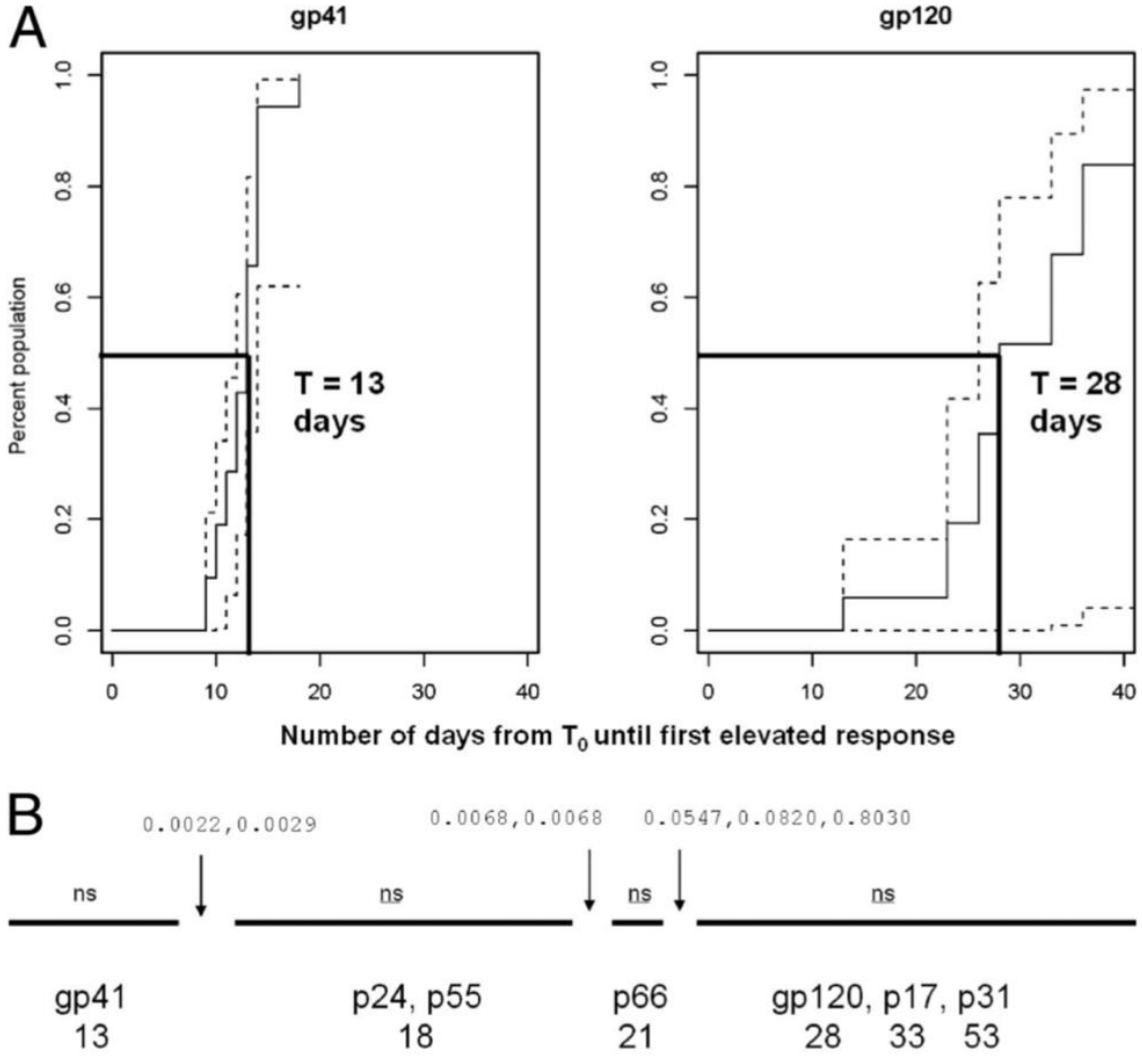

Figure 5: The Appearance of anti-HIV Antibodies. A: T_0 = date of first detectable HIV RNA, approximately 10 DPI. Anti-gp41 Abs are the first to appear at 13 days post-T_0 or 23 DPI. Anti-gp120 Abs appear later, a median of 38 DPI, and with greater variability within the cohort. B: differences in the appearance of anti-HIV Abs, arrows represent significant differences in timing of appearance with p-values above, the appearance of antigens listed under a line were non-significantly different from one another. *Image reproduced from "Initial B-Cell Responses to Transmitted Human Immunodeficiency Virus Type 1: Virion-Binding Immunoglobulin M (IgM) and IgG Antibodies Followed by Plasma Anti-gp41 Antibodies with Ineffective Control of Initial Viremia", Tomaras et al., Journal of Virology, 82(24), 12449, Copyright (2008), with permission from the American Society for Microbiology.*

cause escape mutations in the HIV sequence (Caskey et al., 2017). What has been learned from the study of bnAbs is that their broad potency comes from their targeting of non-overlapping regions in the Env protein, including the V1, V2, and V3 loops, the CD4 binding site, the membrane proximal external region, and a series of epitopes spanning the gp120 and gp41 regions (Caskey et al., 2017). The emphasis on targeting non-overlapping regions is key as resistance would develop more quickly if only one or overlapping regions of the protein were targeted. The V1, V2 and V3 regions of the gp120 protein have been identified as especially important targets for therapy based on several studies demonstrating their highly conserved nature, which may even allow for cross-neutralization of strains by a single antibody (Pinter et al., 1998; Gottardo et al., 2013). The humoral response to HIV infection is truly dynamic and many current studies are consequently focusing on harnessing its power for use in treatments and prevention.

Fc-Dependent Functions

In addition to the anti-viral activities exhibited by nAbs and bnAbs, the activity of non-neutralizing Abs (nnAbs) has been shown to correlate with protection from infection. Instead of acting directly on HIV-infected cells, nnAbs recruit immune effector cells and factors to perform neutralization or cell lysis of the infected cells they opsonize (Boesch et al., 2015). Such functions were found to correlate with protection from infection in the modestly effective RV144 vaccine trial (Haynes et al., 2012; Rerks-Ngarm et al., 2009). The recruitment of immune cells and factors, such as complement, that support effector functions directed to infected cells depends on both the binding of the antigen binding site of the Ab to the target cell, as well as interaction between the fragment crystallizable (Fc) region of the Ab to receptors on immune cells and the first element of the complement cascade. A particular interest in the Fc region of Abs has emerged after several studies have linked it to the essential action of both nnAbs and bnAbs (Bournazos et al., 2014; Chung et al., 2014; Halper-Stromberg et al., 2014). Knock-down experiments have demonstrated reduced protection from infection in the absence of a functional Fc region, suggesting that it is key for ensuring the immune action against infected cells (Halper-Stromberg et al., 2014). Fc-dependent functions (FcDFs) of Abs have also been proposed to be predictive of the development of bnAbs during chronic infection (Richardson et al., 2018). While many FcDFs exist, there are several which have been the focus of additional attention due to their proposed role in fighting infection, namely antibody-dependent cellular cytotoxicity (ADCC), antibody-dependent complement

deposition (ADCD), antibody-dependent cellular phagocytosis (ADCP), and antibody-dependent cellular trogocytosis (ADCT). ADCC describes the targeted killing of infected cells by Ab-recruited NK cells expressing the CD16 Fc Receptor (FcR). The cross-linking of CD16 by Ab-bound target cells results in the release of cytotoxic granules containing perforin and granzymes from the NK cell, which penetrate the infected cell, causing cell lysis (Dourmashkin et al, 1980; Perussia et al., 1983).

ADCC is the function which has gained the most prominence of the four as it was claimed to be a correlate of protection in the RV144 trial (Bonsignori et al., 2012; Haynes et al., 2012). It was discovered that in the presence of low anti-HIV Env gp120 specific IgA levels, ADCC activity was significantly higher in recipients of the vaccine who did not succumb to infection, compared to those who did (Tomaras et al., 2013; Haynes et al., 2012). These results have been criticized as the techniques used to quantify ADCC used HIV targets not representative of the Env protein's conformation in productively infected cells, thus leading to skepticism as to whether the same levels of ADCC were achieved in vivo. Nonetheless, ADCC had gained a reputation as a protective function, based on the RV144 trial and other studies (Baul et al., 1996; Wren et al., 2013).

ADCD describes the deposition of components of the complement cascade, most often C3b, on the surface of infected cells. The activation of the complement cascade and deposition of its components precedes the formation of a membrane attack complex that can lead to cell death (Medof et al., 1982). ADCD activity has also become a potential correlate of the protection seen in the RV144 trial due to a study which found that higher complement deposition on V1/V2 coated beads occurred in the presence of serum from RV144 vaccine recipients compared to that of unvaccinated subjects (Perez et al., 2017). This study again used a model target cell expressing monomeric Env gp120. Other studies have also supported the role of ADCD in the immune response to HIV. One such study observed increased levels of complement components in an HIV-infected brain compared to an uninfected brain, though the authors did point out that this inflammatory response may also contribute to HIV-associated non-AIDS events (Liu et al., 2014). In contrast, a study on the role of bnAbs in protection against HIV infection found that Abs that lost their complement binding ability had no loss of protective activity (Hessell et al., 2007). Whether ADCD has a net beneficial impact on HIV outcomes is still uncertain, though the

evidence strongly suggests that the complement cascade is upregulated in response to HIV infection.

ADCP is the process whereby monocytes and macrophages bind antibody-opsonized infected cells and phagocytose them, leading to cell death (Tay et al., 2019). The internalization of the target cell leads to the destruction of the HIV structures by phagolysosomal degradation along with the components of the host $CD4^+$ T cell. It has been shown that ADCP is partially responsible for the clearance of HIV immune complexes, with increased phagocytic activity observed in HIV controllers, who control their viral load in the absence of treatment, and untreated progressors (Ackerman et al., 2013). Additionally, while it was demonstrated that ADCP did not play a significant role in prevention of HIV acquisition, it has been suggested that it likely plays a role in elimination of infected cells (Gach et al., 2017).

ADCT involves monocytes binding to antibody-bound infected cells, extracting surface molecules and membrane fragments, and expressing them in their own membrane (Taylor et al., 2015). This process of extraction may lead to cell death due to membrane destabilization. The role of ADCT in HIV infection has not been extensively studied though the presence of high levels of ADCT activity at 6 months post-infection were predictive of the development of bnAbs in one study (Richardson et al., 2018). Theories around ADCT's role in protection are largely borrowed from the field of cancer research, where it has been observed that the removal of membrane fragments from tumorigenic cells resulted in cell killing (Velmurugan et al., 2016). Taken separately or together, the literature on the FcDP immune responses to HIV infection supports an important role for these Ab-dependent functions in the control of infection.

Elite Controllers

A unique opportunity for the study of successful immune responses to HIV infection comes in the form of a population know as HIV controllers. More specifically, 'elite controllers' are HIV-infected people capable of controlling their infection to a level of less than 50 copies of HIV RNA/ mL of plasma without treatment (Walker, 2007). Below this limit of detection, subjects maintain healthy levels of $CD4^+$ T cells, are at low risk of progressing to AIDS, and are unlikely to transmit the infection to others (Sheppard et al., 1993; Eisinger et al., 2019). Elite controllers are

exceptionally rare, however, representing less than 1% of the HIV-infected population (Okulicz et al., 2011). Due to their exceptional resistance to diseases progression, extensive studies have attempted to determine the mechanisms underlying their control of infection. A prevalent commonality between elite controllers is the presence of protective human leukocyte antigen (HLA) alleles. HLA-B57 and HLA-B27 are two alleles that are enriched in elite controller populations, said to offer an adaptive immune advantage due to the improved antigen recognition mediated by the HLA molecules (Kiepiela et al., 2004). The protective effects of these HLA alleles are especially pronounced in individuals who co-express KIR3DS1, an inhibitory killer-cell immunoglobulin-like receptor (KIR) (Martin et al., 2007). It is hypothesized that improved epitope presentation in individuals carrying favourable HLA alleles causes mutations in HIV that come at a large fitness cost to the virus, thus reducing its infectivity. Another leading school of thought looks at the enriched $CD8^+$ T cell responses in HIV controllers. $CD8^+$ T cell responses occur at higher frequencies and have a demonstrated enhanced capacity to suppress HIV infection in controllers compared to non-controllers (Sáez-Cirión et al., 2007; Kou et al., 2004). Various functions carried out by $CD8^+$ T cells are also enriched in controllers such as proliferative ability, cytokine production, and production of perforin, all of which play a role in eliminating infected cells (Borrow et al., 2004; Migueles et al., 2007; Zimmerli et al., 2005). The $CD8^+$ T cell phenotype may play a role in protection as surface markers such as PD-1, CD57 and CD127 differentiate the $CD8^+$ T cells of controllers from those of untreated progressors (Petrovas et al., 2006; Trautmann et al., 2006; Paiardini et al., 2005). $CD8^+$ T cell avidity and polyfunctionality are other potential causes of the enhanced protection, allowing them to detect and kill more antigens at lower antigen concentrations (Almeida et al., 2007; Betts et al., 2006). It is hypothesized that the HLA-B57 allele may contribute to this response by presenting a broad number of HIV antigens to activate a greater number of $CD8^+$ T cells (Altfeld et al., 2003). Though there is no consensus on a single cause of elite control in certain HIV-infected subjects, various studies point to an important role for enhanced $CD8^+$ T cell responses coupled with antigen presentation by favourable HLA alleles.

1.5 Treatments and Cure Research

The success of ART has not eliminated the need to design a treatment that will permanently prevent acquisition of HIV or fully eliminate it from the body post-infection. Discussed here are some of

the leading past and present efforts for preventing and eliminating HIV infection in relation to the development of the pandemic.

The HIV Pandemic

As of the virus' discovery in 1981, the number of deaths due to HIV increased each year until 2006 where it peaked at nearly 2 million deaths per year (Institute for Health Metrics and Evaluation, 2018). The subsequent slowing was in large part due to the spread of ART to the areas with the highest burden of disease. Of the 35 million people living with HIV in 2012, 70% lived in Sub-Saharan Africa with infections especially concentrated in southern Africa (UNAIDS, 2013). While the global annual incidence of HIV declined from 2006 to 2012, the global prevalence increased due to the higher longevity of people on ART (UNAIDS, 2013; WHO, 2013). Contemporarily there is cause for cautious optimism as the yearly rate of new infections continues to decline, despite the fact that the UNAIDS goals for 90% diagnosis, treatment, and viral control were not achieved by 2020 (UNAIDS, 2019). In recent years, gains against the epidemic have been positive but relatively more modest year-to-year, with great geographical variation. Between 2010 and 2018 eastern and southern Africa saw a 28% decline in new infections, however in eastern Europe and central Asia there was a 29% increase in new infections (UNAIDS, 2019). Additionally, while 2016 was the first year that more than half of HIV-infected people were accessing ART, there have also been troubling rises in resistance to ART, as high as 10% to certain regimens in key regions (UNAIDS, 2017; WHO, 2019). The current state of the pandemic demonstrates that while great strides have been made, new, more efficient prevention and treatment options are needed to end the era of HIV/AIDS.

ART

The introduction and popularization of ART after 1996 was a major success in the fight against HIV, limiting the disease to a chronic rather than fatal diagnosis (Collier et al., 1996; Staszewski et al., 1996). Use of ART continues to spread globally and is estimated to have saved millions of lives in the years following its availability for treating HIV infection (WHO, 2011). While ART implementation greatly altered the course of the HIV pandemic, the reality for many HIV-infected patients remains the burden of taking several daily medications and fearing development of resistance, disease progression, or death if treatment is stopped (Hogg et al., 2002). ART does not cure HIV but it can reduce the viral load to below detectable levels of 50 copies of virus/mL of

plasma (Fischl, 1999). Below these levels, HIV infected people do not progress to AIDS and do not transmit the virus, however, they still experience higher mortality than the general population due to co-morbidities such as cancer, kidney disease, and cardiovascular disease (Eisinger et al., 2019; Abbar et al., 2020; Mallipattu et al., 2014; Ballocca et al., 2017). As ART has become less toxic over time, the severity of these comorbidities has declined but they have not disappeared completely. The typical ART regimen includes three drugs that are taken daily: two nucleoside reverse transcriptase inhibitors (NRTIs) plus one of either a non-nucleoside reverse transcriptase inhibitor (NNRTI), an integrase inhibitor (INI), or a protease inhibitor (PI) (Johnson, 2016). Each inhibitor acts by blocking a step in HIV's replication corresponding to the given protein (RTr, IN, or PI). Two of the first-line regimens recommended by practitioners are abacavir/lamivudine/dolutegravir and tenofovir alafenamide/emtricitabine/bictegravir, both containing two NRTIs and one INI (Merrick, 2019). The exact regimen can vary between patients based on preferences and may need to be changed over time as resistance to a regimen can develop as well as negative interactions with other medications. While ART offers a lengthened life of improved quality to those diagnosed with HIV, the reality is that many people with HIV are not undergoing successful treatment. When considering the number of people who are unaware of their HIV status, are not on treatment, or who are on an ineffective regimen, it is estimated that barely half (53%) of HIV infected people are virally suppressed (UNAIDS, 2019). A preventative drug treatment with a similar regimen to ART is called pre-exposure prophylaxis (PrEP). The typical PREP regimen includes two nucleoside reverse transcriptase inhibitors, tenofovir disoproxil fumarate and emtricitabine, taken daily (Spinner et al., 2016). The prescription of PrEP to individuals at heightened risk for HIV infection, such as men who have sex with men (MSM), uninfected partners in sero-discordant couples, and injection drug users, has been used as a strategy to reduce the incidence rate (Grant et al., 2010; McMahon et al., 2014; Choopanya et al., 2013). The timing of ART initiation has been a subject of debate since its advent into the list of prescribed treatments. As of a 2006 report, the WHO's official recommendation was to only begin ART once a patient had reached the clinical definition of AIDS, a $CD4^+$ T cell count of less than 200 cells/mm^3 (WHO, 2006). Over the years this threshold gradually increased until 2015 when the WHO's official stance became that ART should be initiated immediately after diagnosis regardless of $CD4^+$ T cell count or disease stage (WHO, 2015). The WHO report maintained that earlier initiation of ART resulted in better clinical outcomes for people with ART regardless of the

potential side effects of the drugs. An additional benefit of initiating ART as early as possible is that it has been shown to limit the size of the HIV reservoir, a high priority in HIV cure research (Vandergeeten et al., 2014; Luo et al., 2019). On the other hand, less is known about the impact of the timing of the initiation of ART on host immune responses, which may become especially important in the face of mounting resistance to ART drugs. In summary, ART has arguably been the most important breakthrough for the treatment of HIV/AIDS to date, preventing millions of new infections in addition to saving millions of lives. The ART regimen options have evolved greatly since its relatively recent introduction to the management of HIV infection, so there is still much to learn about its effects on the human body in early infection and over time. In addition, ART does not cure HIV and if therapy is stopped, viral rebound and progressive infection will ensue, so there is still great incentive to develop new treatments.

RV144 Vaccine Trial

One of the largest efforts towards curbing the HIV epidemic is the creation of a preventative vaccine that would induce long-lasting protection against infection. The only modestly successful preventative HIV vaccine to date was tested in the RV144 study whose results were published as part of a phase 3 clinical trial in 2009 (Rerks-Ngarm et al., 2009). The trial recruited 16,400 Thai men and women between the ages of 18 and 30 years old, split equally into a vaccine-receiving and placebo arm. The vaccine regimen included an, ALVAC-HIV prime, which contained recombinant HIV-1 Gag, gp120, and gp41 proteins and an AIDSVAX B/E boost, which contained a combination of two gp120 variants. The goal of the vaccine was to elicit anti-gp120 and anti-gp41 Abs that would offer protection against infection during HIV exposure post-vaccination. The results showed that the vaccine offered 31.2% protection against HIV infection up to three years post-infection compared to the placebo, which was significant ($p = 0.04$) (Figure 6) (Rerks-Ngarm et al., 2009). Dissecting the specifics of protection seen in the RV144 trial has been the basis of several subsequent studies that have uncovered two primary correlates of the protection seen in the trial. Foremost, reduced risk of infection was correlated with IgG Abs targeting the scaffolded

V1/V2 regions of the gp120 protein (Karasavvas et al., 2012; Haynes, 2012). Higher levels of anti-V1/V2 Abs were found in the uninfected vaccinated subjects compared to infected subjects, leading to the hypothesis that Ab binding to these regions of gp120 offered protection against infection. The second correlate was ADCC, though this correlation only held true in vaccine recipients with low anti-Env IgA levels (Haynes et al., 2012). IgA Ab levels were found to correlate with infection due to their competitive binding at the same sites as IgG, thus they offered no protection against infection while concomitantly blocking the protective action of IgG Abs (Tomaras et al., 2013). Additionally, IgG3 responses were preferentially induced, eliminating IgG3 resulted in a decline of 30% of overall Ab activity and correspondingly lower levels of ADCC (Yates et al., 2014; Chung et al., 2014). IgG1 titers were also found to correlate with protection compared to IgG2 and IgG4, and depletion analysis suggested that it functions in coordination with IgG3 (Chung et al., 2014). Notably, there has been much criticism of the trial since its concept was originally proposed, including disapproval of the rationale for the trial before it began, and

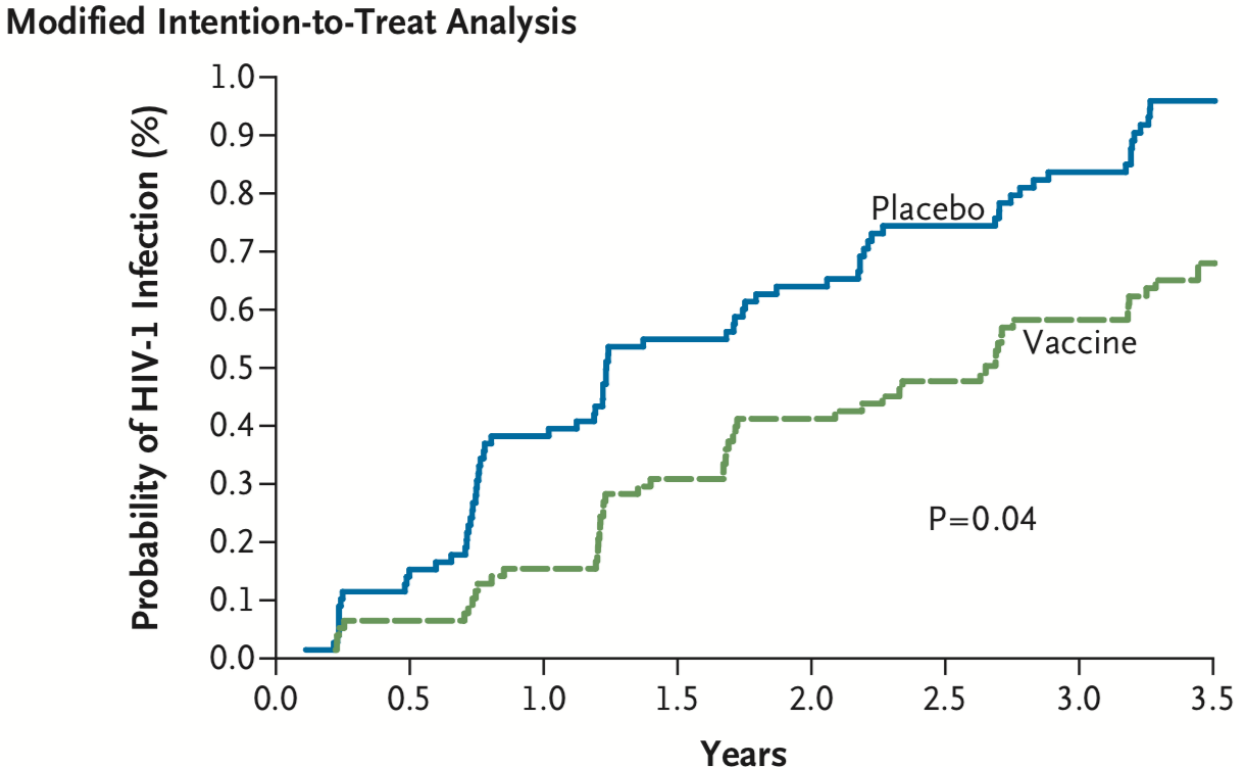

Figure 6: Protective Efficacy of the RV144 Vaccine. The RV144 vaccine regimen offered 31.2% protection against HIV infection compared to a placebo three years after vaccination, significant at p = 0.04. *Image reproduced from "Vaccination with ALVAC and AIDSVAX to Prevent HIV-1 Infection in Thailand", Rerks-Ngarm, S et al., 2009, New England Journal of Medicine, 361(23), 2209-2220.*

scrutiny surrounding the exclusion of subjects to reach statistical significance following its publication (Frantz, 2004; Desrosiers, 2017). Despite its critics, the focus of many follow-up trials has been to elicit the same ADCC-capable IgG Abs as RV144 through varying prime-boost strategies. A phase 3 clinical trial testing a clade-C adapted vaccine regimen in South Africa was recently cancelled due to lack of protection, likely due to differences in Env conformation, thus highlighting the need for accurate models and correlates of protection tests (NIAID, 2020). The strain of HIV most common in Thailand is a recombinant form of subtypes A and E called CRF01_AE, which carries a unique substitution in its Env protein sequence (Carr et al., 1996). In most HIV strains there is a Serine at position 375 in the gp120 sequence whereas in the CRF01_AE strain found in Thailand, a larger Histidine residue naturally occurs in this position (Richard et al., 2017). The result is a slight change in Env conformation that results in the exposure of CD4-induced (CD4i) epitopes, which are targets for anti-HIV Abs and not usually exposed on native Env trimers present at the surface of genuinely infected cells. It was predicted that the conformation of Env present in the Thai strain was responsible for the protection seen in the RV144 trial as Abs induced by the vaccine were able to recognize cells infected with CRF01_AE HIV. Several vaccine trials continue presently as hope for an HIV vaccine has not dissipated. It is hoped that in future efficacy evaluations and correlates of protection analysis, full consideration will be given to the strain of HIV studied so that results will be more substantial and generalizable.

Chapter 2: Introduction

Recent progress in HIV-1 treatment has allowed HIV-positive patients to live long and fulfilling lives thanks to advances such as PrEP and ART. Current ART regimens are less toxic with fewer side-effects compared to those used in the past, and they are available to more HIV infected persons than ever. Nevertheless, drug resistance, unequal access, and lack of affordability persist for many HIV-infected people, meaning that there is still an incentive to eradicate the disease by limiting its spread and/or by finding a long sought-after cure. Past efforts in this field have highlighted the importance of the humoral response in the defense against infection. BnAbs, capable of neutralizing many strains of the virus, have been a focus of much research due to their potential for effectiveness in a wide range of settings. Experiments testing protection derived from infusion of bnAbs in primates as well as humans have shown promising results and a regimen including the bnAbs 10-1074 and 3BNC117 is now being tested in humans in a phase 1 trial (Nishimura et al., 2017; Caskey et al., 2017; Lavelle, 2018). Infusion of bnAbs is necessary as they appear too late in infection to offer protection against acquisition and no vaccine to date has been successful at eliciting them. Conversely, the RV144 trial found that nnAbs and FcDFs develop just weeks after infection and were correlated with the protection they observed in the vaccine-recipient group (Karasavvas et al., 2012; Haynes et al., 2012). These Ab responses appear weeks after HIV challenge rather than years later as with bnAbs. Anti-gp120 IgG and ADCC in the presence of low IgA were found to be associated with prevention of infection in the trial, responses which developed in response to the gp120 antigens present in the vaccine (Rerks-Ngarm et al., 2009; Haynes et al., 2012; Tomaras et al., 2013).

While studies have convincingly demonstrated that Abs can be key for protection from and control of HIV infection, the data supporting this are often misinterpreted due to the use of models that do not accurately reflect in vivo interactions between HIV infected cells and anti-HIV Env specific Abs. HIV Env is the only HIV gene product expressed on the surface of HIV infected cells (Checkley et al., 2011). Therefore, measuring the concentration of Abs to Env and the FcDFs of these Abs is relevant. However, many assays used to quantify HIV Env gp120-specific IgG titers use microtitre plates or target cells coated with monomeric gp120. Many assays used to measure FcDFs such as ADCC use monomeric gp120 coated target cells or cultured HIV infected target cells. Gp120 coated target cells expose Env epitopes such as CD4i epitopes that are hidden on

genuinely HIV-infected CD4+ T cells, which express Env in a native trimeric closed conformation. In productively HIV-infected cell cultures, the HIV proteins Nef and Vpu mediate the downregulation of CD4 from the cell membrane, thus preventing the exposure of CD4i epitopes (Willey et al., 1992; Schwartz et al., 1995). However, only a fraction (5 to 20%) of the CD4+ T cells in HIV-infected cell cultures are HIV infected (Kiani et al., 2019; Kiani et al., 2019). Infected cells shed gp120, which is taken up by CD4 on uninfected bystander cells. This leads to exposure of CD4i epitopes (Richard et al., 2018). In other words, most of the assays used to measure anti-gp120 concentrations and FcDFs to date have used target cells that bind CD4i Ab preferentially expressed on uninfected bystander cells leading to the pathogenic killing of uninfected rather than the protective lysis of genuinely infected cells. Because many studies neglect this crucial distinction, including those involved in the correlates of protection analysis for RV144, Ab responses are often overestimated and misinterpreted. Thus it is important to use more suitable target cell models that measure Abs to the closed Env conformation on HIV infected cells.

Our lab has developed such a target cell by infecting CEM.NKr.CCR5 cells with NL4-3-BaL-IRES-HSA, a kind gift from Dr. Michel J. Tremblay, Université Laval (Imbeault et al., 2009). This HIV vector expresses the selection marker heat stable antigen (HSA/murine CD24) and replication competent HIV using the CCR5 Env from $HIV_{Bal.}$. After infection, these infected CEM cells were sorted for HSA+ cells. The resulting sorted HIV infected CEM (siCEM) cells are virtually all HSA+ and p24+, marking them as HIV infected. The siCEM cells are CD4- as CD4 has been downmodulated by wild type Nef and Vpu. The binding of a panel of bnAbs recognizing the CD4 binding site, V3 loop and V1/V2 structures shows that Env on siCEM is expressed in a closed conformation. NnAb to CD4i epitope, including the prototypic A32 monoclonal Ab fail to bind Env on siCEM cells, further confirming the closed conformation of HIV Env on these siCEM cells (Kant et al., 2019; Dupuy et al., 2019).

The recommendations surrounding the timing of ART treatment initiation have evolved over time, though the WHO's most recent position supports initiating ART as soon as HIV infection is detected, citing more favourable outcomes for patients who start treatment early (WHO, 2015). It has also been well established that early initiation of ART contributes to limiting the size of the viral reservoir, an important consideration for cure research (Vandergeeten et al., 2014; Luo et al.,

2019). Less is known, however, about the impact of ART initiation timing on the humoral response, in terms of both quantity and functionality. In most HIV infected individuals, non-specific hypergammaglobulinemia is observed after acquiring HIV, with higher virus concentration correlating with greater B cell proliferation (Lane et al., 1983; Schnittman et al., 1986). This trend appears to reverse once ART is initiated, as Ab levels correlated with HIV DNA decline once free plasma viral loads decline (Keating et al., 2019). Our knowledge on trends in FcDF activity before and after ART initiation is incomplete.

The objective of this project is to improve our understanding of Ab FcD immunity in HIV positive subjects through two primary aims: 1) To characterize the fate of Ab FcD functions in untreated subjects using cross-sectionally collected samples, and 2) To describe the evolution of Ab concentrations and FcD functions in subjects starting ART at defined times post infection using longitudinally collected samples. This line of investigation will contribute to several key outcomes: bettering our understanding of Fc-mediated immune activity, informing novel strategies on the ideal time to initiate ART, and providing information on which vaccine induced Ab responses to target for HIV protection or control.

Here we report an increase in HIV-specific Ab concentration and FcDF in untreated HIV positive individuals. Higher concentrations of Abs binding monomeric gp120 were detected than Abs capable of binding Env on the surface of iCEM cells. We also observed a decline in HIV-specific Abs and FcDFs after treatment initiation, with a more pronounced decline in subjects treated more than 90 DPI.

Chapter 3: Methodology

Study population

The plasma and peripheral blood mononuclear cell (PBMC) samples used in this study were collected from subjects enrolled in the Montreal HIV Primary Infection Cohort initiated in 1996 (principal investigator, Dr. Jean-Pierre Routy, McGill University). The cohort includes untreated and treated subjects, including those who initiated treatment after enrolment in the cohort. The data analysis in this thesis includes samples from 99 subjects, including cross-sectional untreated samples and longitudinally collected samples from treated individuals, collected by physicians located at several hospital-based and community clinic sites in the Montreal area. Subjects range in age from 19-78 years old and 93 of 99 of the subjects are male. The reason for the predominance of males in the study population is that the population at highest risk for HIV infection over the time span of recruitment to the Montreal PI cohort were MSM. The data presented in this thesis comes from my own experimental work and that of a previous Masters' student named Chris Leeks. The samples of the 99 subjects enrolled in the Primary Infection Cohort used in the study were split evenly between myself and previous Masters student Chris Leeks, and we each performed the Total IgG and anti-gp120 quantifications, ADCC, ADCT, ADCD, and ADCP assays on our own portion of the samples. I performed the HIV infected cell-based assay and the integrated HIV reservoir quantification on samples from both Chris and my study subjects.

CEM and siCEM cell lines

The uninfected CEM.NKr.CCR5 (uniCEM) and siCEM cell lines were the basis of many of the experiments described in the thesis. The CEM cell line was derived from the lymphocytes of a 2-year old female leukemia patient (Foley et al., 1965). The cells have been selected for resistance to NK cell-mediated lysis and for expression of CCR5, which make them excellent targets for measuring FcDFs (Howell et al., 1985; Trkola et al., 1999). The virus used to infect the siCEM is the NL4-3-BaL-IRES-HSA construct, an NL4-3 backbone with an envelope protein derived from the Bal strain, bound to the HSA reporter gene, and containing an internal ribosome entry site (IRES) allowing for replication, kindly provided by Dr. Michel J. Tremblay (Université Laval) (Imbeault et al., 2009). Briefly, preparation of siCEMs was as follows: uniCEM cells were HIV-infected by adding the supernatant from NL4-3-Bal-IRES-HSA transfected 293 T cells to 10_6 CEM cells followed by spinoculation at 2000 x g for 90 mins (Kant et al., 2019). Cell surface HSA

expression was used to identify infected cells, which were sorted using a FACSAria cell sorter instrument (BD Biosciences, San Jose, CA). Pre-experiments, both uniCEM and siCEM were cultured in RPMI 1640;10% fetal bovine serum (FBS); 2 mM L-glutamine; 100 IU/mL penicillin; 100 mg/mL streptomycin, all from Wisent) (R10).

Total IgG quantification

The concentration of total IgG Ab in subject plasma was quantified using the plate-based human IgG ELISA Quantification Set (Bethyl Laboratories, Montgomery, TX). First, 100µL of 1mg/mL affinity purified goat anti-human IgG-Fc coating Ab was added to each well of a round-bottomed 96-well plate (Thermo Fisher, St. Laurent, QC, Canada) and incubated at room temperature (RT) for 1 hr. The plate was then washed five times with 100µL/well ELISA Wash Solution (50mM Tris [Sigma Aldrich, St. Louis, MO, USA]; 0.14M NaCl [American Chemicals Ltd, Montreal, QC, Canada]; 0.05% Tween 20 [Sigma- Aldrich]) before adding 200µL of ELISA Blocking Solution (50mM Tris; 0.14M NaCl; 1% Bovine Serum Albumin [BSA, Sigma Aldrich]) in phosphate buffered saline (PBS, Wisent Bio Products, St-Jean-Baptiste, QC, Canada) to each well at RT for 30 min. The following additions were made to the plate with five 100µL/well plate washes between steps. 100µL of subject plasma diluted 1:150,000 in Sample Diluent (50mM Tris; 0.14 M NaCl; 1% BSA; 0.05% Tween 20) was added in duplicate for 1 hr at RT. A human reference serum IgG positive control diluted to concentrations ranging from 500ng/µL to 7.8ng/µL was also added in duplicate to each plate at the same time as the test plasma. 100µL per well of 1mg/mL Horse Radish Peroxidase-conjugated goat anti-human IgG polyclonal detection Ab (HRP-conjugated detection Ab) (Bethyl Laboratories), diluted 1:150,000, was then added for 1 hr at RT. 100µL of Tetramethylbenzidine (TMB) substrate solution was added to each well and allowed to develop in the dark at RT for 15 mins. The reaction was stopped with addition of 100µL of stop solution (1M H_3PO_4) to each well. Absorbance was measured on a Tecan ELISA plate reader (Tecan, Männedorf, CH) at 450nm and optical density values were calculated for each well. Total IgG Ab concentration values were obtained using GraphPad Prism 7 software (GraphPad Software, San Diego, CA), which interpolates IgG concentration values for the plasma samples against the optical density of a standard curve of known IgG concentrations of the human reference serum.

Anti-gp120 Ab detection

Anti-gp120 Ab concentrations were measured using a plate-based ELISA. First, 100uL of 2.5μg/mL affinity-purified sheep polyclonal anti-HIV-1-gp120 Ab (Aalto Bio Reagents, Dublin, Ireland) was added to each well of a round-bottom 96-well plate and incubated at 4ºC overnight. The plate was then washed three times with 100μL/well gp120 ELISA Wash Solution (0.05% Tween 20 in PBS) before adding 100μL of ELISA Blocking Solution to each well for 30 mins at 37$_{o}$C. The following additions were made to the plate with three plate washes of 100μL/well of gp120 ELISA Wash Solution between each step. 100μL of diluted HIV-1 Bal gp120 recombinant protein (from the NIH AIDS Reagent Program, Division of AIDS, NIAID, NIH: HIV-1BaL gp120 from DAIDS, NIAID) at 100ng/mL was added per well, for 3 hrs at RT. 100μL of subject plasma was added at four dilutions: (1:100, 1:200, 1:400, and 1:800) in ELISA Blocking Solution to the plate in addition to a standard curve of HIV$_{+}$IG (a pool of polyclonal IgG isolated from HIV-infected donors from the NIH Reagent Bank, NABI and NHLBI), containing IgG concentrations ranging from 150ng/μL to 0.21ng/μL for 60 mins at 37ºC. 100μL of HRP-conjugated detection Ab diluted 1:150,000 was added to each well for 30 mins at RT. 100μL of TMB substrate solution was added to each well and allowed to develop in the dark for 15 mins at RT. The reaction was stopped with addition of 100μL of stop solution (1M H_3PO_4) to each well. Absorbance was measured on a Tecan ELISA plate reader at 450nm and optical density values were calculated for each well. Anti-gp120 Ab values were obtained using Graphpad Prism 7 software (GraphPad Software), which plots a standard curve based on the optical density and known concentrations of the HIV$_{+}$IG standard and interpolates values for the plasma samples. The concentration of anti-gp120 Abs in HIV$_{+}$IG is unknown so an exact concentration or quantity of anti-gp120 Abs in plasma cannot be determined. Therefore, the relative amount of "Arbitrary Units" of anti-gp120 Abs was calculated for each plasma sample.

Anti-Env Ab detection

Anti-Env Abs were detected using a cell-based assay that uses flow cytometry to detect Abs capable of binding the native, trimeric closed Env conformation on the surface of an HIV-infected cell. uniCEM cells served as a negative control to determine non-specific binding to uninfected cells in addition to a no-Ab control well. HIV infected CEM cells expressing Nef and Vpu, which downregulate CD4 surface expression, serve as the model to determine Ab-binding to closed

conformation Env.

Target cells for detecting Abs to cell surface Env were prepared as follows: uniCEM were first suspended at 2.0x10$_6$ cells/mL in PBS and stained with CFSE by mixing equal volumes of the cell suspension and a pre-diluted CFSE solution for 10 mins at RT followed by addition of an equal volume of FBS (Wisent Bio Products) for 10 min to stop the reaction. CFSE stained uniCEM and unstained iCEM cells were both washed twice with PBS and resuspended at 4x10$_6$ cells/mL in FACS buffer (PBS; 4% FBS). Equal volumes of each cell suspension were combined and 25µL (i.e. 100,000 cells) of this mixture was distributed into each well of a 96-well V-bottomed plate (Thermo Fisher). 25µL of diluted subject plasma or a standard curve of HIV$^+$IG dilutions, with IgG concentrations ranging from 450ng/µL to 0.6ng/µL was added in duplicate to the wells or the microtitre plate and incubated at RT for 20 mins in the dark. The wells were then washed twice with 150µL of FACS buffer followed by the addition of 50µL of a 1:50 dilution of APC conjugated anti-human IgG Fc (BioLegend, San Diego, CA) in FACS buffer to each well. The plate was incubated for 20 mins in the dark at 4ºC, then washed twice with 150µL of FACS buffer. The cell pellet was fixed in 100µL per well of 2% paraformaldehyde (PFA) (Santa Cruz Biotechnology, Dallas, TX, USA) in PBS. APC fluorescence was detected by flow cytometry using an LSRFortessa X-20 instrument (BD Biosciences) and results were analyzed with FlowJo software version 10 (Treestar Inc., Ashland, OR, USA). Values generated in the no-Ab negative control wells were subtracted from those of the HIV$^+$IG and plasma-containing wells. CFSE$^+$ uniCEM served as a within-well internal negative control measuring non-HIV Env-specific binding. Binding levels to uniCEM were subtracted from results generated by the same Ab dilution used to assess binding to iCEM cells. Anti-Env Ab values were obtained using GraphPad Prism 7 software, which plots a standard curve based on the MFI and known concentrations of the HIV$^+$-IG standard and interpolates values for the plasma samples. The concentration of anti-Env Abs in HIV$^+$IG is unknown, therefore the relative amount of "Arbitrary Units" of anti-Env antibodies was calculated for each plasma sample.

ADCC

ADCC activity was measured by quantifying phosphatidylserine (PS) as an indicator of NK-mediated target cell apoptosis. PS is a phospholipid and a component of the cell membrane present

on the inner cytosolic side of the membrane in live, healthy cells. When a cell undergoes apoptosis, the membrane becomes unstable and PS is exposed on the extracellular side (Verhoven et al., 1995). Thus, when a cell is undergoing apoptosis, PS becomes detectable at its surface and its quantification is indicative of the number of apoptotic cells in a sample. In our assay, target iCEM cells were incubated with NK cells and subject plasma containing Abs able to induce ADCC-driven apoptosis of the iCEM by the NK cells.

First, iCEM cells were suspended at $2.0x10^6$ cells/mL in PBS and stained with CFSE as described in the previous section. The CFSE-stained cells were then washed twice with R10 and re-suspended at $0.2x10^6$ cells/mL in R10. 50µL of this iCEM cell suspension was added to the wells of a V-bottomed plate and mixed with 50µL of diluted subject plasma at RT for 20 mins to allow binding of plasma Abs to the iCEM cells. Subject plasma and positive control HIV^+IG were serially diluted to 500, 50 and 5µg IgG/mL in R10. A negative control of Ab-free R10 was also added to duplicate wells in each plate. Next, NK cells isolated from donor PBMCs by negative selection using the Human NK enrichment kit (Stem Cell, Vancouver, BC, Canada) were added as effector cells to wells containing iCEM target cells at an Effector: Target ratio of 5:1 ($5x10^4$ NK cells and 10^4 iCEM per well) and incubated for 1 hr at 37ºC. Post-incubation, the plate was centrifuged at 2000rpm for 3 mins and washed once with 150µL of 1x Annexin V buffer (BD Biosciences, Mississauga, ON, Canada). 100µL of Annexin V-APC conjugated Ab (BD Biosciences) diluted 1:100 in Annexin V buffer was added to each well and incubated for 10 mins at RT in the dark. The plate was centrifuged at 2000rpm for 3 mins and washed once with 150µL of 1x Annexin V buffer before removing the supernatant and fixing the cells in 100µL of 2% PFA in Annexin V buffer. APC fluorescence was detected by flow cytometry using an LSRFortessa instrument (BD Biosciences) and results were analyzed using FlowJo software. The gating strategy focused on detecting live, singlet $CFSE^+$ iCEM cells that were AnV^+. ADCC scores were determined by measuring the percent (%) of AnV^+ iCEM cells in a well, minus the value generated by the plate's negative control, at three concentrations so that an area under the curve (AUC) could be calculated for each sample. The following formula was used to calculate AUC:

$$AUC = \frac{((\%AnV^+_{\frac{5\mu g}{mL}} + \%AnV^+_{\frac{50\mu g}{mL}}) \times (50-5))}{2} + \frac{((\%AnV^+_{\frac{50\mu g}{mL}} + \%AnV^+_{\frac{500\mu g}{mL}}) \times (500-50))}{2}$$

To allow for inter-plate comparability, results were normalized by dividing sample AUC values by the AUC value of the HIV+IG positive control.

ADCT

ADCT activity was measured by quantifying the transfer of PKH26-stained membrane from iCEM cells to co-cultured monocytes. PKH26 is a lipophilic membrane dye that remains intact and detectable as cell membrane fragments are transferred between cells during ADCT (Richardson et al, 2018). In this assay, iCEM cells were stained with PKH26 dye then incubated with subject plasma and PBMC effector cells, whose PKH26 positivity was used as an indicator of ADCT activity.

First, iCEM cells were stained with CFSE, as described above, washed once with R10 and once with RPMI. The cell pellet was resuspended in diluent C from the PKH26 staining kit (Cell Linker Mini Kit, Sigma Aldrich, St. Louis, MO) at a concentration of $2x10^7$ cells/mL. An equal volume of PKH26 dye in diluent C was prepared at a concentration of 4µL dye/mL diluent, then mixed with the iCEM suspension for 2 mins at RT with periodic mixing by pipette. An equal volume of FBS was then added for 1 min to stop the reaction. The stained iCEM were washed twice with R10 then resuspended at a concentration of $2x10^5$ cells/mL in R10. 50µL of this iCEM suspension was added to the wells of a 96-well V-bottomed plate and mixed with 50µL of diluted subject plasma for 20 mins at RT. The subject plasma and HIV+IG positive control were serially diluted to 500, 167 and 56µg IgG/mL in R10. 100µL of PBMC effector cells at $3x10^6$ cells/mL in R10 were added to each well, (i.e. at 30:1 PBMCs: iCEM) and incubated for 1 hr at 37ºC. Post-incubation, the plates were spun at 2000rpm for 3 mins and washed with 150µL of 2% FACS buffer (PBS; 2% FBS). The supernatant from the wash was removed and 50µL of a staining mixture composed of 0.1µL Live/Dead fixable dead cell stain (Invitrogen, St Laurent, QC, Canada), 1µL anti-human CD14 Ab (BioLegend), and 49µL 2% FACS buffer was added to each well for 20 mins in the dark at 4ºC. After the incubation, the plate was washed twice with 150µL of 2% FACS buffer, then fixed in 100µL of a 2% PFA in FACS buffer. Fluorescence was detected by flow cytometry using an LSRFortessa instrument (BD Biosciences) and results were analyzed using FlowJo software. The frequency of CFSE fluorescent monocytes was determined by gating on live, singlet PKH26+ CD14+ monocytes. ADCT scores were determined using the % PKH26+

monocyte population minus the value generated by the no-Ab negative control. An AUC was calculated for each sample using the same formula as used for ADCC but adapted to the 500, 167 and 56µg IgG/mL dilutions. To allow for inter-plate comparability, results were normalized to the HIV+IG positive control.

ADCD

ADCD activity was measured by quantifying the deposition of complement component C3b on the surface of target iCEM cells. The classical complement pathway is initiated upon binding of C1 to an Ab-antigen complex. C1 becomes activated and cleaves C2 into C2a and C2b, and C4 into C4a and C4b. C2b and C4b combine to form a protease called C3 convertase, which cleaves C3 into C3a and C3b. C3a promotes inflammation while C3b attaches to the surface of the antigen-coated cell, recruiting additional complement components leading to the assembly of the membrane attack complex (MAC), which precedes the formation of a pore resulting in cell lysis (Fischinger et al., 2019). In our assay, deposition of C3b on target iCEM cells was measured as an indicator of ADCD activity presumed to lead to cell lysis.

First, iCEM were washed in R0 and resuspended at $2x10^6$ cells/mL in R0. A 50µL volume of iCEM cells (i.e. 100,000 cells) was added to the wells of a V-bottommed 96-well plate with 50µL of diluted subject plasma or HIV+IG positive control, serially diluted to 500 and 100µg IgG/mL in PBS, were added in duplicate for 20 mins at RT. A volume of 150µL of freshly frozen and thawed human serum as a source of complement was diluted 1:10 in Veronal buffer (Boston BioProducts, MA, USA); 0.1% gelatin (Fisher Scientific Company, Fair Lawn, NJ, USA) was added to each well and incubated for 20 mins at 37ºC. The plates were spun at 2000 rpm for 3 mins and washed two times with PBS; 15mM EDTA (Invitrogen). The plate was vortexed and 50µL of anti-human C3b-FITC conjugated Ab (Cedarlane, Burlington, ON, Canada) diluted 1:50 in in PBS was added to each well and incubated for 20 mins at RT in the dark. After washing twice with PBS, the cell pellet was fixed by resuspending cells in 100µL of 2% PFA in PBS. Fluorescence was detected by flow cytometry using an LSRFortessa instrument (BD Biosciences) and analyzed using FlowJo software. The gating strategy focused on measuring the frequency and MFI of singlet, C3b+ iCEM cells. To calculate the ADCD score, the % of C3b+ iCEM was multiplied by the MFI of the parent gate and an AUC was calculated based on the two dilutions. Duplicates were averaged and the no-

Ab negative control value was subtracted. To allow for inter-plate comparisons, results were normalized to the HIV+IG positive control.

ADCP

ADCP activity was measured as the ingestion of Ab-opsonized, gp120-coated fluorescent beads by a phagocytosis-competent cell line. The assay utilized the phagocytic THP-1 monocytic cell line derived from a human monocytic leukemia patient (Tsuchiya et al., 1980). First, HIV-1 Bal recombinant gp120 protein (from the NIH AIDS Reagent Program, Division of AIDS, NIAID, NIH: HIV-1BaL gp120 from DAIDS, NIAID) was biotinylated. 100 µL of gp120, diluted to 0.5mg/mL in PBS was combined with 5µL of 9 mM biotin from the EZ-Link Sulfo-NHS-LC-Biotinylation Kit (Thermo Fisher) in DMSO for 2 hrs on ice. The gp120-biotin solution was then applied to the resin bed of an equilibrated Zebra Spin Desalting Column (Thermo Fisher) and centrifuged at 1000 x g for 2 mins. The flow-through protein solution was collected and stored at 4ºC until use. Biotinylated gp120 and fluorescent NeutrAvidin beads (Invitrogen) were mixed at a ratio of 1µg: 1µL for 2 hrs at 37ºC. The beads were washed twice with 1mL PBS; 0.1% BSA and resuspended at a dilution of 10µL of beads per 1mL PBS; 0.1% BSA.

Subject plasma and the HIV+IG positive control were diluted to 100 and 2µg IgG/mL in PBS. 10µL of the gp120-bead solution and 10 µL of diluted plasma were added to each well of a 96-well V-bottomed plate in triplicate. Plates were centrifuged at 300 x g for 1 min and incubated for 2 hs at 37ºC. After washing twice with PBS, 200µL THP-1 cells at $1.25x10^5$ cells/mL (i.e. 25,000 cells) in R10 were added to each well and incubated for 3 hrs at 37ºC. The plates were centrifuged and 100µL of supernatant was removed and replaced with the same volume of 2% PFA in PBS. Fluorescence was detected by flow cytometry using an LSRFortessa instrument (BD Biosciences) and analyzed using FlowJo software. The gating strategy involved gating on the FITC+ THP-1 monocytes, which detected cells that had phagocytosed gp120-coated beads. To calculate the ADCP score, the % of FITC+ monocytes was multiplied by the FITC+ MFI of the parent monocyte gate and an AUC was calculated based on the two dilutions. Triplicates were averaged and the no-Ab negative control value subtracted. To allow for inter-plate comparisons, results were normalized to the HIV+IG positive control present in each plate tested.

Integrated HIV DNA quantification

The quantity of integrated HIV DNA in the $CD4^+$ T cells of virally suppressed individuals on ART was quantified with a PCR-based method. The forward primer ULF1 (5'- ATG CCA CGT AAG CGA AAC TCT GGG TCT CTC TDG TTA GAC-3') and reverse primers Alu1 (5'-TCC CAG CTA CTG GGG AGG CTG AGG-3') and Alu2 (5'-GCC TCC CAA AGT GCT GGG ATT ACA G-3') bind to the integrated HIV DNA in isolated $CD4^+$ cells, which is pre-amplified in a first round of amplification, followed by a real-time nested PCR, which quantifies the number of $CD3^+$ cells and HIV copies in the sample (Vandergeeten et al., 2014). The forward primer ULF1 corresponds to the 3' LTR region of the HIV genome and the reverse Alu1 and Alu2 primers correspond to a repeat element common in the human genome, appearing approximately once per 3,000 base pairs.

First, $CD4^+$ T cells were isolated from PBMC samples from ART-treated subjects that reached undetectable viral loads (<50 copies/mL plasma). The isolation was performed using the EasySep Human $CD4^+$ T cell Isolation Kit (Stem Cell). Briefly, frozen PBMCs were thawed and resuspended in R10, counted, washed and resuspended at $5x10^7$ cells/mL in EasySep buffer. A negative selection enrichment Ab cocktail was added at a volume of 25µL/mL of sample, gently vortexed, and incubated for 5 mins at RT. The same volume (25µL/mL of sample) of RapidSpheres was added to the mix followed by incubation for 5 mins at RT. EasySep buffer was added to the mixture to bring the volume up to 5mL before transferring the cell mixture to an EasyEights magnet for 5 mins at RT. This was repeated a second time on cells remaining in suspension to increase purity. The purified cell suspension was centrifuged at 2000 rpm for 5 mins and resuspended in PBS for cell counting. Cells were resuspended at 600,000 cells/mL and frozen as 500µL pellets of 300,000 cells, then stored at -20ºC until use. Cell suspension purity was verified using flow cytometry before freezing and was considered in the final reservoir size calculation.

Isolated $CD4^+$ T cell aliquots were thawed and resuspended in 45uL of Proteinase K (PK) in PK lysis buffer (Invitrogen) and vortexed before being incubated overnight in a ThermoMixer (Eppendorf, Mississauga, ON, Canada) at 450rpm for 20 hrs at 55ºC. Samples were then placed in a Multi-Blokblock heater (American Scientific Products, OH, USA) at 95ºC for 10 mins to inactivate the Proteinase K. The samples were vortexed and placed on ice with the ACH-2 cells

required for the standard dilution. ACH-2 cells are derived from the A3.01 sub-clone of the CEM cell line and each cell harbours 1 copy of integrated HIV proviral DNA (Clouse et al., 1989). ACH-2 cells underwent the same processing as isolated $CD4^+$ T cells: they were thawed and incubated overnight in a ThermoMixer (Eppendorf) at 450rpm for 20 hrs at 55ºC then frozen as 10^7 cells in 500µL PK lysis buffer.

The pre-amplification Master Mix consisted of 0.15µL ULF1, 0.3 µL Alu1, 0.3µL Alu2, 0.3µL HCD3OUT5' (5'-ACT GAC ATG GAA CAG GGG AAG-3'), 0.3µL HCD3OUT3' (5'-CCA GCT CTG AAG TAG GGA ACA TAT-3'), 5µL Taq Buffer (Invitrogen), 1.5µL dNTP, 3µL $MgCl_2$ (Invitrogen), and 0.5µL Taq Polymerase (Invitrogen) in 23.65µL ddH_2O per well. 35µL of Master Mix was distributed to the wells of a 96-well PCR plate on ice, followed by 15µL of the digested samples, the ddH_2O cell-free negative control, and the ACH-2 standard dilution. The plate was sealed and loaded into the PCR thermal cycler (Biometra, Göttingen, Germany) where it underwent the following steps: an 8-min denaturation phase at 95°C followed by 12 cycles of amplification (1 min at 95°C, 40 s at 55°C, 1 min at 72°C), followed by a final elongation phase for 15 mins at 72°C for 15 min. The plate was stored overnight at 4ºC in the dark. The next day, two separate Master Mixes were prepared, one for measuring $CD3^+$ cells, containing 2.6µL RNase-Free water (Qiagen, Toronto, ON, Canada), 0.25µL HCD3IN5' (5'-GGC TAT CAT TCT TCT TCA AGG T-3'), 0.25µL HCD3IN3' (5'-CCT CTC TTC AGC CAT TTA AGT A-3'), 0.5µL CD3 FamZen probe, 10µL Rotor-Gene Probe Master Mix (Qiagen) and 0.2µL Taq Polymerase (Invitrogen) per well, and another Master Mix for measuring copies of integrated HIV DNA, containing 2.6µL RNase-Free water (Qiagen), 0.25µL LambdaT, 0.25µL UR2, 0.5µL UHIV FamZen probe, 10µL Rotor-Gene Probe Master Mix (Qiagen) and 0.2µL Taq Polymerase (Invitrogen). The previous day's PCR products were gently centrifuged for 15 s at 2000 rpm and diluted in a new PCR plate with 20µL of PCR products in 180µL of sterile water (Wisent). The required number of 4-strip PCR tubes (Axygen, Union City, CA) were filled with 13.6µL of the HIV Master Mix followed by 6.4µL of the mixed, diluted PCR products. The tubes were capped then loaded into the Rotor-Gene Q instrument (Qiagen) where they underwent the following steps: a 4 min denaturation phase at 95°C followed by 40 cycles of amplification (3 s at 95°C, 10 s at 60°C) to measure the number of HIV copies in each sample. A new set of PCR tubes were filled with 13.6µL of the CD3 Master Mix followed by 6.4µL of the diluted PCR products. The tubes

were loaded into the Rotor-Gene Q instrument and completed the same cycle as for the HIV copy quantification. The number of copies of integrated HIV DNA per 10_6 $CD4_+$ T cells was determined for each sample with the formula:

$$Copies\ HIV\ DNA/10^6 cells\ = \left(\frac{average\ \#\ HIV\ copies}{average\ \#\ CD3\ copies \times CD4\ isolation\ purity}\right) \times 10^6.$$

Data analysis

For comparisons between the early and late treatment groups, a Mann Whitney U test was used to test for significant differences in Ab concentrations or functionality scores between the two groups. A non-parametric test was used as the values within each group were not normally distributed. P values <0.05 were considered statistically significant.

Two parameters were used to compare differences in Ab concentration and functionality score at treatment initiation: Ab concentration at the first treated time point (TP) and y-intercept derived from a best-fit line of a subjects' treated data points. The first treated TP represents the closest approximation of Ab concentration at treatment initiation as data from plasma collected on day 0 or shortly after is included in this analysis. The median number of days post-treatment of the first treated TP is 10 days for the early treatment group and 11 days for the late treatment group. A line of best fit also offers an approximation of Ab concentration at day 0 as it is fitted to a subjects' longitudinal treated TPs. Together, these two parameters offer a way to compare Ab concentrations at day 0 for each subjects.

Chapter 4: Results

Env-specific antibody concentrations increase in early untreated infection

Ab concentrations in subject plasma were measured using coated plate-based assays to quantify total IgG and anti-gp120 Abs. A cell-based assay was used to measure anti-Env Abs. Plasma collected from a single TP for untreated subjects was used to perform cross-sectional analyses of Ab concentration post-infection. The concentration of total IgG increased significantly over time ($p = 0.003$, linear regression) (figure 1a). The increasing IgG level could suggest hypergammaglobulinemia, though the average IgG concentration remained within the normal adult range of 7.5 – 16.0 mg/mL (Sherwood, 2016). Similarly, the concentration of anti-gp120 Abs and anti-Env Abs increased significantly over time in the absence of treatment ($p = 0.0009$ and $p = 0.043$, respectively, linear regression) (figure 1b-c). The quantities of the latter two measures are reported in arbitrary units as the concentration of anti-gp120 and anti-Env Abs in HIV+IG is unknown and all results are reported after normalization to this within-96-well plate control. Therefore, an exact concentration or quantity of anti-gp120 and anti-Env Abs in plasma cannot be determined. Only results within the linear range of HIV+IG positive control standard curve were included. Some samples had undetectable Ab levels or concentrations below the HIV+IG positive control linear range so were not included in the analysis.

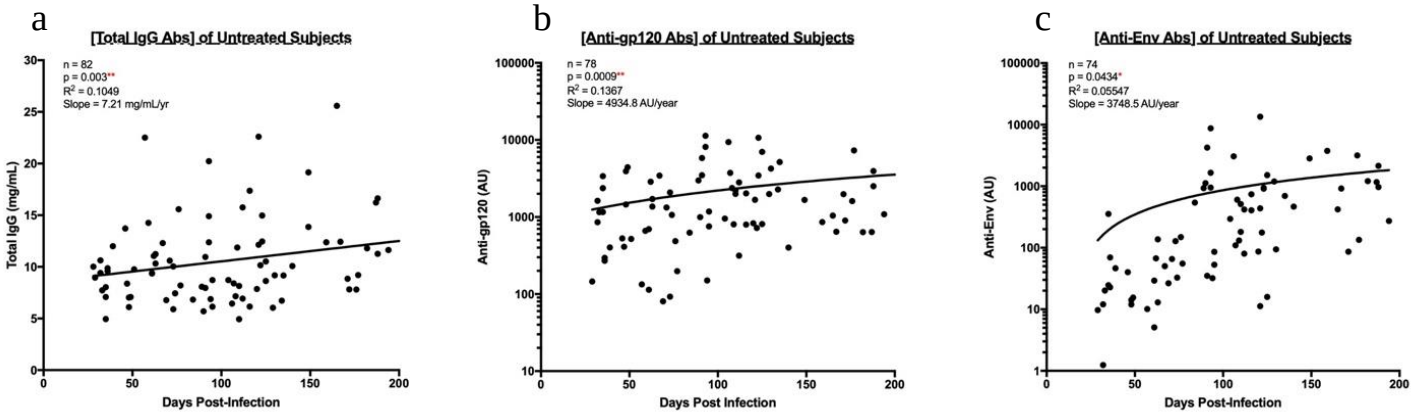

Figure 1: Total IgG, anti-gp120 and anti-Env-specific Ab concentrations increase significantly with days post-infection (DPI) in treatment naïve subjects. The y-axis shows the concentration of Total IgG (a, linear scale), anti-gp120 Abs and anti-Env Abs (b, c log10 scale) The x-axis shows DPI. 1a: Total IgG concentration increases over time with a slope of 7.21 mg/mL/year ($p = 0.003$). 1b: Anti-gp120 Ab concentration increases with a slope of 4934.8 AU/year ($p = 0.0009$). 1c: Anti-Env Ab concentration increases with a slope of 3748.5 AU/year ($p = 0.0434$). AU = Arbitrary Units.

HIV-specific Ab concentrations decline more rapidly when ART is initiated after, compared to before, 90 DPI

Treated subjects were divided into two groups based on whether they initiated treatment less than 90 DPI, called "early treatment" (n = 19) or greater than 90 DPI, called "late treatment" (n = 23). The full list of subjects with the number of DPI at which they started ART is presented in figure 2, colours remain constant across results. The median DPI that treatment was initiated was 60.5 days in the early treatment group with a range of 16 - 87 DPI. The median treatment initiation for the late treatment group was 124.5 days with a range of 93 – 193 DPI. Ab concentrations in plasma were measured at several TPs post-treatment allowing for the collection of longitudinal data. For Total IgG, there was an overall decline in Ab concentration over time in both the early and late treatment groups. The median (inter-quartile range [IQR]) annual slope of decline for all treated subjects was -1.40 (-3.97, -0.61) mg/mL/year. For some subjects this decline started immediately after treatment initiation whereas for others Ab concentration continued increasing until the second visit post-treatment and then proceeded to decline. The median annual slopes of decline were -2.22 (-4.20, -0.75) mg/mL/year and -1.26 (-2.89, -0.47) mg/mL/year for the early and late treatment groups, respectively (figure 3a,b). The concentration of Total IgG declined more steeply in the early than in the late treatment group though this difference was not statistically significant as assessed by a Mann-Whitney U-test comparing the slopes in the treatment groups (Z = 1.16, p = 0.246). Mann-Whitney U-tests were used for all comparisons in this section as the data for treated subjects was not normally distributed. Anti-gp120 Ab concentration also declined over time for both the early and late treated subjects. The median annual slope of decline for all treated subjects was -308.46 (-1116.17, -0.94) AU/year. Anti-gp120 Ab concentration declined more steeply over time in the late treatment group compared to the early treatment group (annual slopes of decline were -70.18 (-426.13, 129.72) and -614.84 (-2946.00, -

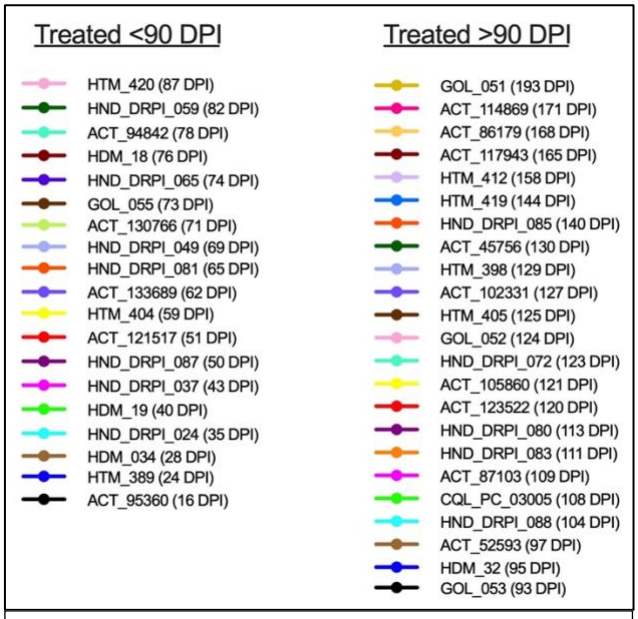

Figure 2: The complete list of subjects included in the longitudinal analyses of treated subjects. To the left of the subject identifier is the number of DPI they initiated treatment in brackets. For subjects treated <90 DPI, n = 19 and for subjects treated >90 DPI, n = 23.

181.68) AU/year in the early versus late treatment groups, respectively (Z = -2.70, p = 0.007, Mann-Whitney test), figure 3c,d). Likewise, the median annual slope of decline in anti-Env Ab concentration for all treated subjects was -53.80 (-369.01, -2.88) AU/year. The concentration of anti-Env Abs also experienced a significantly steeper annual slope of decline in the late treatment group compared to the early group of -4.84 (-63.21, 2.08) and -124.06 (-1033.68, -17.79) AU/year, respectively (Z = -2.49, p = 0.012), Mann-Whitney test, figure 3e,f). The difference between the early and late treatment groups in terms of Ab decline over time was less pronounced for anti-Env Ab concentrations than for anti-gp120 Ab concentrations.

Subjects in the late, compared to early, treatment groups have a higher concentration of Env-specific Abs at treatment initiation

We hypothesized that the differences in slopes of decline between the early and late treatment groups could be explained by higher Ab concentrations at treatment initiation (day 0 post-treatment) in the late treatment group. Not all subjects had plasma collected on the day treatment was initiated so it was impossible to compare Ab concentrations strictly at initiation. Two different parameters were thus used to achieve this comparison: Ab concentration at the first treated TP and y-intercept derived from a best-fit line of a subjects' treated data points, both described in the methods section. Total IgG concentration was not significantly different at treatment initiation between the early and late treatment groups when either method was used to assign an Ab concentration at treatment initiation. The median (IQR) Ab concentrations measured at the first treated TPs were 10.59 (8.09, 13.11) and 8.72 (7.05, 12.30) mg/mL (Z = -1.238, p = 0.215, Mann-Whitney) while the y-intercepts were 10.49 (8.00, 12.25) and 9.51 (7.87, 11.74) mg/mL (Z = -0.909, p = 0.363, Mann-Whitney) for the early and late treatment groups, respectively. Similarly, there were no significant differences in anti-gp120 Ab concentration at treatment initiation between the early and late treatment groups. The Ab concentrations measured at the first treated TPs were 967.56 (489.92, 3353.88) and 1949.31 (915.05, 5109.61) AU (Z = 1.477, p = 0.139, Mann-Whitney) while y-intercepts were 935.30 (656.45, 2672,50) and 2002.00 (900.82, 4650.50) AU (Z = 1.398, p = 0.161, Mann-Whitney) for the early and late treatment groups, respectively. Significant differences were found for both comparisons when comparing the early and late treatment groups for anti-Env Ab concentrations. At the first treated TP, the AU values were 66.46 (16.89, 200.69) AU and 342.28 (86.84, 1517.26) (Z = 2.744, p = 0.006, Mann-Whitney) for the

early and late treatment groups, respectively. The AU y-intercepts for the early and late treatment groups were 65.28 (17.84, 319.87) and 450.90 (84.24, 1210.00), respectively (Z = 2.376, p = 0.017, Mann-Whitney).

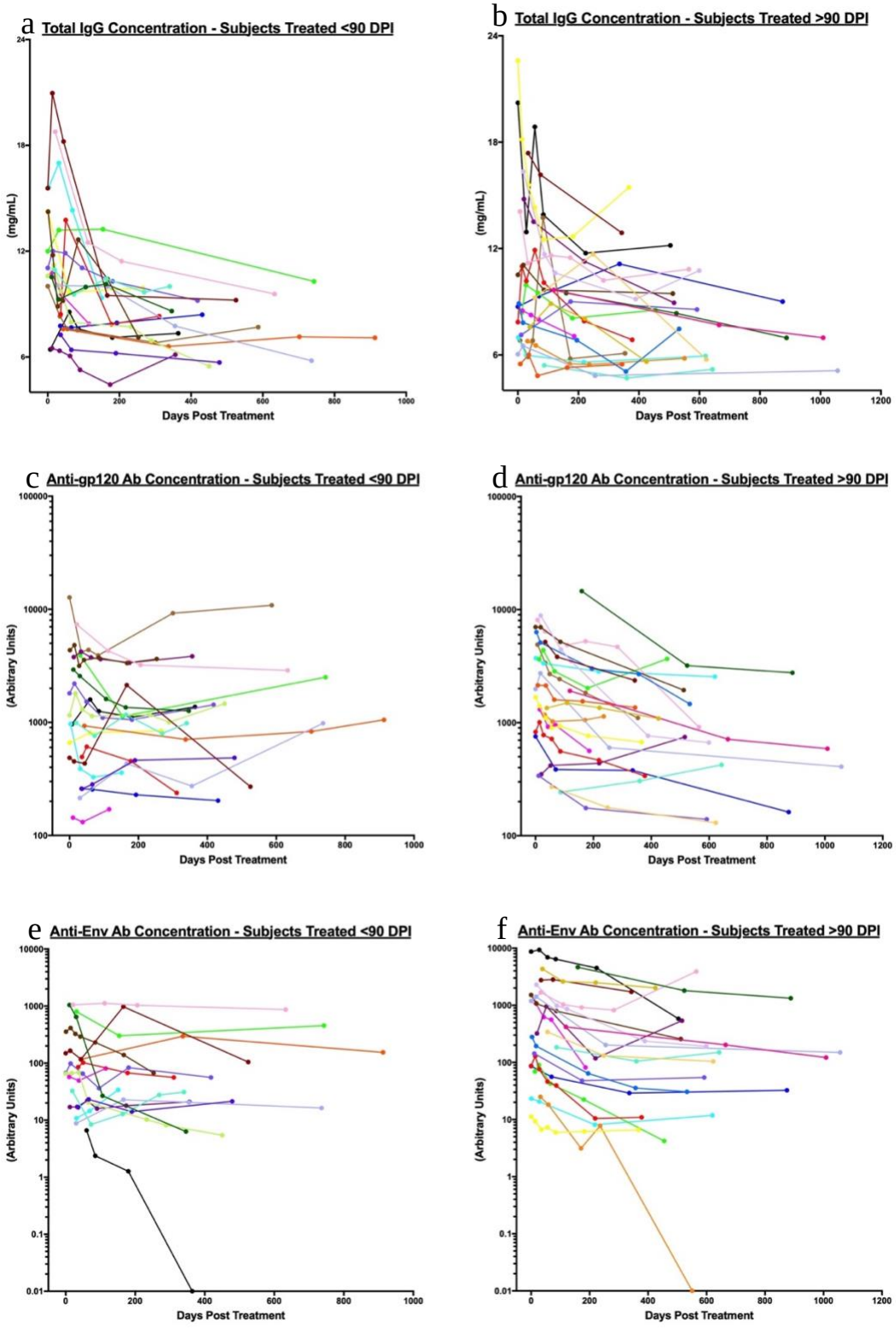

Figure 3: Ab concentrations in subjects followed longitudinally post-treatment. Graphed are longitudinal changes in Total IgG, anti-gp120 and anti-Env Ab concentrations for subjects initiating treatment <90 DPI (a, c, e) and > 90 DPI (b, d, f). The y-axis shows the concentration of Total IgG in mg/mL using a linear scale (a, b) and the concentration of anti-gp120 (c, d) and anti-Env (e, f) Abs in $\log_{10}$ arbitrary units (AU) relative to HIV+IG. Graph (e,f): Anti-Env values of 0 were assigned the value 0.01 to appear on the graph. The x-axis shows days post treatment initiation.

There is an evolving ratio of anti-gp120: anti-Env Abs with a consistently higher concentration of anti-gp120 Abs

We observed a higher concentration of Abs binding to monomeric gp120 in the coated plate-based assay than Abs binding to siCEM in the cell-based assay. For this analysis, all treated TPs available were included (1-6 TPs per subject) whereas figure 3 only included subjects where there was a minimum of three TPs per subject to allow for a truly longitudinal analysis. When all treated and untreated subject TPs were considered there was a 46.1x higher concentration of Abs binding to monomeric gp120 than to the siCEM cells. When subject TPs were divided into untreated and treated groups, the anti-gp120: anti-Env Ab concentration ratios were 40.6 and 48.5, respectively for the untreated and treated groups (figure 4a,b). In the untreated group there was an increase in the ratio of anti-gp120: anti-Env Abs over DPI. The slope of change of anti-gp120 Ab concentration was 4934.8 AU/ year whereas the slope of change of anti-Env Ab concentration was 3602.5 AU/ year, thus a widening gap between the concentrations (figure 4a). The opposite trend was observed in the treated subjects, where the ratio of anti-gp120: anti-Env Ab concentration decreased over time when all treated TPs were considered. The slope of change of anti-gp120 Ab concentration was -295.7 AU/ year whereas the slope of change of anti-Env Ab concentration was -22.2 AU/ year, thus demonstrating a convergence (figure 4b). Similarly, in both the early and late treatment groups there was a convergence in anti-gp120 and anti-Env Ab concentrations over time. For the early treatment group the slope of change of anti-gp120 Ab concentration was -80.9 AU/ year whereas the slope of change of anti-Env Ab concentration was positive at 383.9 AU/ year (figure 4c). For the late treatment group the slope of change of anti-gp120 Ab concentration was -632.9 AU/ year whereas the slope of change of anti-Env Ab concentration was -98.9 AU/ year (figure 4d). The ratio of anti-gp120 : anti-Env Ab concentration was 49.7 for subjects treated <90 DPI and 47.6 for subjects treated >90 DPI.

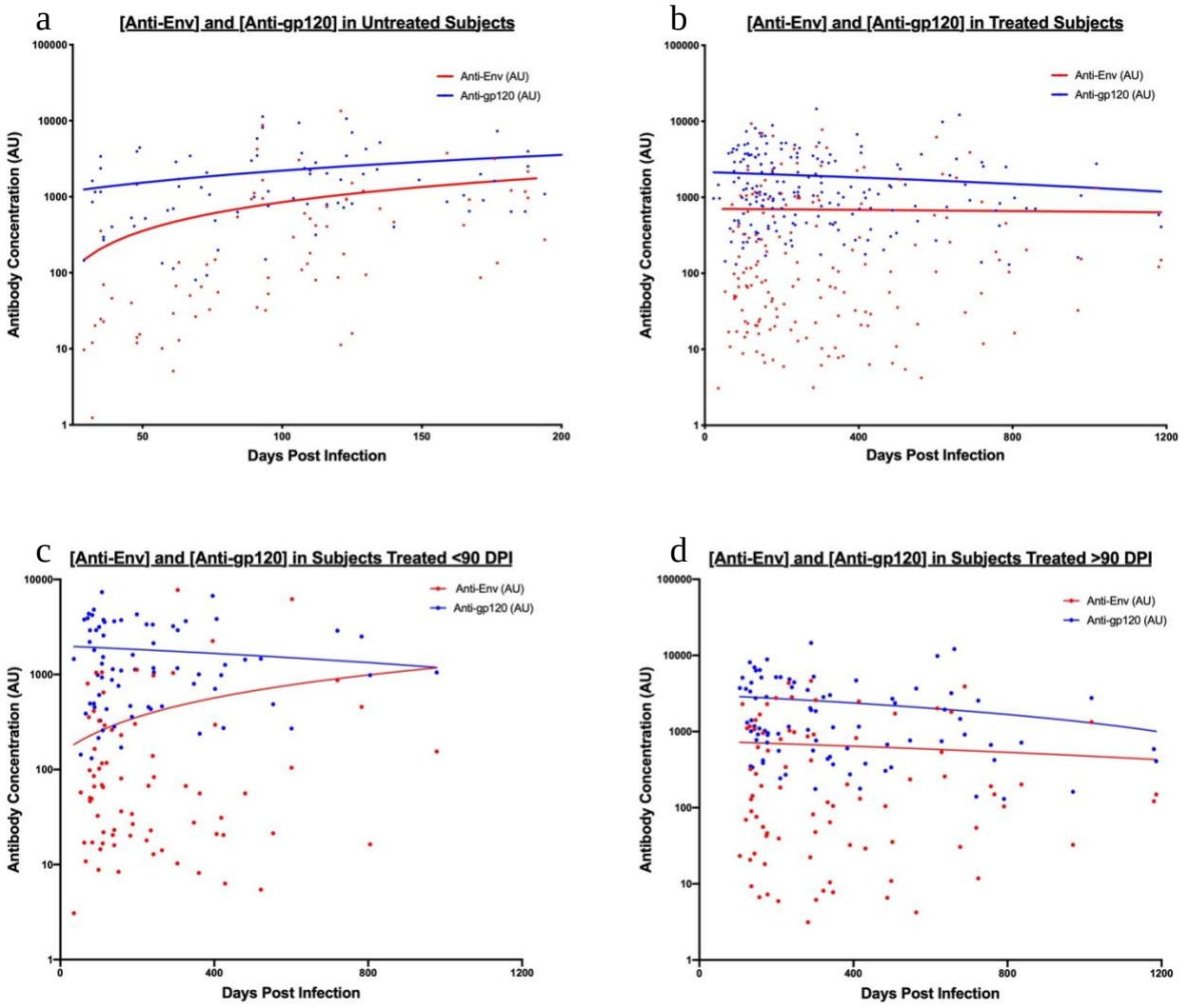

Figure 4: Anti-gp120 (blue) and anti-Env (red) Ab concentrations in subject plasma. The y-axis shows the concentration of Abs in $\log_{10}$ arbitrary units (AU) for untreated (a) and treated subjects (b), and subjects treated <90 DPI (c) and >90 DPI (d). The x-axis shows DPI the sample was collected. The lines of best fit were calculated based on all of the anti-gp120 or anti-Env Ab concentration data points included in each graph.

FcDFs increase in early untreated infection

FcDFs were measured with assays utilizing siCEM for ADCC, ADCT and ADCD and gp120-coated beads to measure ADCP. Plasma collected from a single TP for untreated subjects was used to perform cross-sectional analyses of these FcDFs post-infection. The four functions were given as a score based on the AUC of values produced in the individual assays, represented on the y-axes in figure 5. The slope of change in ADCC and ADCP activity was positive and was significantly different from "0" for the group as a whole ($p = 0.031$ and $p = 0.007$, respectively,

linear regression, figure5a,c). ADCT and ADCD activity also increased at the group level though these slopes did not significantly differ from "0" for the group as a whole ($p = 0.153$ and $p = 0.522$, respectively, linear regression, figure 5b,d). All results were reported relative to the within-96-well plate HIV+IG control standard curve.

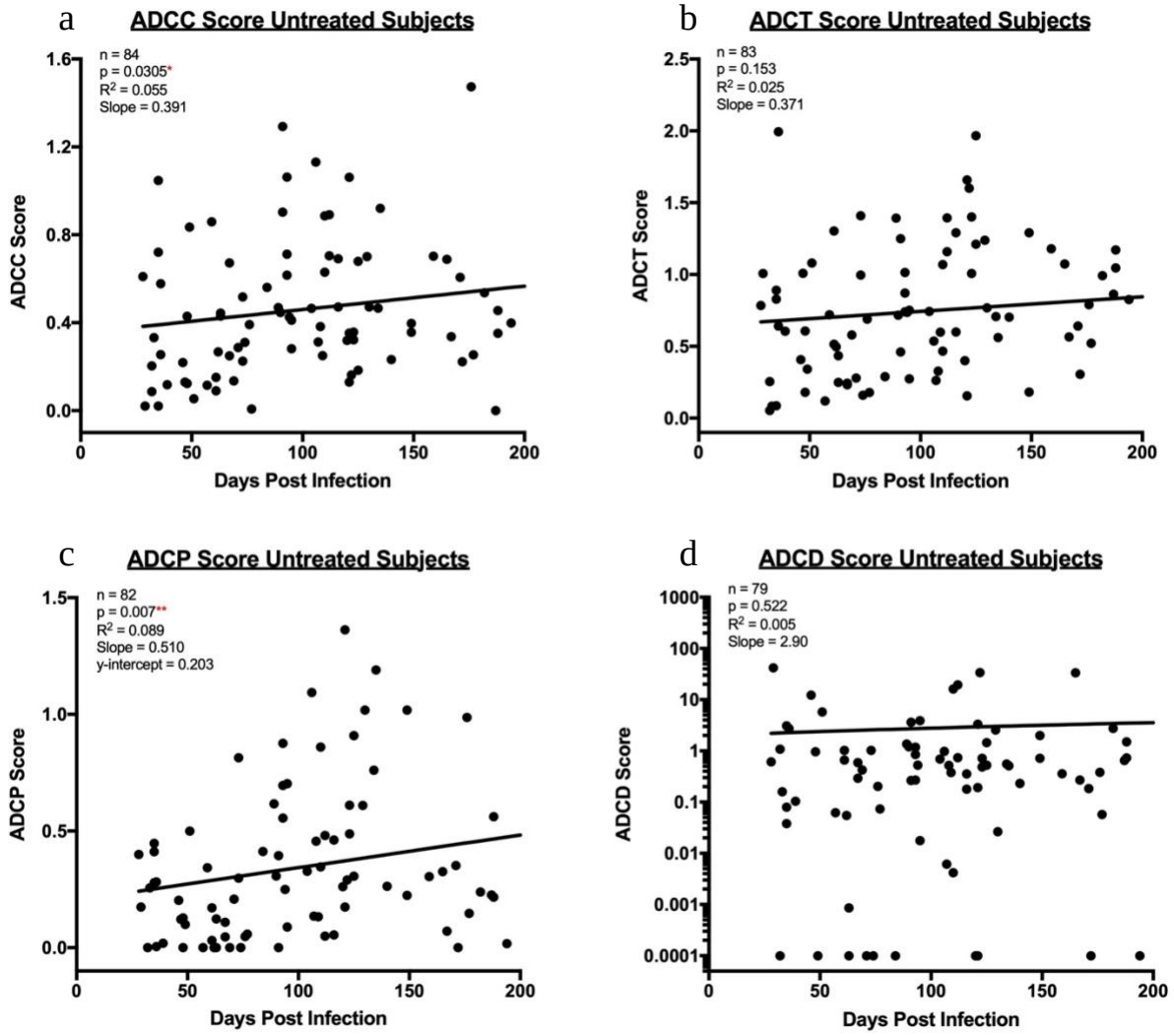

Figure 5: ADCC and ADCP activity increases significantly with days post-infection (DPI) in treatment naïve subjects. ADCT and ADCD activity increases non-significantly. The y-axis shows the scale of functional scores assigned to each assay. ADCC, ADCT, and ADCP Score (a, b,c, linear scale), ADCD Score (d, log10 scale, 0 values were given a value of 0.0001 for graphical representation). The x-axis shows DPI.

There were no significant differences in FcDF decline between early and late treatment groups

Four FcDFs, ADCC, ADCT, ADCP, and ADCD, were measured at several TPs post-treatment allowing for the collection of longitudinal data. For all four functions there was a decline in activity over time post-treatment in both the early and late treatment groups. Similar to the results for Ab concentrations, for the ADCT and ADCP assays there was a steeper slope of decline in the late treatment group compared to the early treatment group. None of these differences reached statistical significance. ADCC and ADCD activity declined more steeply in the early than in the late treatment group though these results were non-significant. The scores for each assay were calculated as an area under the curve (AUC) based on the dilutions used in that assay. The annual slopes of ADCT score decline were -0.12 (-0.28, 0.01) and -0.15 (-0.29, -0.04) for the early and late treatment groups, respectively ($Z = -0.505$, $p = 0.610$, Mann-Whitney, figure 6c,d). The annual slopes of ADCP score decline were -0.06 (-0.11, 0.07) and -0.12 (-0.24, -0.005) for the early and late treatment groups, respectively. The slope of decline for the late treatment group was visibly steeper than that of the early treatment group though this difference only trended towards statistical significance ($Z = -1.748$, $p = 0.08$, Mann-Whitney, figure 6e,f). The annual slopes of ADCC score decline were -0.06 (-0.20, 0.07) and -0.03 (-0.16, 0.02) for the early and late treatment groups, respectively ($Z = -0.025$, $p = 0.976$, Mann-Whitney, figure 6a,b). The annual slopes of ADCD score decline were -0.06 (-0.25, 0.009) and -0.21 (-0.46, 0.02) for the early and late treatment groups, respectively ($Z = -0.420$, $p = 0.674$, Mann-Whitney, figure 6g,h).

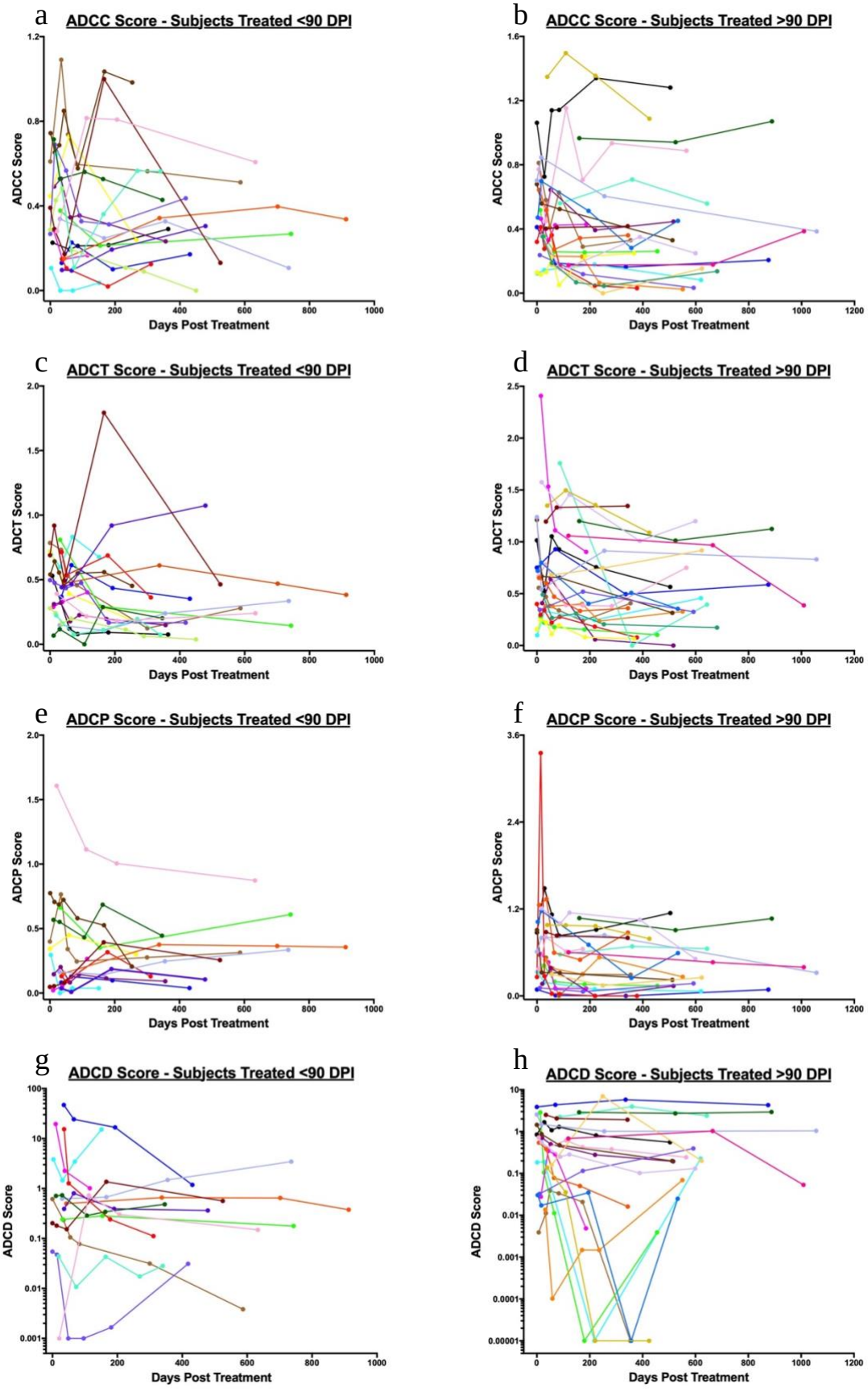
a
ADCC Score - Subjects Treated <90 DPI
ADCC Score
Days Post Treatment
b
ADCC Score - Subjects Treated >90 DPI
ADCC Score
Days Post Treatment
c
ADCT Score - Subjects Treated <90 DPI
ADCT Score
Days Post Treatment
d
ADCT Score - Subjects Treated >90 DPI
ADCT Score
Days Post Treatment
e
ADCP Score - Subjects Treated <90 DPI
ADCP Score
Days Post Treatment
f
ADCP Score - Subjects Treated >90 DPI
ADCP Score
Days Post Treatment
g
ADCD Score - Subjects Treated <90 DPI
ADCD Score
Days Post Treatment
h
ADCD Score - Subjects Treated >90 DPI
ADCD Score
Days Post Treatment

Figure 6: Ab functional scores in subjects followed longitudinally post-treatment. Graphed are longitudinal changes in ADCC, ADCT, ADCP, and ADCD for subjects initiating treatment <90 days (a, c, e, g) and > 90 days from infection (b, d, f, h). The y-axis shows the functional score of ADCC, ADCT, and ADCP using a linear scale relative to HIV+IG (a, b, c, d, e, f) and functional score of ADCD in $\log_{10}$ scale relative to HIV+IG (g,h). ADCD values of 0 were assigned the value 0.00001 for graphical representation. The x-axis shows days post treatment initiation.

Subjects in the late, compared to early, treatment groups have higher ADCT and ADCP activity at treatment initiation

We hypothesized that the differences in slopes of decline between the early and late treatment groups could be explained by higher functional scores at treatment initiation. Functional score at the first treated TP and y-intercept derived from a best-fit line of a subjects' treated data points were used to compare the early and late treatment groups. ADCC score was not significantly different at treatment initiation between the early and late treatment groups when either method was used to assign an Ab concentration at treatment initiation. The ADCC scores measured at the first treated TPs were 0.28 (0.19, 0.52) and 0.46 (0.31, 0.69) (Z = 1.819, p = 0.069, Mann-Whitney) while the y-intercept scores were 0.36 (0.20, 0.53) and 0.41 (0.26, 0.61) (Z = 1.086, p = 0.276, Mann-Whitney) for the early and late treatment groups, respectively. Similarly, there were no significant differences in ADCD score at treatment initiation between the early and late treatment groups. At the first treated TP, the values were 0.56 (0.21, 3.04) and 0.68 (0.14, 2.25) (Z = -0.319, p = 0.749, Mann-Whitney) for the early and late treatment groups, respectively. The y-intercept scores for the early and late treatment groups were 0.43 (0.27, 0.60) and 0.60 (0.14, 1,81), respectively (Z = 0.008, p = 0.936, Mann-Whitney). Significant differences were found in both comparisons when comparing the early and late treatment groups for ADCT score. The ADCT scores measured at the first treated TPs were 0.47 (0.30, 0.69) and 0.72 (0.40, 1.20) (Z = 2.350, p = 0.019, Mann-Whitney) while the y-intercept scores were 0.48 (0.28, 0.63) and 0.72 (0.43, 1.19) (Z = 2.425, p = 0.015, Mann-Whitney) for the early and late treatment groups, respectively. In both cases, the median values were higher at treatment initiation for the late treatment group. The same trend was observed when comparing the early and late treatment groups for ADCP score. The ADCP scores measured at the first treated TPs were 0.16 (0.11, 0.48) and 0.57 (0.34, 0.90) (Z = 2.459, p = 0.014, Mann-Whitney) while the y-intercept scores were 0.16 (0.13, 0.48) and 0.57 (0.35, 1.00) (Z = 2.521, p = 0.011, Mann-Whitney) for the early and late treatment groups, respectively.

Antibody-dependent functions and IgG concentration more strongly correlated with anti-Env Ab concentration than anti-gp120 Ab concentration

We examined how the results of the functional assays were correlated with each other and with the concentration of Total IgG, anti-gp120 and anti-Env Abs. A correlation coefficient (r) and p-value was calculated for each of the pairings (figure 7). The table demonstrates that the functional assays were significantly correlated with one another ($p < 0.0001$ for all pairings except ADCD).

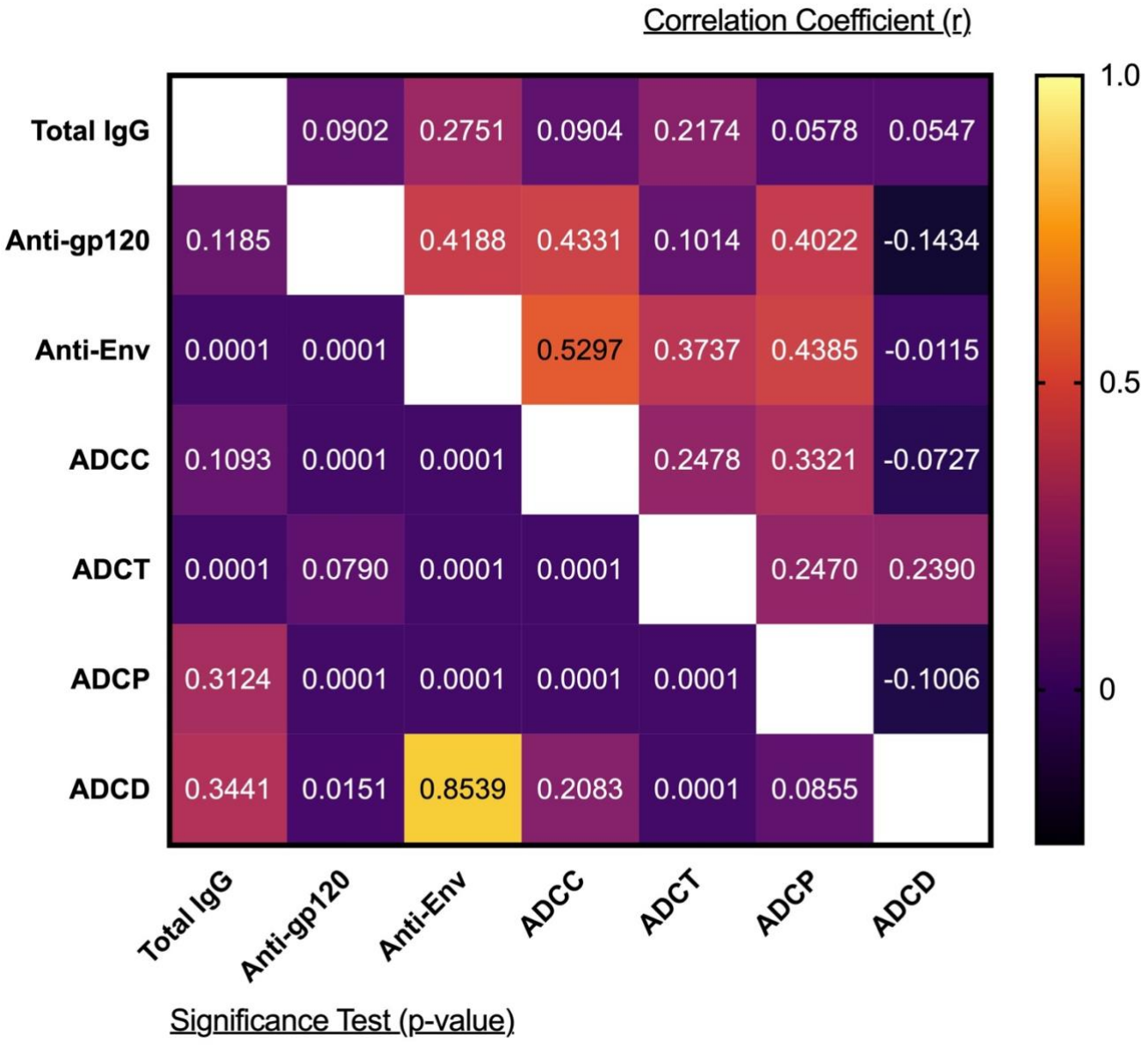

Figure 7: Correlations between the results of the experiments used to evaluate the antibody response in subject plasma. The functional assays correlated well with each other except for ADCD. Anti-Env Ab concentration correlated most strongly with all other assays compared to any other experiment. ADCP and anti-gp120 Ab concentration also correlated significantly with most assays.

The strongest correlation was between the ADCC and ADCP assays (r = 0.3321) whereas the strength of the correlation between the ADCC and ADCT assays compared to the ADCT and ADCP assays was similar (r = 0.2478 and r = 0.2470). Anti-Env Ab concentration correlated with both total IgG and anti-gp120 Ab concentration ($p < 0.0001$ in both cases). Total IgG and anti-gp120 Ab concentrations were not significantly correlated (p = 0.1185). The functional assays correlated more strongly with anti-Env than anti-gp120 Abs, as demonstrated by their correlation coefficients. This result is unsurprising given that the target cells used in these FcDF assays was siCEM cells. Abs capable of binding siCEM exposing Env in a closed conformation are necessary to direct the FcDFs being measured.

Integrated HIV DNA Reservoir Quantification Inconclusive

After learning and optimizing the protocol for the integrated HIV DNA quantification assay, a total of 19 subjects' PBMCs were tested. Subjects tested first were selected because they had notably high or low humoral immune responses in terms of higher anti-HIV Env Ab concentrations and FcDF scores for ADCC, ADCT, and ADCP. Some concerns emerged concerning the reliability of the ADCD assay, considered in the Discussion section below, so these results were not considered in the selection. These samples were chosen first to see if there was a significant difference in reservoir size, the number of copies of integrated HIV DNA per million $CD4_+$ T cells, between subjects considered to have a notably high (n = 12) or low (n = 7) humoral immune response. With these first 19 subjects, no significant difference in reservoir size was observed between the high and low humoral immune response groups (p = 0.8208, Mann-Whitney, figure 8a). The median (IQR) reservoir sizes were 133 (92, 652) and 171 (90, 784) copies/ million $CD4_+$ T cells, respectively for the high and low humoral immune response groups. The 19 subjects were also divided into two groups based on whether they initiated treatment less than 90 DPI (n = 7) or greater than 90 DPI (n = 12). There was a slightly larger reservoir size in the earlier treated group compared to the later group that did not reach significance (p = 0.5492, Mann-Whitney, figure 8b). The median (IQR) reservoir sizes were 161 (117, 1405) and 120 (87, 784) copies/ million $CD4_+$ T cells, respectively for the early and late treatment groups. PBMC samples previously set aside to increase the sample size of this experiment were prepared for the assay, beginning with thawing and $CD4_+$ T cell isolation. Unfortunately, the cells had very poor viability when thawed (<5%), which led to problems with

the CD4+ T cell isolation. The assay requires a minimum 300,000 isolated CD4+ T cells but due to the poor viability this was not achieved. As a result, I could not continue with the experiment and was left with the sample size of n = 19. If more PBMC samples were acquired in the future, the reservoir quantification experiment could continue in another project.

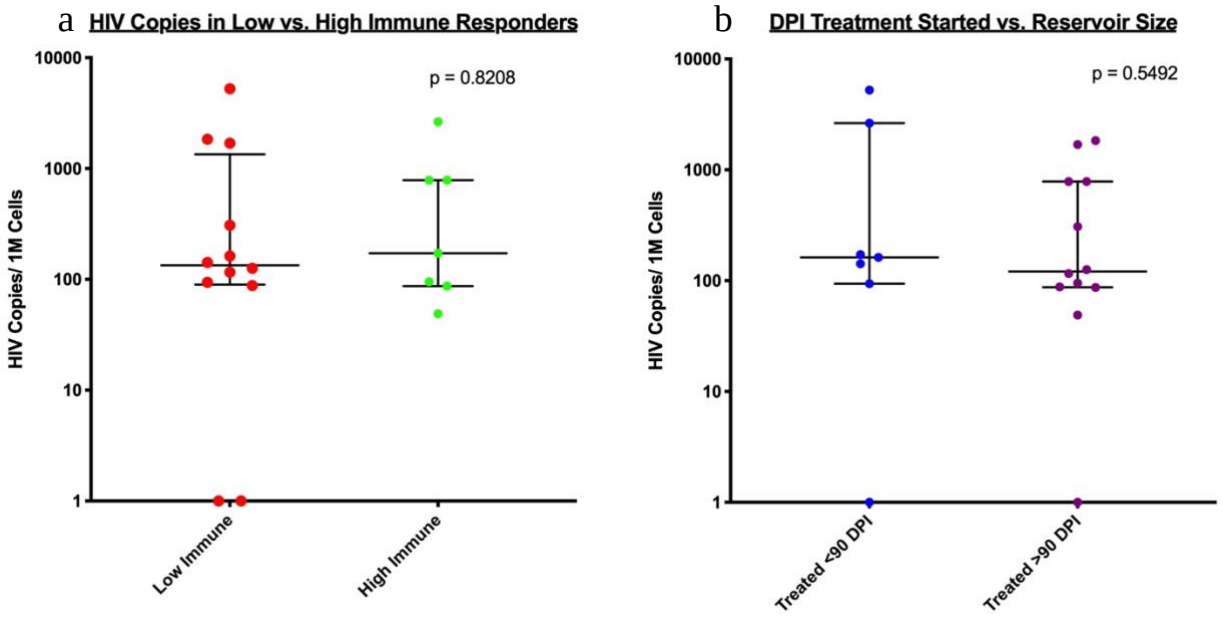

Figure 8: Bar plots representing the integrated HIV DNA reservoir. The y-axis denotes HIV copies/ 1 million CD4+ T cells in both graphs. 1 copy has been added to all values so that subject data points of "0" copies detected could be included on the $\log_{10}$ scale. On the x-axis groups are separated into low and high humoral immune response groups (a) and subjects treated less than vs. greater than 90 DPI (b).

Chapter 5: Discussion

In this study we investigated the relationship between ART initiation in early HIV infection and quantitative and functional anti-HIV Env Ab responses. In untreated HIV positive subjects we observed an increase in total IgG as well as anti-gp120 and anti-Env Ab concentrations post-infection in a cross-sectional analysis. ADCC and ADCP activity increased with a slope that was significantly greater than "0" post-infection in untreated subjects whereas ADCT and ADCD activity also increased with time, though with a slope that did not differ significantly from "0". Anti-gp120 Abs were present at concentrations 46.1x higher than that of anti-Env Abs in subject plasma. Untreated subjects had a lower ratio of anti-gp120: anti-Env Ab concentration than treated subjects and within treated subjects, those treated <90 DPI had a higher anti-gp120: anti-Env Ab concentration ratio than those treated >90 DPI. Treated subjects donating plasma collected at multiple DPI TPs were analysed longitudinally after treatment initiation. Post-treatment, an overall decrease in Ab concentration was observed for total IgG, anti-gp120 Abs and anti-Env Abs. Anti-gp120 as well as anti-Env Ab concentration experienced a significantly steeper slope of decline in subjects treated more than, compared to less than, 90 DPI. No difference was observed between early and late treatment groups for total IgG concentration slope of decline. ADCC, ADCT, ADCP and ADCD activity declined in both the early and late treatment groups with no significant differences between the two groups for any FcDFs. Ab concentration at treatment initiation was also compared and there was no significant difference in total IgG or anti-gp120 Ab concentration between the early and late treatment groups at initiation. In contrast, there was a higher concentration of anti-Env Abs at treatment initiation in the late treatment group compared to the early treatment group. No significant difference in ADCD activity was observed between the early and late treatment groups at treatment initiation. The same was observed for ADCC though ADCC activity at the first treated TP showed a non-significant trend towards being higher in the late than in the early treatment group ($p = 0.068$). ADCT and ADCP activity were significantly higher in the late treatment group at treatment initiation compared to the early treatment group. A correlation analysis demonstrated that the FcDFs correlated significantly with each other except for ADCD. The analysis also showed that the FcDFs were more significantly correlated with anti-Env Ab concentration than anti-gp120 Ab concentration. Unfortunately, I was unable to reach the sample size desired for the integrated HIV DNA reservoir quantification due to low viability of the PBMCs

and no significant conclusions were reached on whether FcDFs modulated HIV DNA reservoir size.

In the face of increasing resistance to ART medications and the protection offered by humoral factors developed in vaccine trials, it is important to consider the interaction between ART initiation and antibody responses in vivo. In situations of ART failure or scheduled treatment interruption, a well-developed humoral response may offer some HIV control. Such control was observed in a study of ART treatment interruption in a group of 14 subjects that had initiated ART during acute infection (Sáez-Cirión et al., 2013). Of these 14 subjects, five initiated ART during Fiebig stages I-IV (10-30 DPI) while the other nine subjects initiated therapy during Fiebig stage V (30- 100 DPI). Subjects were treated with ART for a median of 36.5 (range 12 – 92) months before treatment interruption. The 14 subjects studied, called post-treatment controllers, maintained undetectable viral loads for up to thirteen years post-treatment interruption. The controllers had very low HIV reservoirs and lower CD8+ T cell activation than viremic and treated subjects. Ab-dependent responses were not measured or considered in this study so the role of anti-HIV Env nnAbs and FcDFs in the control observed is unknown. As several studies have pointed to a role for anti-Env Abs and FcDFs in infection control, it would be interesting to know how these responses evolved in the cohort. Additionally, nnAbs with FcDFs usually precede the production of bnAbs, a key goal of several modern vaccine trials and therapies (Richardson et al., 2018). Nonetheless, this study provides evidence that the body's immune system is capable of controlling infection post-treatment interruption, though the cause of this control is not well understood. There is thus incentive to better understand the interaction between the timing of ART initiation and a multi-faceted humoral response.

The only successful vaccine trial to date, the RV144 trial conducted in Thailand, correlated protection from infection with IgG Abs targeting gp120 as well as ADCC activity in the presence of low IgA levels to competing specificities (Karasavvas et al., 2012; Haynes et al., 2012, Tomaras et al., 2013). The immune correlates analysis of the RV144 trial used gp120-coated cells to measure ADCC activity (Haynes et al., 2012). This means that they measured vaccine induced Abs to a component of Env that was monomeric. Monoclonal Abs made from the vaccinees enrolled in the RV144 trial recognized CD4i epitopes in the HIV Env cluster A region that are normally hidden in native trimeric closed conformation Env (Bonsignori et al., 2012). As

mentioned before, these Abs bind preferentially to healthy uninfected bystander that have taken up gp120 shed from infected cells rather than HIV infected cells (Richard et al., 2018; Dupuy et al., 2019). This raises the question as to why these Abs were associated with protection in the RV144 vaccine trial. As it turns out, the efficaciousness seen in this trial was exceptional and likely due to the strain of HIV present in Thailand. The CRF01_AE circulating recombinant form predominates in Thailand. It is a recombinant between Clade A and E viruses with a unique mutation in gp120 at position 375 of its amino acid sequence (Zoubchenok et al., 2017). The location typically occupied by a Serine is filled by a Histidine residue in the CRF01_AE strain, causing a conformational discrepancy that partially opens the Env conformation, exposing CD4i epitopes at the surface of infected cells and virions and renders the virus more easily recognized by the nnAbs induced by the RV144 vaccine (Xiang et al., 2002; Richard et al., 2017). Supporting the idea that the RV144 trial's success was due to the HIV strain present in Thailand are the results of the HVTN 702 trial in South Africa, which used the original clade B/E vaccine with a clade C adapted formula (Gray et al., 2019; Bekker et al., 2018; NIAID, 2016). In this phase 3 placebo-controlled clinical trial, which enrolled 5,400 participants, interim analyses found that the vaccine offered no significant protection against infection, with equal numbers of vaccine and placebo recipients becoming infected (NIAID, 2020). This is despite both the RV144 vaccine regimen and the clade C version of the vaccine regimen used in the HVTN 702 trial inducing even stronger anti-gp120 Abs and ADCC-competent Abs in this South African than in the Thai populations (Grey et al., 2019). Again, the immune correlates analysis of ADCC activity on samples from HVTN 702 vaccine recipients used gp120 coated cells as ADCC target cells and therefore probed for plasma Abs to CD4i epitopes rather than to closed conformation Env on genuinely HIV infected cells (Gray et al., 2019). The lack of efficacy for HIV protection in the HVTN trial led to the trial being stopped in February 2020. The lack of generalizability of the RV144 results highlights the need for caution when interpreting responses to HIV due to target and virus strain-specific differences that can cause unwarranted optimism.

In this study we observed an increase in both of the RV144 correlates of protection, anti-gp120 Ab concentration and ADCC activity, in early untreated HIV infection. Both anti-gp120 Abs and ADCC activity were detectable as early as 30 DPI and both increased with a slope of change significantly different from "0" through the first 200 DPI in a cross-sectional analysis of untreated

subjects. A significant increase was also observed for total IgG, anti-Env Ab concentration and ADCP activity in the same period of early untreated infection. These results are in line with the findings of a study by Dugast et al. that looked at the early evolution of the functional Ab response, including nnAbs and ADCC (Dugast et al., 2014). In line with our results, they found that anti-gp120 Abs appeared as early as one month post-infection. However, they used a plate-based ELISA assay for the quantification rather than an infected cell target. They also observed a rise and fall in ADCC activity within the first year of infection, noting a peak in ADCC activity at 120 DPI followed by a gradual decline in subsequent months and years. In our study we saw a similar increase in ADCC activity in acute infection but did not observe a peak or decline in acute-phase untreated subjects, rather a continuous increase in ADCC activity through 200 DPI. Importantly, the decline in ADCC seen in their study occurred without treatment, so this decline cannot be compared to that observed after treatment initiation in our study. They used two assays to quantify FcDF activity, an antibody-dependent cellular viral inhibition assay measuring the reduction of p24 production by infected $CD4_+$ T cells in the presence of NK cells, and an AD NK cell activation assay that measured NK cell cytokine secretion and/or degranulation as surrogates for NK cell cytolysis. Our ADCC assay directly measured Fc-mediated apoptosis of siCEM by NK cells in the presence in subject plasma, an explicit indicator of in vivo ADCC ability. They also observed a loss of Fc activity associated with a decline of HIV-specific IgG3 responses. This result is unsurprising as Abs are required to coordinate FcDFs. The results presented in my thesis correspond with several findings presented in this 2014 study. The evolution of Env-specific responses in HIV infection have not been described until now as no target cells have been available to probe for Abs and FcDFs targeting cells expressing closed conformation Env. The results of this thesis therefore present an important first look at these responses.

Post-treatment there was an overall decline in anti-gp120 and anti-Env Ab concentration with a significantly steeper annual slope of decline in those treated later compared to those treated earlier for both specific Abs. The activity of all four FcDFs also declined post-treatment with no significant difference in annual slope of decline between the early and late treatment groups. At treatment initiation there was a significantly higher Anti-Env Ab concentration in the late treatment group compared to the early treatment group. The same held true for ADCT and ADCP activity, which was higher at treatment initiation in those starting treatment later compared to earlier. No

significant difference was observed in anti-gp120 Ab concentration, ADCC or ADCD activity between the early and late treatment groups. We can speculate as to the cause of the steeper slope of decline in anti-gp120 and anti-Env Ab concentration in the late treatment group compared to the early one. It could be due to the higher concentration of specific Abs at treatment initiation, thus the levels have farther to fall once treatment is initiated. While there were higher levels of anti-gp120 and anti-Env Abs at treatment initiation in the late treatment group in both cases, the difference between the early and late groups was only statistically significant for anti-Env Abs and not for anti-gp120 Abs. Another explanation could be that in subjects treated later, the immune system is more compromised by the time treatment is initiated and thus the humoral response is lost as soon as the HIV antigen level declines. HIV antigen, or viral load, is needed to maintain anti-HIV Env specific Ab concentrations and FcDF activity. It is possible that in subjects treated earlier, for whom there is less time for $CD4_+$ T cell depletion and immune exhaustion during infection, there is the prospect of sustaining the humoral immune response after the antigen level declines. In a more exhausted immune system, it may not be possible to sustain the response once treatment eliminates the antigen. As the results of this thesis have not been compared to the clinical outcomes of the subjects enrolled, we can only display the trends in AbDF activity but not conclude how it is correlated to protection from or control of infection. This information is not likely to be forthcoming as we can no longer make assumptions on the natural history of infection once treatment is started. After treatment initiation it becomes difficult to disentangle the infection control offered by the body's immune system and that of ART.

In this thesis, I have used siCEM cells as target cells for the ADCC, ADCD and ADCT assays. Using these target cells allows us to probe plasma samples for Abs to HIV infected cells rather than to uninfected bystander cells (Dupuy et al., 2019). It should be noted, however, that while present, the concentration of these Abs is much lower than those specific for CD4i epitopes. In our experiments, Abs to native trimeric Env were first detected at low levels at 30 DPI while those to gp120 on coated cells were present at relatively higher levels at the earliest TPs 30 DPI. Furthermore, there was a 46.1x higher concentration of Abs binding monomeric gp120 in the plate-based assay than Abs binding Env of the surface of siCEM cells in the cell-based quantification assay on average. This observation was amplified in the samples of treated subjects where there was a 48.5x higher concentration of anti-gp120 Abs compared to anti-Env

Abs, in contrast to the untreated subjects where the ratio of anti-gp120 to anti-Env Ab concentration was only 40.6x. This result was unexpected as I would have predicted that in the context of untreated infection, there would be a greater frequency of infected cells shedding gp120 to bystander cells, which would be targeted by Abs to monomeric gp120. However, in the absence of genuinely infected cells as targets after treatment initiation, it is possible that the concentration of anti-Env Abs decline more rapidly than anti-gp120 Abs. The median annual slopes of decline of anti-gp120 and anti-Env Ab concentrations for all treated subjects were -308.46 and -53.80 AU/year, respectively. It is difficult to directly compare these slopes of change as the Ab concentrations had different starting points. The median Ab concentrations at the first treated time point for all treated subjects were 1348.03 and 149.02 AU for anti-gp120 and anti-Env Abs, respectively. More advanced statistical analysis could help explain this relationship in future studies. The ratio of anti-gp120: anti-Env Ab concentration was higher in the early than late treatment group, ratios of 49.6x and 47.6x, respectively. It seems likely that due to their later appearance, it may take longer for anti-Env Ab titres to develop, and thus later treatment initiation could result in a reduction in the ratio of anti-gp120: anti-Env Abs as anti-Env Ab titres have more time to develop before treatment limits the presence of infected cell targets. It is interesting to speculate that Abs binding siCEM cells may be able to exert HIV control through FcDFs while those to gp120 coated cells and uninfected bystander cells may be pathogenic. Consistent with the later point, in a mother to child transmission cohort followed in Kenya, ADCC activity targeting CD4i epitopes was associated with mortality in HIV infected infants (Naiman et al., 2019). More work needs to be done to more formally address whether Abs to closed conformation Env on HIV infected cells that are ADCC competent exert HIV control. In order to do this, ADCC assays such as ours, with target siCEM expressing closed conformation Env, should be used for assessment of ADCC activity (Dupuy et al., 2019). An assay like this will allow for more accurate evaluation of correlates of protection in vaccine or treatment clinical trials.

We observed that the FcDF assays correlated more strongly with anti-Env Ab concentration than anti-gp120 Ab concentration. This result was unsurprising as the siCEM used to measure the FcDFs replicate the conformation of Env present on the surface of cells in vivo. Ab binding necessarily precedes the development of FcDFs so it makes sense that HIV Env-specific Ab titres

are correlated to FcDF activity. Studies often use targets such as monomeric gp120 to test immune responses to HIV but this target does not reflect HIV's appearance in vivo. For example, assays using plates or cells coated with monomeric gp120 allow binding at epitopes that would not be accessible in vivo. Assays using such target cells likely overestimate the antibody response to Env in vivo, as our results demonstrated an average of 46.1x higher binding of Abs to monomeric gp120 compared to Env expressed on the surface of the siCEM target cells. Furthermore, gp120-coated target cells are not expressing an Env conformation present on infected cells. FcDF assays using the gp120 coated target cells could lead to misinformed decisions on treatments and trials that are ultimately useless. Thus it is important to use the most accurate models possible. The anti-Env Ab quantification assay and ADCC assay developed by our lab uses the HIV-infected siCEM cell line, likely the most realistic in vitro model for quantifying the binding and functionality of anti-Env specific Abs (Kant et al., 2019, Dupuy et al., 2019). The key feature of this cell line is that it is close to 100% infected by a virus that expresses Nef and Vpu, which downregulate CD4 from the cell surface allowing Env to maintain a closed conformation, analogous to what would present on genuinely HIV infected cells in vivo. Assays using target cells expressing an Env conformation that mimics that present on $CD4_+$ T cells infected with replication competent HIV will be vital to detecting the presence of FcDF-competent Abs targeting HIV-infected and not uninfected bystander cells as anti-HIV Abs and FcDFs have been repeatedly implicated in protection against infection (Naiman et al., 2019).

Modern recommendations suggest that initiating ART as soon as possible after infection leads to better clinical outcomes and a smaller reservoir size (WHO, 2015). Historically and in resource-limited settings, this is almost certainly the right course of action. While there is motivation to initiate ART as soon as possible in order to limit the size of the reservoir, it is possible that early ART also limits the magnitude and functionality of the humoral immune response. Our study demonstrated a statistically significant increase in total IgG, anti-gp120 and anti-Env Abs in early untreated infection through the first 200 DPI. We also observed an increase in the FcDFs pre-treatment, increases which were significant for ADCC and ADCP activity. This result is in agreement with a study that observed a rapidly generated Fc-derived immune response during acute HIV infection, which peaked at 6 months post-infection (Dugast et al., 2014). Post-treatment, we observed a decline in Ab concentrations and FcDFs across in all assays. This is in agreement

with studies showing that hypergammaglobulinemia and B cell proliferation in HIV positive subjects seems to be reversed once ART is initiated, which may prevent or delay the development of a protective response (Lane et al., 1983; Schnittman et al., 1986). Studies have observed an increase in ADCC activity post-ART initiation, correlated with improved NK cell activity as opposed to Ab titre, pointing to a potential increase in Ab potency over time on ART (Jensen et al., 2015; Jensen et al., 2015). Research on the relationship between ADCP and ART has revealed that the phagocytic activity of monocytes and neutrophils was equal to or lower in treated individuals compared to treatment naïve subjects, while their phagocytic indicators were higher than in those who had initiated and ceased treatment (Michailidis et al., 2012). In our study, ADCP activity was measured as the phagocytosis of gp120-coated beads rather than siCEM cells. In an in vitro model, the siCEM are too large to be phagocytosed by the THP-1 monocyte cell line consisting of cells of a similar size. It would be beneficial to develop an assay that would allow for measurement of ADCP of HIV-infected cells in the future. It is unclear whether complement activation plays a protective or antagonistic role in HIV infection. It has been shown that complement inhibitors are necessary in many infections to limit initiation of the complement cascade in order to prevent inflammation and tissue damage, pointing to an antagonistic role (Meri and Jarva, 2013). Another study highlighting the importance of the Fc receptor in Ab-based protection noted that the complement system was not a part of this protection (Hessell et al., 2007). While it remains inconclusive whether ADCD plays an antagonistic or perhaps neutral role in infection, it has been observed that complement activity increases following initiation of ART, with undefined clinical results, suggesting there is at minimum a direct response (Yu et al., 2010; Spear et al., 1999). The relationship between ADCT and ART has not been studied aside from the work presented in my thesis. My results demonstrated that ADCT activity increased slightly in untreated subjects during the first 200 DPI, though this increase was not statistically significant. At treatment initiation, ADCT activity was significantly higher in subjects initiating treatment greater than 90 DPI compared to those starting treatment less than 90 DPI. Post-treatment ADCT activity declined with no significant difference in slope of decline between those initiating treatment less than or more than 90 DPI. While the above mentioned studies provide a broad picture of the dynamics of FcDFs after ART initiation, our study is crucial for addressing existing knowledge gaps surrounding the differences in these functions in subjects initiating ART at different intervals post-infection.

The results of the ADCD assays performed for this thesis were somewhat divergent from those of the other three functional assays. In almost every case the trends in slope and differences between early and late treatment groups were the opposite for ADCD compared to the results of the other three functional assays. In addition, the ADCD results correlated poorly with both the anti-gp120 and anti-Env Ab concentrations and the results of the other functional assays. As mentioned in the Methods section, the functional assays performed on half of the subjects, including ADCD, were done by a previous Masters' student in the lab. There was a notable difference in the ADCD values obtained by this student and my own, suggesting that the assay is not sufficiently replicable on different dates. Some of the values obtained by this other student were 100-fold higher than the rest of the values obtained. This was unprecedented in the other functional assays. If there were a few extreme values these could be considered outliers but there were at least a dozen values that I would consider extremely out of the reasonable range, so I could not dismiss them completely. A difference between the assays performed by the previous Masters' student and my own is the source of human complement used. This could be a cause of the significant difference seen between our results. I decided to include the ADCD results in my thesis because the work was done and it would seem irresponsible to ignore them completely. However, I would not consider these results a reliable representation of the ADCD response in untreated and treated HIV infection.

In our study we observed differences in Ab concentration and FcDFs based on whether subjects initiated treatment less than or greater than 90 DPI. Anti-gp120 and anti-Env Abs declined with a significantly steeper slope of decline in the late compared to the early treatment group. At treatment initiation, there was a significantly higher concentration of anti-Env Abs as well as higher ADCT and ADCP activity in the late compared to the early treatment group. These results incite an interesting discussion about priorities surrounding treatment initiation going forward. Is it wiser to treat early to limit the size of the viral reservoir at a TP that prevents the development of anti-HIV humoral immune responses that may play a role in HIV control, or to delay treatment to allow for the development of these immune response? This is of course dependent on what can be achieved in either scenario. Jain et al. reported that treatment initiation less than six months post-infection shrinks the reservoir size compared to treating later, while Laanani et al. have demonstrated lower

reservoir setpoints related to treatment initiation at intervals less than 6 months post-infection (Jain et al., 2013; Laanani et al., 2015). Work done by Ananworanich et al. with the untreated RV217 cohort and acute-treated RV254 cohort in Thailand supports the concept of limiting the size of the HIV reservoir through early ART initiation (Ananworanich et al., 2016). At every TP post-enrollment, the acute treated RV254 subjects had smaller HIV reservoirs than the untreated RV217 subjects. This held true for three reservoir quantification measures, total HIV DNA, integrated HIV DNA, and 2LTR circles, providing strong evidence that early ART initiation can limit the size of the reservoir. However, another report demonstrated that despite ART, reservoir size increased in 27% of subjects and the impact of ART within one year played little role in long-term reservoir dynamics (Bachmann et al., 2019). In terms of humoral immune benefits, it would be unreasonable to delay treatment until the development of bnAbs, which generally do not appear until years after infection, though delaying treatment may allow for the induction of Ab responses that may precede the formation of these bnAbs (Caskey et al., 2017; Richardson et al., 2018). Furthermore, by the time bnAbs appear, if they do, they are unable to neutralize contemporaneous viral isolates due to the accumulation of HIV escape mutations (Wei et al., 2003). Treatment initiation timing appears to require the necessary trade-off between limiting the reservoir and allowing for the development of an HIV-specific immune response. Repeating this study with samples from subjects starting ART in the earliest Feibig stages would help to elucidate whether a compromise is found in a "sweet spot" whereby you could get the best of both worlds – a limited reservoir and an effective humoral response. If such an ideal timing of treatment existed, past studies would predict it to occur at less than 6 months post-infection. Similarly, our data presented here suggest this would occur at less than 3 months post-infection as subjects treated less than 90 DPI had less of a drop-off of Env-specific Ab concentration and FcDF activity after treatment initiation than those treated more than 90 DPI.

One limitation of this study is the nature of the Montreal HIV Primary Infection Cohort, in which subjects studied in the work described in this thesis were enrolled. Positive aspects of the cohort include the relatively large sample size and the longitudinal collection of plasma and PBMC samples over long periods of time, allowing for analysis of trends over time. Unfortunately, it is rare to have samples in this cohort from the earliest Fiebig stages since subjects are only enrolled after their diagnosis, which is often at least one month post-infection. Additionally, subject visit

dates and sample collections were scheduled at approximate but not precise intervals post-infection and post-treatment. While the aim may have been to have subject visits at specific TPs, the reality is that there is a range in DPI at which subjects came in for clinic visits, and some clinic visits were missed altogether. This is the reality of working with human volunteers. The consequence of this is that it was challenging to group subjects and compare their humoral development post-infection and post-treatment.

Another limitation of the cohort was that the participants were predominantly male as the highest risk group in Montreal was and still is MSM, making it difficult to study sex differences. It is known that HIV pathogenesis differs in men and women, which would have been interesting to observe in this study, had it not been for the fact that 93 of the 99 subjects were male (Scully, 2018). Additionally, data on co-infections was somewhat limited. For example, CMV infection status was unknown for (57%) of the participants studied. Co-infection of HIV and CMV are very common, and of the subjects whose status was known, 42/43 (98%) were CMV positive (Gianella et al., 2015). If sufficient data existed, it would be interesting to look at the effect of CMV co-infection on the humoral response in future studies. Finally, the sample size of the study was somewhat of a limitation. For the Ab quantification and FcDF functional assays, we were limited to 42 subject who had three or more longitudinal treated TPs. As a consequence, there were several analyses that trended towards statistical significance but did not achieve it. It is possible that with a larger sample size we would have observed more significant trends meriting further investigation. The sample size was also a limitation in the quantification of the integrated HIV DNA reservoir. The poor viability of the cells post-thaw meant that I did not have the necessary cell numbers required to perform more tests and was left with the sample size of n = 19. Preliminary results suggested there may be a relationship between the treatment initiation timing and the size of the viral reservoir, an interesting association to investigate further. If more PBMC samples are acquired in the future, the reservoir quantification could continue in future studies.

Another limitation of the study is the need to use arbitrary units for the quantification of anti-gp120 and anti-Env Abs, and for the scoring of the FcDFs. Unfortunately, the precise concentration of anti-gp120 and anti-Env Abs in HIV^{+}IG is unknown so an exact concentration or quantity of anti-

gp120/ anti-Env Abs in plasma could not be calculated. Therefore, the relative amount of "Arbitrary Units" of Abs was calculated for each plasma sample, allowing for comparisons of relative Ab concentrations but not absolute values. For the functional assays, in ADCC and ADCT, the unit "%" cancelled out when values were normalized to the inter-plate HIV+IG control. For the ADCP and ADCD assays, the output value was the product of "%" and MFI, which gives a unit-less arbitrary number. For this reason, each functional assay was reported in terms of a functional score, which still allowed for comparisons between samples, assays, and Ab concentrations in a relative manner as opposed to in terms of an absolute value. However, the fact that the input IgG concentration used in each assay is standardized represents an improvement in terms of between subject comparisons in anti-gp120 and FcDF measures compared to work done by others (Ackerman et al., 2016; Richardson et al., 2018).

Chapter 6: Conclusion

The battle against HIV has been fought long and hard, resulting in discoveries that have changed the lives of those afflicted. In the years following its discovery, an HIV/AIDS diagnosis was almost surely a death sentence, accompanied by fear and stigma that also had to be endured. Hope emerged as the virus itself was identified and traced, and continued to grow with the invention of combination ART. An incredible breakthrough, ART allowed HIV-infected people to live long lives without fear of progressing to AIDS despite several persistent co-morbidities. A major obstacle to curing HIV is the persistent latent HIV reservoir, which persists despite ART. Early initiation of ART can limit the size of the reservoir, though it is not well understood what impact the timing of treatment initiation has on the humoral immune response. In this thesis I have helped to fill this knowledge gap by comparing the Ab concentrations and FcDFs of subjects initiating treatment less than or greater than 90 DPI. The functional experiments performed used siCEM cells as targets, which display a closed conformation Env at their surface, representative of the conformation present on a genuinely infected cell. In the study I observed a statistically significant increase in total IgG, anti-gp120 and anti-Env Abs in early untreated infection as well as an increase in four FcDFs, increases which were statistically significant for ADCC and ADCP. I also observed differences in Ab concentration and FcDF activity based on whether subjects initiated treatment less than or greater than 90 DPI. Anti-gp120 and anti-Env Abs declined with a significantly steeper slope of decline in the late compared to early treatment group. At treatment initiation, there was a significantly higher concentration of anti-Env Abs as well as higher ADCT and ADCP activity in the late compared to the early treatment group. Unsurprisingly, the FcDFs correlated more strongly with anti-Env Ab concentration than anti-gp120 Ab concentration likely because the siCEM used to measure the FcDFs reproduce the conformation of Env present on the infected cell surface in vivo. Additionally, there was a 46.1x higher concentration of anti-gp120 Abs than anti-Env Abs on average in subject plasma. This ratio was augmented in treated compared to untreated subjects and in those treated <90 DPI compared to those treated > 90 DPI. The results of this thesis help to inform the field on the effects of timing of ART treatment on Ab concentration and FcDF activity. These results may contribute to novel strategies regarding the optimal time to start ART that balance allowing development of persistent anti-HIV immune responses that exert HIV control with limiting the size of the viral reservoir.

References

[1] Zhu, T., Korber, B. T., Nahmias, A. J., Hooper, E., Sharp, P. M., and Ho, D. D. (1998) An African HIV-1 sequence from 1959 and implications for the origin of the epidemic, *Nature 391*, 594-597.

[2] Korber, B., Muldoon, M., Theiler, J., Gao, F., Gupta, R., Lapedes, A., Hahn, B. H., Wolinsky, S., and Bhattacharya, T. (2000) Timing the Ancestor of the HIV-1 Pandemic Strains, *Science 288*, 1789-1796.

[3] Worobey, M., Gemmel, M., Teuwen, D. E., Haselkorn, T., Kunstman, K., Bunce, M., Muyembe, J.-J., Kabongo, J.-M. M., Kalengayi, R. M., Van Marck, E., Gilbert, M. T. P., and Wolinsky, S. M. (2008) Direct evidence of extensive diversity of HIV-1 in Kinshasa by 1960, *Nature 455*, 661-664.

[4] Garry, R. F., Witte, M. H., Gottlieb, A. A., Elvin-Lewis, M., Gottlieb, M. S., Witte, C. L., Alexander, S. S., Cole, W. R., and Drake, W. L., Jr. (1988) Documentation of an AIDS virus infection in the United States in 1968, *JAMA 260*, 2085-2087.

[5] Dufoort, G., Couroucé, A.-M., Ancelle-Park, R., and Bletry, O. (1988) No clinical signs 14 years after HIV-2 transmission via blood transfusion, *The Lancet 332*, 510.

[6] Guyader, M., Emerman, M., Sonigo, P., Clavel, F., Montagnier, L., and Alizon, M. (1987) Genome organization and transactivation of the human immunodeficiency virus type 2, *Nature 326*, 662-669.

[7] Gao, F., Bailes, E., Robertson, D. L., Chen, Y., Rodenburg, C. M., Michael, S. F., Cummins, L. B., Arthur, L. O., Peeters, M., Shaw, G. M., Sharp, P. M., and Hahn, B. H. (1999) Origin of HIV-1 in the chimpanzee Pan troglodytes troglodytes, *Nature 397*, 436-441.

[8] Hirsch, V. M., Olmsted, R. A., Murphey-Corb, M., Purcell, R. H., and Johnson, P. R. (1989) An African primate lentivirus (SIVsmclosely related to HIV-2, *Nature 339*, 389-392.

[9] De Leys, R., Vanderborght, B., Vanden Haesevelde, M., Heyndrickx, L., van Geel, A., Wauters, C., Bernaerts, R., Saman, E., Nijs, P., and Willems, B. (1990) Isolation and partial characterization of an unusual human immunodeficiency retrovirus from two persons of west-central African origin, *Journal of Virology 64*, 1207-1216.

[10] Simon, F., Mauclère, P., Roques, P., Loussert-Ajaka, I., Müller-Trutwin, M. C., Saragosti, S., Georges-Courbot, M. C., Barré-Sinoussi, F., and Brun-Vézinet, F. (1998) Identification of a new human immunodeficiency virus type 1 distinct from group M and group O, *Nature Medicine 4*, 1032-1037.

[11] Plantier, J.-C., Leoz, M., Dickerson, J. E., De Oliveira, F., Cordonnier, F., Lemée, V., Damond, F., Robertson, D. L., and Simon, F. (2009) A new human immunodeficiency virus derived from gorillas, *Nature medicine 15*, 871-872.

[12] Mourez, T., Simon, F., and Plantier, J.-C. (2013) Non-M variants of human immunodeficiency virus type 1, *Clin Microbiol Rev 26*, 448-461.

[13] Magiorkinis, G., Angelis, K., Mamais, I., Katzourakis, A., Hatzakis, A., Albert, J., Lawyer, G., Hamouda, O., Struck, D., Vercauteren, J., Wensing, A., Alexiev, I., Åsjö, B., Balotta, C., Gomes, P., Camacho, R. J., Coughlan, S., Griskevicius, A., Grossman, Z., Horban, A., Kostrikis, L. G., Lepej, S. J., Liitsola, K., Linka, M., Nielsen, C., Otelea, D., Paredes, R., Poljak, M., Puchhammer-Stöckl, E., Schmit, J. C., Sönnerborg, A., Staneková, D.,

Stanojevic, M., Stylianou, D. C., Boucher, C. A. B., program, S., Nikolopoulos, G., Vasylyeva, T., Friedman, S. R., van de Vijver, D., Angarano, G., Chaix, M.-L., de Luca, A., Korn, K., Loveday, C., Soriano, V., Yerly, S., Zazzi, M., Vandamme, A.-M., and Paraskevis, D. (2016) The global spread of HIV-1 subtype B epidemic, *Infect Genet Evol 46*, 169-179.

[14] CDC. (1981) Morbidity and mortality weekly report, 30(21), June 5, 1981.

[15] CDC. (1981) Morbidity and mortality weekly report, 30(25), July 3, 1981.

[16] Barre-Sinoussi, F., Chermann, J. C., Rey, F., Nugeyre, M. T., Chamaret, S., Gruest, J., Dauguet, C., Axler-Blin, C., Vezinet-Brun, F., Rouzioux, C., Rozenbaum, W., and Montagnier, L. (1983) Isolation of a T-lymphotropic retrovirus from a patient at risk for acquired immune deficiency syndrome (AIDS), *Science 220*, 868-871.

[17] Gallo, R. C., Salahuddin, S. Z., Popovic, M., Shearer, G. M., Kaplan, M., Haynes, B. F., Palker, T. J., Redfield, R., Oleske, J., Safai, B., and et, a. (1984) Frequent detection and isolation of cytopathic retroviruses (HTLV-III) from patients with AIDS and at risk for AIDS, *Science 224*, 500-503.

[18] Case, K. (1986) Nomenclature: Human Immunodeficiency Virus, p 133, Annals of Internal Medicine.

[19] Shearer, G. M., Bernstein, D. C., Tung, K. S., Via, C. S., Redfield, R., Salahuddin, S. Z., and Gallo, R. C. (1986) A model for the selective loss of major histocompatibility complex self-restricted T cell immune responses during the development of acquired immune deficiency syndrome (AIDS), *The Journal of Immunology 137*, 2514-2521.

[20] Müller, H., Falk, S., and Stutte, H. J. (1986) Accessory cells as primary target of human immunodeficiency virus HIV infection, *Journal of Clinical Pathology 39*, 1161-a.

[21] Siliciano, R. F., Lawton, T., Knall, C., Karr, R. W., Berman, P., Gregory, T., and Reinherz, E. L. (1988) Analysis of host-virus interactions in AIDS with anti-gp120 T cell clones: Effect of HIV sequence variation and a mechanism for CD4+ cell depletion, *Cell 54*, 561-575.

[22] Robb, M. L., Eller, L. A., Kibuuka, H., Rono, K., Maganga, L., Nitayaphan, S., Kroon, E., Sawe, F. K., Sinei, S., Sriplienchan, S., Jagodzinski, L. L., Malia, J., Manak, M., de Souza, M. S., Tovanabutra, S., Sanders-Buell, E., Rolland, M., Dorsey-Spitz, J., Eller, M. A., Milazzo, M., Li, Q., Lewandowski, A., Wu, H., Swann, E., O'Connell, R. J., Peel, S., Dawson, P., Kim, J. H., and Michael, N. L. (2016) Prospective Study of Acute HIV-1 Infection in Adults in East Africa and Thailand, *New England Journal of Medicine 374*, 2120-2130.

[23] CDC. (1993) 1993 Revised Classification System for HIV Infection and Expanded Surveillance Case Definition for AIDS Among Adolescents and Adults, *JAMA 269*, 729-730.

[24] Pitchenik, A. E., Fischl, M.A., Dickinson, G.M., Becker, D.M., Fournier, A.M., O'Connell, M.T., Colton, R.M., Spira, T.J. (1983) Opportunistic Infections and Kaposi's Sarcoma Among Haitians: Evidence of a New Acquired Immunodeficiency State, *Annals of Internal Medicine 98*, 277-284.

[25] Lifson, A. R. (1988) Do Alternate Modes for Transmission of Human Immunodeficiency Virus Exist?: A Review, *JAMA 259*, 1353-1356.

[26] Maartens, G., Celum, C., and Lewin, S. R. (2014) HIV infection: epidemiology, pathogenesis, treatment, and prevention, *The Lancet 384*, 258-271.

[27] Moore, M. D., and Hu, W. S. (2009) HIV-1 RNA dimerization: It takes two to tango, *AIDS Rev 11*, 91-102.

[28] German Advisory Committee Blood, S. A. o. P. T. b. B. (2016) Human Immunodeficiency Virus (HIV), *Transfus Med Hemother 43*, 203-222.
[29] Muesing, M. A., Smith, D. H., Cabradilla, C. D., Benton, C. V., Lasky, L. A., and Capon, D. J. (1985) Nucleic acid structure and expression of the human AIDS/lymphadenopathy retrovirus, *Nature 313*, 450-458.
[30] Wain-Hobson, S., Sonigo, P., Danos, O., Cole, S., and Alizon, M. (1985) Nucleotide sequence of the AIDS virus, LAV, *Cell 40*, 9-17.
[31] Gelderblom, H. R. (1991) Assembly and morphology of HIV: potential effect of structure on viral function, *AIDS 5*, 617-638.
[32] Campbell, E. M., and Hope, T. J. (2015) HIV-1 capsid: the multifaceted key player in HIV-1 infection, *Nat Rev Microbiol 13*, 471-483.
[33] Thomas, J. A., and Gorelick, R. J. (2008) Nucleocapsid protein function in early infection processes, *Virus Res 134*, 39-63.
[34] Robey, W. G., Safai, B., Oroszlan, S., Arthur, L. O., Gonda, M. A., Gallo, R. C., and Fischinger, P. J. (1985) Characterization of envelope and core structural gene products of HTLV-III with sera from AIDS patients, *Science 228*, 593-595.
[35] Veronese, F. D., DeVico, A. L., Copeland, T. D., Oroszlan, S., Gallo, R. C., and Sarngadharan, M. G. (1985) Characterization of gp41 as the transmembrane protein coded by the HTLV-III/LAV envelope gene, *Science 229*, 1402-1405.
[36] Zhang, C. W. H., Chishti, Y., Hussey, R. E., and Reinherz, E. L. (2001) Expression, Purification, and Characterization of Recombinant HIV gp140: The gp41 ectodomain of HIV or Simian Immunodeficiency virus is sufficient to maintain the retroviral envelope glycoprotein as a trimer., *Journal of Biological Chemistry 276*, 39577-39585.
[37] Eckert, D. M., and Kim, P. S. (2001) Mechanisms of Viral Membrane Fusion and Its Inhibition, *Annual Review of Biochemistry 70*, 777-810.
[38] Wilen, C. B., Tilton, J.C., Doms, R.W. (2012) HIV: Cell Binding and Entry, *Cold Spring Harb Perspect Med 2*, a006866.
[39] Stein, B. S., Gowda, S. D., Lifson, J. D., Penhallow, R. C., Bensch, K. G., and Engleman, E. G. (1987) pH-independent HIV entry into CD4-positive T cells via virus envelope fusion to the plasma membrane, *Cell 49*, 659-668.
[40] Tersmette, M., Gruters, R. A., de Wolf, F., de Goede, R. E., Lange, J. M., Schellekens, P. T., Goudsmit, J., Huisman, H. G., and Miedema, F. (1989) Evidence for a role of virulent human immunodeficiency virus (HIV) variants in the pathogenesis of acquired immunodeficiency syndrome: studies on sequential HIV isolates, *Journal of Virology 63*, 2118-2125.
[41] Yaniz-Galende, E., and Hajjar, R. J. (2014) Stem cell and gene therapy for cardiac regeneration, In *Cardiac Regeneration and Repair* (Li, R.-K., and Weisel, R. D., Eds.), pp 347-379, Woodhead Publishing.
[42] Sousa, R., Chung, Y. J., Rose, J. P., and Wang, B.-C. (1993) Crystal structure of bacteriophage T7 RNA polymerase at 3.3 Å resolution, *Nature 364*, 593-599.
[43] Figiel, M., Krepl, M., Poznański, J., Gołąb, A., Šponer, J., and Nowotny, M. (2017) Coordination between the polymerase and RNase H activity of HIV-1 reverse transcriptase, *Nucleic Acids Research 45*, 3341-3352.

[44] Beilhartz, G. L., and Götte, M. (2010) HIV-1 Ribonuclease H: Structure, Catalytic Mechanism and Inhibitors, *Viruses 2*, 900-926.
[45] Tsuchihashi, Z., and Brown, P. O. (1994) DNA strand exchange and selective DNA annealing promoted by the human immunodeficiency virus type 1 nucleocapsid protein, *Journal of Virology 68*, 5863-5870.
[46] Accola, M. A., Strack, B., and Göttlinger, H. G. (2000) Efficient Particle Production by Minimal Gag Constructs Which Retain the Carboxy-Terminal Domain of Human Immunodeficiency Virus Type 1 Capsid-p2 and a Late Assembly Domain, *Journal of Virology 74*, 5395-5402.
[47] Barré-Sinoussi, F. (1996) HIV as the cause of AIDS, *The Lancet 348*, 31-35.
[48] Preston, B. D., Poiesz, B. J., and Loeb, L. A. (1988) Fidelity of HIV-1 reverse transcriptase, *Science 242*, 1168-1171.
[49] Goodenow, M., Huet, T., Saurin, W., Kwok, S., Sninsky, J., Wain-Hobson, S. (1989) HIV-1 Isolates Are Rapidly Evolving Quasispecies : Evidence for Viral Mixtures and Preferred Nucleotide Substitutions, *Journal of Acquired Immune Deficiency Syndromes 2*, 344-352.
[50] Bowerman, B., Brown, P. O., Bishop, J. M., and Varmus, H. E. (1989) A nucleoprotein complex mediates the integration of retroviral DNA, *Genes & Development 3*, 469-478.
[51] Farnet, C. M., and Bushman, F. D. (1997) HIV-1 cDNA Integration: Requirement of HMG I(Y) Protein for Function of Preintegration Complexes In Vitro, *Cell 88*, 483-492.
[52] Mitchell, R. S., Beitzel, B. F., Schroder, A. R. W., Shinn, P., Chen, H., Berry, C. C., Ecker, J. R., and Bushman, F. D. (2004) Retroviral DNA Integration: ASLV, HIV, and MLV Show Distinct Target Site Preferences, *PLOS Biology 2*, e234.
[53] Sundquist, W. I., and Kräusslich, H.-G. (2012) HIV-1 assembly, budding, and maturation, *Cold Spring Harb Perspect Med 2*, a006924.
[54] Perelson, A. S., Neumann, A. U., Markowitz, M., Leonard, J. M., and Ho, D. D. (1996) HIV-1 Dynamics in Vivo: Virion Clearance Rate, Infected Cell Life-Span, and Viral Generation Time, *Science 271*, 1582-1586.
[55] Mellors, J. W., Rinaldo, C. R., Gupta, P., White, R. M., Todd, J. A., and Kingsley, L. A. (1996) Prognosis in HIV-1 Infection Predicted by the Quantity of Virus in Plasma, *Science 272*, 1167-1170.
[56] Brenchley, J. M., Schacker, T. W., Ruff, L. E., Price, D. A., Taylor, J. H., Beilman, G. J., Nguyen, P. L., Khoruts, A., Larson, M., Haase, A. T., and Douek, D. C. (2004) CD4+ T Cell Depletion during all Stages of HIV Disease Occurs Predominantly in the Gastrointestinal Tract, *Journal of Experimental Medicine 200*, 749-759.
[57] Brenchley, J. M., Price, D. A., Schacker, T. W., Asher, T. E., Silvestri, G., Rao, S., Kazzaz, Z., Bornstein, E., Lambotte, O., Altmann, D., Blazar, B. R., Rodriguez, B., Teixeira-Johnson, L., Landay, A., Martin, J. N., Hecht, F. M., Picker, L. J., Lederman, M. M., Deeks, S. G., and Douek, D. C. (2006) Microbial translocation is a cause of systemic immune activation in chronic HIV infection, *Nature Medicine 12*, 1365-1371.
[58] Cecchinato, V., Trindade, C. J., Laurence, A., Heraud, J. M., Brenchley, J. M., Ferrari, M. G., Zaffiri, L., Tryniszewska, E., Tsai, W. P., Vaccari, M., Parks, R. W., Venzon, D., Douek, D. C., O'Shea, J. J., and Franchini, G. (2008) Altered balance between Th17 and Th1 cells at mucosal sites predicts AIDS progression in simian immunodeficiency virus-infected macaques, *Mucosal Immunology 1*, 279-288.

[59] Salgado, M., Rallón, N. I., Rodés, B., López, M., Soriano, V., and Benito, J. M. (2011) Long-term non-progressors display a greater number of Th17 cells than HIV-infected typical progressors, *Clinical Immunology 139*, 110-114.
[60] Henrard, D. R., Phillips, J. F., Muenz, L. R., Blattner, W. A., Wiesner, D., Eyster, M. E., and Goedert, J. J. (1995) Natural History of HIV-1 Cell-Free Viremia, *JAMA 274*, 554-558.
[61] Patrikar, S., Basannar, D. R., Bhatti, V. K., Kotwal, A., Gupta, R. M., and Grewal, R. S. (2014) Rate of decline in CD4 count in HIV patients not on antiretroviral therapy, *Med J Armed Forces India 70*, 134-138.
[62] Fiebig, E. W., Wright, D. J., Rawal, B. D., Garrett, P. E., Schumacher, R. T., Peddada, L., Heldebrant, C., Smith, R., Conrad, A., Kleinman, S. H., and Busch, M. P. (2003) Dynamics of HIV viremia and antibody seroconversion in plasma donors: implications for diagnosis and staging of primary HIV infection, *AIDS 17*, 1871-1879.
[63] Cohen, M. S., Shaw, G. M., McMichael, A. J., and Haynes, B. F. (2011) Acute HIV-1 Infection, *New England Journal of Medicine 364*, 1943-1954.
[64] McMichael, A. J., Borrow, P., Tomaras, G. D., Goonetilleke, N., and Haynes, B. F. (2009) The immune response during acute HIV-1 infection: clues for vaccine development, *Nature Reviews Immunology 10*, 11-23.
[65] Whitney, J. B., Hill, A. L., Sanisetty, S., Penaloza-MacMaster, P., Liu, J., Shetty, M., Parenteau, L., Cabral, C., Shields, J., Blackmore, S., Smith, J. Y., Brinkman, A. L., Peter, L. E., Mathew, S. I., Smith, K. M., Borducchi, E. N., Rosenbloom, D. I. S., Lewis, M. G., Hattersley, J., Li, B., Hesselgesser, J., Geleziunas, R., Robb, M. L., Kim, J. H., Michael, N. L., and Barouch, D. H. (2014) Rapid seeding of the viral reservoir prior to SIV viraemia in rhesus monkeys, *Nature 512*, 74-77.
[66] Chun, T.-W., Engel, D., Berrey, M. M., Shea, T., Corey, L., and Fauci, A. S. (1998) Early establishment of a pool of latently infected, resting CD4+ T cells during primary HIV-1 infection, *Proceedings of the National Academy of Sciences 95*, 8869-8873.
[67] Kulpa, D. A., Chomont, N. (2015) HIV persistence in the setting of antiretroviral therapy: when, where and how does HIV hide?, *J Virus Erad 1*, 59-66.
[68] Procopio, F. A., Fromentin, R., Kulpa, D. A., Brehm, J. H., Bebin, A.-G., Strain, M. C., Richman, D. D., O'Doherty, U., Palmer, S., Hecht, F. M., Hoh, R., Barnard, R. J. O., Miller, M. D., Hazuda, D. J., Deeks, S. G., Sékaly, R.-P., and Chomont, N. (2015) A Novel Assay to Measure the Magnitude of the Inducible Viral Reservoir in HIV-infected Individuals, *EBioMedicine 2*, 874-883.
[69] Bruner, K. M., Wang, Z., Simonetti, F. R., Bender, A. M., Kwon, K. J., Sengupta, S., Fray, E. J., Beg, S. A., Antar, A. A. R., Jenike, K. M., Bertagnolli, L. N., Capoferri, A. A., Kufera, J. T., Timmons, A., Nobles, C., Gregg, J., Wada, N., Ho, Y.-C., Zhang, H., Margolick, J. B., Blankson, J. N., Deeks, S. G., Bushman, F. D., Siliciano, J. D., Laird, G. M., and Siliciano, R. F. (2019) A quantitative approach for measuring the reservoir of latent HIV-1 proviruses, *Nature 566*, 120-125.
[70] Hosmane, N. N., Kwon, K. J., Bruner, K. M., Capoferri, A. A., Beg, S., Rosenbloom, D. I. S., Keele, B. F., Ho, Y.-C., Siliciano, J. D., and Siliciano, R. F. (2017) Proliferation of latently infected CD4 T cells carrying replication-competent HIV-1: Potential role in latent reservoir dynamics, *The Journal of Experimental Medicine 214*, 959-972.

[71] Letendre, S., Marquie-Beck, J., Capparelli, E., Best, B., Clifford, D., Collier, A. C., Gelman, B. B., McArthur, J. C., McCutchan, J. A., Morgello, S., Simpson, D., Grant, I., Ellis, R. J., and Group, C. (2008) Validation of the CNS Penetration-Effectiveness Rank for Quantifying Antiretroviral Penetration Into the Central Nervous System, *JAMA Neurology 65*, 65-70.

[72] Chun, T.-W., Carruth, L., Finzi, D., Shen, X., DiGiuseppe, J. A., Taylor, H., Hermankova, M., Chadwick, K., Margolick, J., Quinn, T. C., Kuo, Y.-H., Brookmeyer, R., Zeiger, M. A., Barditch-Crovo, P., and Siliciano, R. F. (1997) Quantification of latent tissue reservoirs and total body viral load in HIV-1 infection, *Nature 387*, 183-188.

[73] Siliciano, J. D., Kajdas, J., Finzi, D., Quinn, T. C., Chadwick, K., Margolick, J. B., Kovacs, C., Gange, S. J., and Siliciano, R. F. (2003) Long-term follow-up studies confirm the stability of the latent reservoir for HIV-1 in resting CD4+ T cells, *Nature Medicine 9*, 727-728.

[74] Finzi, D., Blankson, J., Siliciano, J. D., Margolick, J. B., Chadwick, K., Pierson, T., Smith, K., Lisziewicz, J., Lori, F., Flexner, C., Quinn, T. C., Chaisson, R. E., Rosenberg, E., Walker, B., Gange, S., Gallant, J., and Siliciano, R. F. (1999) Latent infection of CD4+ T cells provides a mechanism for lifelong persistence of HIV-1, even in patients on effective combination therapy, *Nature Medicine 5*, 512-517.

[75] Kamat, A., Ravi, V., Desai, A., Satishchandra, P., Satish, K. S., Borodowsky, I., Subbakrishna, D. K., and Kumar, M. (2007) Quantitation of HIV-1 RNA levels in plasma and CSF of asymptomatic HIV-1 infected patients from South India using a TaqMan real time PCR assay, *Journal of Clinical Virology 39*, 9-15.

[76] Hey-Nguyen, W. J., Xu, Y., Pearson, C. F., Bailey, M., Suzuki, K., Tantau, R., Obeid, S., Milner, B., Field, A., Carr, A., Bloch, M., Cooper, D. A., Kelleher, A. D., Zaunders, J. J., and Koelsch, K. K. (2017) Quantification of Residual Germinal Center Activity and HIV-1 DNA and RNA Levels Using Fine Needle Biopsies of Lymph Nodes During Antiretroviral Therapy, *AIDS Research and Human Retroviruses 33*, 648-657.

[77] Vandergeeten, C., Fromentin, R., Merlini, E., Lawani, M. B., DaFonseca, S., Bakeman, W., McNulty, A., Ramgopal, M., Michael, N., Kim, J. H., Ananworanich, J., and Chomont, N. (2014) Cross-Clade Ultrasensitive PCR-Based Assays To Measure HIV Persistence in Large-Cohort Studies, *Journal of Virology 88*, 12385-12396.

[78] Ho, Y.-C., Shan, L., Hosmane, Nina N., Wang, J., Laskey, Sarah B., Rosenbloom, Daniel I. S., Lai, J., Blankson, Joel N., Siliciano, Janet D., and Siliciano, Robert F. (2013) Replication-Competent Noninduced Proviruses in the Latent Reservoir Increase Barrier to HIV-1 Cure, *Cell 155*, 540-551.

[79] Pardons, M., Baxter, A. E., Massanella, M., Pagliuzza, A., Fromentin, R., Dufour, C., Leyre, L., Routy, J.-P., Kaufmann, D. E., and Chomont, N. (2019) Single-cell characterization and quantification of translation-competent viral reservoirs in treated and untreated HIV infection, *PLOS Pathogens 15*, e1007619.

[80] Heil, F., Hemmi, H., Hochrein, H., Ampenberger, F., Kirschning, C., Akira, S., Lipford, G., Wagner, H., and Bauer, S. (2004) Species-Specific Recognition of Single-Stranded RNA via Toll-like Receptor 7 and 8, *Science 303*, 1526-1529.

[81] Gringhuis, S. I., van der Vlist, M., van den Berg, L. M., den Dunnen, J., Litjens, M., and Geijtenbeek, T. B. H. (2010) HIV-1 exploits innate signaling by TLR8 and DC-SIGN for productive infection of dendritic cells, *Nature Immunology 11*, 419-426.

[82] Henrick, B. M., Yao, X.-D., Rosenthal, K. L., and team, I. s. (2015) HIV-1 Structural Proteins Serve as PAMPs for TLR2 Heterodimers Significantly Increasing Infection and Innate Immune Activation, *Front Immunol 6*.
[83] Nazli, A., Kafka, J. K., Ferreira, V. H., Anipindi, V., Mueller, K., Osborne, B. J., Dizzell, S., Chauvin, S., Mian, M. F., Ouellet, M., Tremblay, M. J., Mossman, K. L., Ashkar, A. A., Kovacs, C., Bowdish, D. M. E., Snider, D. P., Kaul, R., and Kaushic, C. (2013) HIV-1 gp120 Induces TLR2- and TLR4-Mediated Innate Immune Activation in Human Female Genital Epithelium, *The Journal of Immunology 191*, 4246-4258.
[84] Stacey, A. R., Norris, P. J., Qin, L., Haygreen, E. A., Taylor, E., Heitman, J., Lebedeva, M., DeCamp, A., Li, D., Grove, D., Self, S. G., and Borrow, P. (2009) Induction of a Striking Systemic Cytokine Cascade prior to Peak Viremia in Acute Human Immunodeficiency Virus Type 1 Infection, in Contrast to More Modest and Delayed Responses in Acute Hepatitis B and C Virus Infections, *Journal of Virology 83*, 3719-3733.
[85] Hotter, D., Sauter, D., and Kirchhoff, F. (2013) Emerging Role of the Host Restriction Factor Tetherin in Viral Immune Sensing, *Journal of Molecular Biology 425*, 4956-4964.
[86] Simon, V., Bloch, N., and Landau, N. R. (2015) Intrinsic host restrictions to HIV-1 and mechanisms of viral escape, *Nature Immunology 16*, 546-553.
[87] Kramer, H. B., Lavender, K. J., Qin, L., Stacey, A. R., Liu, M. K. P., di Gleria, K., Simmons, A., Gasper-Smith, N., Haynes, B. F., McMichael, A. J., Borrow, P., and Kessler, B. M. (2010) Elevation of Intact and Proteolytic Fragments of Acute Phase Proteins Constitutes the Earliest Systemic Antiviral Response in HIV-1 Infection, *PLOS Pathogens 6*, e1000893.
[88] Tomescu, C., Chehimi, J., Maino, V. C., and Montaner, L. J. (2007) NK Cell Lysis of HIV-1-Infected Autologous CD4 Primary T Cells: Requirement for IFN-Mediated NK Activation by Plasmacytoid Dendritic Cells, *The Journal of Immunology 179*, 2097-2104.
[89] Alter, G., Teigen, N., Ahern, R., Streeck, H., Meier, A., Rosenberg, E. S., and Altfeld, M. (2007) Evolution of Innate and Adaptive Effector Cell Functions during Acute HIV-1 Infection, *The Journal of Infectious Diseases 195*, 1452-1460.
[90] Waggoner, S. N., Cornberg, M., Selin, L. K., and Welsh, R. M. (2012) Natural killer cells act as rheostats modulating antiviral T cells, *Nature 481*, 394-398.
[91] Altfeld, M., and Gale Jr, M. (2015) Innate immunity against HIV-1 infection, *Nature Immunology 16*, 554-562.
[92] Hersperger, A. R., Pereyra, F., Nason, M., Demers, K., Sheth, P., Shin, L. Y., Kovacs, C. M., Rodriguez, B., Sieg, S. F., Teixeira-Johnson, L., Gudonis, D., Goepfert, P. A., Lederman, M. M., Frank, I., Makedonas, G., Kaul, R., Walker, B. D., and Betts, M. R. (2010) Perforin Expression Directly Ex Vivo by HIV-Specific CD8+ T-Cells Is a Correlate of HIV Elite Control, *PLOS Pathogens 6*, e1000917.
[93] Alter, G., Heckerman, D., Schneidewind, A., Fadda, L., Kadie, C. M., Carlson, J. M., Oniangue-Ndza, C., Martin, M., Li, B., Khakoo, S. I., Carrington, M., Allen, T. M., and Altfeld, M. (2011) HIV-1 adaptation to NK-cell-mediated immune pressure, *Nature 476*, 96-100.
[94] Tomaras, G. D., Yates, N. L., Liu, P., Qin, L., Fouda, G. G., Chavez, L. L., Decamp, A. C., Parks, R. J., Ashley, V. C., Lucas, J. T., Cohen, M., Eron, J., Hicks, C. B., Liao, H.-X., Self, S. G., Landucci, G., Forthal, D. N., Weinhold, K. J., Keele, B. F., Hahn, B. H., Greenberg, M. L., Morris, L., Karim, S. S. A., Blattner, W. A., Montefiori, D. C., Shaw, G. M., Perelson, A. S.,

and Haynes, B. F. (2008) Initial B-Cell Responses to Transmitted Human Immunodeficiency Virus Type 1: Virion-Binding Immunoglobulin M (IgM) and IgG Antibodies Followed by Plasma Anti-gp41 Antibodies with Ineffective Control of Initial Viremia, *Journal of Virology 82*, 12449-12463.

[95] Weiss, R. A., Clapham, P. R., Weber, J. N., Dalgleish, A. G., Lasky, L. A., and Berman, P. W. (1986) Variable and conserved neutralization antigens of human immunodeficiency virus, *Nature 324*, 572-575.

[96] Richman, D. D., Wrin, T., Little, S. J., and Petropoulos, C. J. (2003) Rapid evolution of the neutralizing antibody response to HIV type 1 infection, *Proceedings of the National Academy of Sciences 100*, 4144-4149.

[97] Payne, S. (2017) Chapter 6 - Immunity and Resistance to Viruses, In *Viruses* (Payne, S., Ed.), pp 61-71, Academic Press.

[98] Wei, X., Decker, J. M., Wang, S., Hui, H., Kappes, J. C., Wu, X., Salazar-Gonzalez, J. F., Salazar, M. G., Kilby, J. M., Saag, M. S., Komarova, N. L., Nowak, M. A., Hahn, B. H., Kwong, P. D., and Shaw, G. M. (2003) Antibody neutralization and escape by HIV-1, *Nature 422*, 307-312.

[99] Landais, E., Huang, X., Havenar-Daughton, C., Murrell, B., Price, M. A., Wickramasinghe, L., Ramos, A., Bian, C. B., Simek, M., Allen, S., Karita, E., Kilembe, W., Lakhi, S., Inambao, M., Kamali, A., Sanders, E. J., Anzala, O., Edward, V., Bekker, L.-G., Tang, J., Gilmour, J., Kosakovsky-Pond, S. L., Phung, P., Wrin, T., Crotty, S., Godzik, A., and Poignard, P. (2016) Broadly Neutralizing Antibody Responses in a Large Longitudinal Sub-Saharan HIV Primary Infection Cohort, *PLOS Pathogens 12*, e1005369.

[100] Caskey, M., Schoofs, T., Gruell, H., Settler, A., Karagounis, T., Kreider, E. F., Murrell, B., Pfeifer, N., Nogueira, L., Oliveira, T. Y., Learn, G. H., Cohen, Y. Z., Lehmann, C., Gillor, D., Shimeliovich, I., Unson-O'Brien, C., Weiland, D., Robles, A., Kümmerle, T., Wyen, C., Levin, R., Witmer-Pack, M., Eren, K., Ignacio, C., Kiss, S., West Jr, A. P., Mouquet, H., Zingman, B. S., Gulick, R. M., Keler, T., Bjorkman, P. J., Seaman, M. S., Hahn, B. H., Fätkenheuer, G., Schlesinger, S. J., Nussenzweig, M. C., and Klein, F. (2017) Antibody 10-1074 suppresses viremia in HIV-1-infected individuals, *Nature Medicine 23*, 185.

[101] Nishimura, Y., and Martin, M. A. (2017) Of Mice, Macaques, and Men: Broadly Neutralizing Antibody Immunotherapy for HIV-1, *Cell Host & Microbe 22*, 207-216.

[102] Gottardo, R., Bailer, R. T., Korber, B. T., Gnanakaran, S., Phillips, J., Shen, X., Tomaras, G. D., Turk, E., Imholte, G., Eckler, L., Wenschuh, H., Zerweck, J., Greene, K., Gao, H., Berman, P. W., Francis, D., Sinangil, F., Lee, C., Nitayaphan, S., Rerks-Ngarm, S., Kaewkungwal, J., Pitisuttithum, P., Tartaglia, J., Robb, M. L., Michael, N. L., Kim, J. H., Zolla-Pazner, S., Haynes, B. F., Mascola, J. R., Self, S., Gilbert, P., and Montefiori, D. C. (2013) Plasma IgG to Linear Epitopes in the V2 and V3 Regions of HIV-1 gp120 Correlate with a Reduced Risk of Infection in the RV144 Vaccine Efficacy Trial, *PLOS ONE 8*, e75665.

[103] Pinter, A., Honnen, W. J., Kayman, S. C., Trochev, O., and Wu, Z. (1998) Potent neutralization of primary HIV-1 isolates by antibodies directed against epitopes present in the V1V2 domain of HIV-1 gp120, *Vaccine 16*, 1803-1811.

[104] Boesch, A. W., Brown, E. P., and Ackerman, M. E. (2015) The role of Fc receptors in HIV prevention and therapy, *Immunological Reviews 268*, 296-310.

[105] Richardson, S. I., Chung, A. W., Natarajan, H., Mabvakure, B., Mkhize, N. N., Garrett, N., Abdool Karim, S., Moore, P. L., Ackerman, M. E., Alter, G., and Morris, L. (2018) HIV-specific Fc effector function early in infection predicts the development of broadly neutralizing antibodies, *PLoS pathogens 14*, e1006987.
[106] Dourmashkin, R. R., Deteix, P., Simone, C. B., and Henkart, P. (1980) Electron microscopic demonstration of lesions in target cell membranes associated with antibody-dependent cellular cytotoxicity, *Clinical & Experimental Immunology 42*, 554-560.
[107] Perussia, B., Starr, S., Abraham, S., Fanning, V., and Trinchieri, G. (1983) Human natural killer cells analyzed by B73.1, a monoclonal antibody blocking Fc receptor functions. I. Characterization of the lymphocyte subset reactive with B73.1, *The Journal of Immunology 130*, 2133-2141.
[108] Lewis, G., Ackerman, ME., Scarlatti, G., Moog, C., Robert-Guroff, M., Kent, SJ., Overbaugh, J., Reeves, RK., Ferrari, G., Thyagarajan, B. (2019) Knowns and Unknowns of Assaying Antibody-Dependent Cell-Mediated Cytotoxicity Against HIV-1, *Front Immunol 10*.
[109] Bonsignori, M., Pollara, J., Moody, M. A., Alpert, M. D., Chen, X., Hwang, K.-K., Gilbert, P. B., Huang, Y., Gurley, T. C., Kozink, D. M., Marshall, D. J., Whitesides, J. F., Tsao, C.-Y., Kaewkungwal, J., Nitayaphan, S., Pitisuttithum, P., Rerks-Ngarm, S., Kim, J. H., Michael, N. L., Tomaras, G. D., Montefiori, D. C., Lewis, G. K., DeVico, A., Evans, D. T., Ferrari, G., Liao, H.-X., and Haynes, B. F. (2012) Antibody-Dependent Cellular Cytotoxicity-Mediating Antibodies from an HIV-1 Vaccine Efficacy Trial Target Multiple Epitopes and Preferentially Use the VH1 Gene Family, *Journal of Virology 86*, 11521-11532.
[110] Haynes, B. F., Gilbert, P. B., McElrath, M. J., Zolla-Pazner, S., Tomaras, G. D., Alam, S. M., Evans, D. T., Montefiori, D. C., Karnasuta, C., Sutthent, R., Liao, H.-X., DeVico, A. L., Lewis, G. K., Williams, C., Pinter, A., Fong, Y., Janes, H., DeCamp, A., Huang, Y., Rao, M., Billings, E., Karasavvas, N., Robb, M. L., Ngauy, V., de Souza, M. S., Paris, R., Ferrari, G., Bailer, R. T., Soderberg, K. A., Andrews, C., Berman, P. W., Frahm, N., De Rosa, S. C., Alpert, M. D., Yates, N. L., Shen, X., Koup, R. A., Pitisuttithum, P., Kaewkungwal, J., Nitayaphan, S., Rerks-Ngarm, S., Michael, N. L., and Kim, J. H. (2012) Immune-Correlates Analysis of an HIV-1 Vaccine Efficacy Trial, *New England Journal of Medicine 366*, 1275-1286.
[111] Baum, L. L., Cassutt, K. J., Knigge, K., Khattri, R., Margolick, J., Rinaldo, C., Kleeberger, C. A., Nishanian, P., Henrard, D. R., and Phair, J. (1996) HIV-1 gp120-specific antibody-dependent cell-mediated cytotoxicity correlates with rate of disease progression, *The Journal of Immunology 157*, 2168-2173.
[112] Wren, L. H., Chung, A. W., Isitman, G., Kelleher, A. D., Parsons, M. S., Amin, J., Cooper, D. A., investigators, A. s. c., Stratov, I., Navis, M., and Kent, S. J. (2013) Specific antibody-dependent cellular cytotoxicity responses associated with slow progression of HIV infection, *Immunology 138*, 116-123.
[113] Medof, M. E., Iida, K., Mold, C., and Nussenzweig, V. (1982) Unique role of the complement receptor CR1 in the degradation of C3b associated with immune complexes, *Journal of Experimental Medicine 156*, 1739-1754.
[114] Perez, L. G., Martinez, D. R., deCamp, A. C., Pinter, A., Berman, P. W., Francis, D., Sinangil, F., Lee, C., Greene, K., Gao, H., Nitayaphan, S., Rerks-Ngarm, S., Kaewkungwal, J., Pitisuttithum, P., Tartaglia, J., O'Connell, R. J., Robb, M. L., Michael, N. L., Kim, J. H.,

Gilbert, P., and Montefiori, D. C. (2017) V1V2-specific complement activating serum IgG as a correlate of reduced HIV-1 infection risk in RV144, *PLOS ONE 12*, e0180720.
[115] Liu, F., Dai, S., Gordon, J., and Qin, X. (2014) Complement and HIV-I infection/HIV-associated neurocognitive disorders, *Journal of NeuroVirology 20*, 184-198.
[116] Hessell, A. J., Hangartner, L., Hunter, M., Havenith, C. E. G., Beurskens, F. J., Bakker, J. M., Lanigan, C. M. S., Landucci, G., Forthal, D. N., Parren, P. W. H. I., Marx, P. A., and Burton, D. R. (2007) Fc receptor but not complement binding is important in antibody protection against HIV, *Nature 449*, 101-104.
[117] Tay, M. Z., Wiehe, K., Pollara, J. (2019) Antibody-Dependent Cellular Phagocytosis in Antiviral Immune Responses, *Front Immunol 10*.
[118] Ackerman, M. E., Dugast, A.-S., McAndrew, E. G., Tsoukas, S., Licht, A. F., Irvine, D. J., and Alter, G. (2013) Enhanced Phagocytic Activity of HIV-Specific Antibodies Correlates with Natural Production of Immunoglobulins with Skewed Affinity for FcγR2a and FcγR2b, *Journal of Virology 87*, 5468-5476.
[119] Gach, J. S., Bouzin, M., Wong, M. P., Chromikova, V., Gorlani, A., Yu, K.-T., Sharma, B., Gratton, E., and Forthal, D. N. (2017) Human immunodeficiency virus type-1 (HIV-1) evades antibody-dependent phagocytosis, *PLOS Pathogens 13*, e1006793.
[120] Velmurugan, R., Challa, D. K., Ram, S., Ober, R. J., and Ward, E. S. (2016) Macrophage-Mediated Trogocytosis Leads to Death of Antibody-Opsonized Tumor Cells, *Molecular Cancer Therapeutics 15*, 1879-1889.
[121] Walker Bruce, D. B. (2007) Elite control of HIV Infection: implications for vaccines and treatment, *Topics in HIV medicine : a publication of the International AIDS Society, USA 15*, 134-136.
[122] Sheppard, H. W., Lang, W., Ascher, M.S., Vittinghoff, E., Winkelstein, W. (1993) The characterization of non-progressors: long-term HIV-1 infection with stable CD4+ T-cell levels, *AIDS 7*, 1159-1166.
[123] Eisinger, R. W., Dieffenbach, C.W., Fauci, A.S. (2019) HIV viral load and transmissibility of HIV infection: undetectable equals untransmittable, *Journal of The American Medical Association 321*, 451-452.
[124] Okulicz, J. F., and Lambotte, O. (2011) Epidemiology and clinical characteristics of elite controllers, *Current Opinion in HIV and AIDS 6*, 163-168.
[125] Kiepiela, P., Leslie, A. J., Honeyborne, I., Ramduth, D., Thobakgale, C., Chetty, S., Rathnavalu, P., Moore, C., Pfafferott, K. J., Hilton, L., Zimbwa, P., Moore, S., Allen, T., Brander, C., Addo, M. M., Altfeld, M., James, I., Mallal, S., Bunce, M., Barber, L. D., Szinger, J., Day, C., Klenerman, P., Mullins, J., Korber, B., Coovadia, H. M., Walker, B. D., and Goulder, P. J. R. (2004) Dominant influence of HLA-B in mediating the potential co-evolution of HIV and HLA, *Nature 432*, 769-775.
[126] Martin, M. P., Pascal, V., Yeager, M., Phair, J., Kirk, G. D., Hoots, K., O'Brien, S. J., Anderson, S. K., and Carrington, M. (2007) A mutation in KIR3DS1 that results in truncation and lack of cell surface expression, *Immunogenetics 59*, 823-829.
[127] Sáez-Cirión, A., Lacabaratz, C., Lambotte, O., Versmisse, P., Urrutia, A., Boufassa, F., Barré-Sinoussi, F., Delfraissy, J.-F., Sinet, M., Pancino, G., and Venet, A. (2007) HIV controllers exhibit potent CD8 T cell capacity to suppress HIV infection ex vivo and peculiar

cytotoxic T lymphocyte activation phenotype, *Proceedings of the National Academy of Sciences 104*, 6776-6781.

[128] Koup, R. A., Safrit, J. T., Cao, Y., Andrews, C. A., McLeod, G., Borkowsky, W., Farthing, C., and Ho, D. D. (1994) Temporal association of cellular immune responses with the initial control of viremia in primary human immunodeficiency virus type 1 syndrome, *Journal of Virology 68*, 4650-4655.

[129] Borrow, P., Lewicki, H., Hahn, B. H., Shaw, G. M., and Oldstone, M. B. (1994) Virus-specific CD8+ cytotoxic T-lymphocyte activity associated with control of viremia in primary human immunodeficiency virus type 1 infection, *Journal of Virology 68*, 6103-6110.

[130] Zimmerli, S. C., Harari, A., Cellerai, C., Vallelian, F., Bart, P.-A., and Pantaleo, G. (2005) HIV-1-specific IFN-γ/IL-2-secreting CD8 T cells support CD4-independent proliferation of HIV-1-specific CD8 T cells, *Proceedings of the National Academy of Sciences of the United States of America 102*, 7239-7244.

[131] Petrovas, C., Casazza, J. P., Brenchley, J. M., Price, D. A., Gostick, E., Adams, W. C., Precopio, M. L., Schacker, T., Roederer, M., Douek, D. C., and Koup, R. A. (2006) PD-1 is a regulator of virus-specific CD8+ T cell survival in HIV infection, *Journal of Experimental Medicine 203*, 2281-2292.

[132] Trautmann, L., Janbazian, L., Chomont, N., Said, E. A., Gimmig, S., Bessette, B., Boulassel, M.-R., Delwart, E., Sepulveda, H., Balderas, R. S., Routy, J.-P., Haddad, E. K., and Sekaly, R.-P. (2006) Upregulation of PD-1 expression on HIV-specific CD8+ T cells leads to reversible immune dysfunction, *Nature Medicine 12*, 1198-1202.

[133] Paiardini, M., Cervasi, B., Albrecht, H., Muthukumar, A., Dunham, R., Gordon, S., Radziewicz, H., Piedimonte, G., Magnani, M., Montroni, M., Kaech, S. M., Weintrob, A., Altman, J. D., Sodora, D. L., Feinberg, M. B., and Silvestri, G. (2005) Loss of CD127 expression defines an expansion of effector CD8+ T cells in HIV-infected individuals, *The Journal of Immunology 174*, 2900-2909.

[134] Almeida, J. R., Price, D. A., Papagno, L., Arkoub, Z. n. A. t., Sauce, D., Bornstein, E., Asher, T. E., Samri, A., Schnuriger, A. l., Theodorou, I., Costagliola, D., Rouzioux, C., Agut, H., Marcelin, A.-G. v., Douek, D., Autran, B., and Appay, V. (2007) Superior control of HIV-1 replication by CD8+ T cells is reflected by their avidity, polyfunctionality, and clonal turnover, *Journal of Experimental Medicine 204*, 2473-2485.

[135] Betts, M. R., Nason, M. C., West, S. M., De Rosa, S. C., Migueles, S. A., Abraham, J., Lederman, M. M., Benito, J. M., Goepfert, P. A., Connors, M., Roederer, M., and Koup, R. A. (2006) HIV nonprogressors preferentially maintain highly functional HIV-specific CD8+ T cells, *Blood 107*, 4781-4789.

[136] Altfeld, M., Addo, M. M., Rosenberg, E. S., Hecht, F. M., Lee, P. K., Vogel, M., Yu, X. G., Draenert, R., Johnston, M. N., Strick, D., Allen, T. M., Feeney, M. E., Kahn, J. O., Sekaly, R. P., Levy, J. A., Rockstroh, J. K., Goulder, P. J. R., and Walker, B. D. (2003) Influence of HLA-B57 on clinical presentation and viral control during acute HIV-1 infection, *AIDS 17*, 2581-2591.

[137] IHME. (2018) Deaths - HIV/AIDS, Institute for Health Metrics and Evaluation, Seattle, United States.

[138] UNAIDS. (2013) Report on the global AIDS epidemic 2013., (HIV/AIDS, J. U. N. P. o., Ed.).

[139] UNAIDS. (2019) UNAIDS Data 2019, (HIV/AIDS, J. U. N. P. o., Ed.).

[140] UNAIDS. (2017) Progress Towards the 90-90-90 targets., In *Ending AIDS* (HIV/AIDS, J. U. N. P. o., Ed.).
[141] WHO. (2019) HIV Drug Resistance Report 2019, (Organisation, W. H., Ed.), Geneva, Switzerland.
[142] Hammer, S. M., Squires, K. E., Hughes, M. D., Grimes, J. M., Demeter, L. M., Currier, J. S., Eron, J. J., Feinberg, J. E., Balfour, H. H., Deyton, L. R., Chodakewitz, J. A., Fischl, M. A., Phair, J. P., Pedneault, L., Nguyen, B.-Y., and Cook, J. C. (1997) A Controlled Trial of Two Nucleoside Analogues plus Indinavir in Persons with Human Immunodeficiency Virus Infection and CD4 Cell Counts of 200 per Cubic Millimeter or Less, *New England Journal of Medicine 337*, 725-733.
[143] Collier, A. C., Coombs, R. W., Schoenfeld, D. A., Bassett, R. L., Timpone, J., Baruch, A., Jones, M., Facey, K., Whitacre, C., McAuliffe, V. J., Friedman, H. M., Merigan, T. C., Reichman, R. C., Hooper, C., and Corey, L. (1996) Treatment of Human Immunodeficiency Virus Infection with Saquinavir, Zidovudine, and Zalcitabine, *New England Journal of Medicine 334*, 1011-1018.
[144] Gulick, R. M., Mellors, J. W., Havlir, D., Eron, J. J., Gonzalez, C., McMahon, D., Richman, D. D., Valentine, F. T., Jonas, L., Meibohm, A., Emini, E. A., Chodakewitz, J. A., Deutsch, P., Holder, D., Schleif, W. A., and Condra, J. H. (1997) Treatment with Indinavir, Zidovudine, and Lamivudine in Adults with Human Immunodeficiency Virus Infection and Prior Antiretroviral Therapy, *New England Journal of Medicine 337*, 734-739.
[145] Staszewski, S. M., Veronica ; Rehmet, Sibylle ; Stark, Thomas ; De Creé, Jean ; De Brabander, Marc ; Peeters, Monika ; Andries, Koen ; Moeremans, Marc ; De Raeymaeker, Marc ; Pearce, Gillian ; Van Den Broeck, Remi ; Verbiest, Werner ; Stoffels, Paul. (1996) Virological and immunological analysis of a triple combination pilot study with loviride, lamivudine and zidovudine in HIV-1-infected patients, *AIDS 10*, F1-F7.
[146] WHO. (2011) Global HIV/AIDS Response: Epidemic update and health sector progress towards Universal Access, World Health Organization, Geneva, Switzerland.
[147] Hogg, R. S., Heath, K., Bangsberg, D., Yip, B., Press, N., O'Shaughnessy, M. V., and Montaner, J. S. G. (2002) Intermittent use of triple-combination therapy is predictive of mortality at baseline and after 1 year of follow-up, *AIDS 16*, S123-S124.
[148] Fischl, M. A. (1999) Antiretroviral therapy in 1999 for antiretroviral-naive individuals with HIV infection, *AIDS 13 Supplemental*, S49-59.
[149] Abbar, B., Veyri, M., Solas, C., Poizot-Martin, I., and Spano, J.-P. (2020) VIH et cancer : mise au point en 2020, *Bulletin du Cancer 107*, 21-29.
[150] Mallipattu, S. K., Salem, F., and Wyatt, C. M. (2014) The changing epidemiology of HIV-related chronic kidney disease in the era of antiretroviral therapy, *Kidney International 86*, 259-265.
[151] Ballocca, F., D'Ascenzo, F., Gili, S., Grosso Marra, W., and Gaita, F. (2017) Cardiovascular disease in patients with HIV, *Trends in Cardiovascular Medicine 27*, 558-563.
[152] Johnson, S. C. (2016) Antiretroviral Therapy for HIV Infection: When to Initiate Therapy, Which Regimen to Use, and How to Monitor Patients on Therapy, *Topics in Antiviral Medicine 23*, 161-167.
[153] Merrick, S. T. (2019) Selecting an Initial ART Regimen, (Committee, M. C. C., Ed.).

[154] Spinner, C. D., Boesecke, C., Zink, A., Jessen, H., Stellbrink, H.-J., Rockstroh, J. K., and Esser, S. (2016) HIV pre-exposure prophylaxis (PrEP): a review of current knowledge of oral systemic HIV PrEP in humans, *Infection 44*, 151-158.

[155] Grant, R. M., Lama, J. R., Anderson, P. L., McMahan, V., Liu, A. Y., Vargas, L., Goicochea, P., Casapía, M., Guanira-Carranza, J. V., Ramirez-Cardich, M. E., Montoya-Herrera, O., Fernández, T., Veloso, V. G., Buchbinder, S. P., Chariyalertsak, S., Schechter, M., Bekker, L.-G., Mayer, K. H., Kallás, E. G., Amico, K. R., Mulligan, K., Bushman, L. R., Hance, R. J., Ganoza, C., Defechereux, P., Postle, B., Wang, F., McConnell, J. J., Zheng, J.-H., Lee, J., Rooney, J. F., Jaffe, H. S., Martinez, A. I., Burns, D. N., and Glidden, D. V. (2010) Preexposure Chemoprophylaxis for HIV Prevention in Men Who Have Sex with Men, *New England Journal of Medicine 363*, 2587-2599.

[156] McMahon, J. M., Myers, J. E., Kurth, A. E., Cohen, S. E., Mannheimer, S. B., Simmons, J., Pouget, E. R., Trabold, N., and Haberer, J. E. (2014) Oral Pre-Exposure Prophylaxis (PrEP) for Prevention of HIV in Serodiscordant Heterosexual Couples in the United States: Opportunities and Challenges, *AIDS Patient Care and STDs 28*, 462-474.

[157] Choopanya, K., Martin, M., Suntharasamai, P., Sangkum, U., Mock, P. A., Leethochawalit, M., Chiamwongpaet, S., Kitisin, P., Natrujirote, P., Kittimunkong, S., Chuachoowong, R., Gvetadze, R. J., McNicholl, J. M., Paxton, L. A., Curlin, M. E., Hendrix, C. W., and Vanichseni, S. (2013) Antiretroviral prophylaxis for HIV infection in injecting drug users in Bangkok, Thailand (the Bangkok Tenofovir Study): a randomised, double-blind, placebo-controlled phase 3 trial, *The Lancet 381*, 2083-2090.

[158] WHO. (2006) Antiretroviral Therapy for HIV Infection in Adults and Adolescents: Recommendations for a public health approach, World Health Organization, Geneva, Switzerland.

[159] WHO. (2015) Consolidated Guidelines on the use of Antiretroviral Drugs for Treating and Preventing HIV Infection, World Health Organisation, Geneva, Switzerland.

[160] Rerks-Ngarm, S., Pitisuttithum, P., Nitayaphan, S., Kaewkungwal, J., Chiu, J., Paris, R., Premsri, N., Namwat, C., de Souza, M., Adams, E., Benenson, M., Gurunathan, S., Tartaglia, J., McNeil, J. G., Francis, D. P., Stablein, D., Birx, D. L., Chunsuttiwat, S., Khamboonruang, C., Thongcharoen, P., Robb, M. L., Michael, N. L., Kunasol, P., and Kim, J. H. (2009) Vaccination with ALVAC and AIDSVAX to Prevent HIV-1 Infection in Thailand, *New England Journal of Medicine 361*, 2209-2220.

[161] Karasavvas, N., Billings, E., Rao, M., Williams, C., Zolla-Pazner, S., Bailer, R. T., Koup, R. A., Madnote, S., Arworn, D., Shen, X., Tomaras, G. D., Currier, J. R., Jiang, M., Magaret, C., Andrews, C., Gottardo, R., Gilbert, P., Cardozo, T. J., Rerks-Ngarm, S., Nitayaphan, S., Pitisuttithum, P., Kaewkungwal, J., Paris, R., Greene, K., Gao, H., Gurunathan, S., Tartaglia, J., Sinangil, F., Korber, B. T., Montefiori, D. C., Mascola, J. R., Robb, M. L., Haynes, B. F., Ngauy, V., Michael, N. L., Kim, J. H., and de Souza, f. t. M. T. C. M. S. (2012) The Thai Phase III HIV Type 1 Vaccine Trial (RV144) Regimen Induces Antibodies That Target Conserved Regions Within the V2 Loop of gp120, *AIDS Research and Human Retroviruses 28*, 1444-1457.

[162] Tomaras, G. D., Ferrari, G., Shen, X., Alam, S. M., Liao, H.-X., Pollara, J., Bonsignori, M., Moody, M. A., Fong, Y., Chen, X., Poling, B., Nicholson, C. O., Zhang, R., Lu, X., Parks, R., Kaewkungwal, J., Nitayaphan, S., Pitisuttithum, P., Rerks-Ngarm, S., Gilbert, P. B., Kim, J.

H., Michael, N. L., Montefiori, D. C., and Haynes, B. F. (2013) Vaccine-induced plasma IgA specific for the C1 region of the HIV-1 envelope blocks binding and effector function of IgG, *Proceedings of the National Academy of Sciences 110*, 9019-9024.

[163] Yates, N. L., Liao, H.-X., Fong, Y., deCamp, A., Vandergrift, N. A., Williams, W. T., Alam, S. M., Ferrari, G., Yang, Z.-y., Seaton, K. E., Berman, P. W., Alpert, M. D., Evans, D. T., O'Connell, R. J., Francis, D., Sinangil, F., Lee, C., Nitayaphan, S., Rerks-Ngarm, S., Kaewkungwal, J., Pitisuttithum, P., Tartaglia, J., Pinter, A., Zolla-Pazner, S., Gilbert, P. B., Nabel, G. J., Michael, N. L., Kim, J. H., Montefiori, D. C., Haynes, B. F., and Tomaras, G. D. (2014) Vaccine-Induced Env V1–V2 IgG3 Correlates with Lower HIV-1 Infection Risk and Declines Soon After Vaccination, *Science translational medicine 6*, 228-239.

[164] Canver, M. C., Bauer, D. E., Dass, A., Yien, Y. Y., Chung, J., Masuda, T., Maeda, T., Paw, B. H., and Orkin, S. H. (2014) Characterization of Genomic Deletion Efficiency Mediated by Clustered Regularly Interspaced Palindromic Repeats (CRISPR)/Cas9 Nuclease System in Mammalian Cells, *Journal of Biological Chemistry 289*, 21312-21324.

[165] Chung, A. W., Ghebremichael, M., Robinson, H., Brown, E., Choi, I., Lane, S., Dugast, A.-S., Schoen, M. K., Rolland, M., Suscovich, T. J., Mahan, A. E., Liao, L., Streeck, H., Andrews, C., Rerks-Ngarm, S., Nitayaphan, S., de Souza, M. S., Kaewkungwal, J., Pitisuttithum, P., Francis, D., Michael, N. L., Kim, J. H., Bailey-Kellogg, C., Ackerman, M. E., and Alter, G. (2014) Polyfunctional Fc-Effector Profiles Mediated by IgG Subclass Selection Distinguish RV144 and VAX003 Vaccines, *Science Translational Medicine 6*, 228ra238.

[166] Frantz, S. (2004) Scientists slam rationale behind largest HIV vaccine trial, *Nature Reviews Drug Discovery 3*, 195.

[167] Desrosiers, R. C. (2017) Protection against HIV Acquisition in the RV144 Trial, *Journal of Virology 91*, e00905-e00917.

[168] Carr, J. K., Salminen, M. O., Koch, C., Gotte, D., Artenstein, A. W., Hegerich, P. A., St Louis, D., Burke, D. S., and McCutchan, F. E. (1996) Full-length sequence and mosaic structure of a human immunodeficiency virus type 1 isolate from Thailand, *Journal of Virology 70*, 5935-5943.

[169] Richard, J., Ding, S., and Finzi, A. (2017) Unlocking HIV-1 Env: implications for antibody attack, *AIDS Res Ther 14*, 42.

[170] Nishimura, Y., Gautam, R., Chun, T.-W., Sadjadpour, R., Foulds, K. E., Shingai, M., Klein, F., Gazumyan, A., Golijanin, J., Donaldson, M., Donau, O. K., Plishka, R. J., Buckler-White, A., Seaman, M. S., Lifson, J. D., Koup, R. A., Fauci, A. S., Nussenzweig, M. C., and Martin, M. A. (2017) Early antibody therapy can induce long-lasting immunity to SHIV, *Nature 543*, 559-563.

[171] Caskey, M., Schoofs, T., Gruell, H., Settler, A., Karagounis, T., Kreider, E. F., Murrell, B., Pfeifer, N., Nogueira, L., Oliveira, T. Y., Learn, G. H., Cohen, Y. Z., Lehmann, C., Gillor, D., Shimeliovich, I., Unson-O'Brien, C., Weiland, D., Robles, A., Kümmerle, T., Wyen, C., Levin, R., Witmer-Pack, M., Eren, K., Ignacio, C., Kiss, S., West, A. P., Mouquet, H., Zingman, B. S., Gulick, R. M., Keler, T., Bjorkman, P. J., Seaman, M. S., Hahn, B. H., Fätkenheuer, G., Schlesinger, S. J., Nussenzweig, M. C., and Klein, F. (2017) Antibody 10-1074 suppresses viremia in HIV-1-infected individuals, *Nature Medicine 23*, 185-191.

[172] Lavelle, J. (2018) NIH launches study to test combination antibody treatment for HIV infection, (Diseases, N. I. o. A. a. I., Ed.), National Institutes of Health.

[173] Checkley, M. A., Luttge, B. G., and Freed, E. O. (2011) HIV-1 Envelope Glycoprotein Biosynthesis, Trafficking, and Incorporation, *Journal of Molecular Biology 410*, 582-608.
[174] Willey, R. L., Maldarelli, F., Martin, M. A., and Strebel, K. (1992) Human immunodeficiency virus type 1 Vpu protein induces rapid degradation of CD4, *Journal of Virology 66*, 7193-7200.
[175] Schwartz, O., Dautry-Varsat, A., Goud, B., Maréchal, V., Subtil, A., Heard, J. M., and Danos, O. (1995) Human immunodeficiency virus type 1 Nef induces accumulation of CD4 in early endosomes, *Journal of Virology 69*, 528-533.
[176] Kiani, Z., Bruneau, J., Geraghty, D. E., and Bernard, N. F. (2019) HLA-F on Autologous HIV-Infected Cells Activates Primary NK Cells Expressing the Activating Killer Immunoglobulin-Like Receptor KIR3DS1, *Journal of Virology 93*, e00933-00919.
[177] Kiani, Z., Dupuy, F. P., Bruneau, J., Lebouché, B., Retière, C., Geraghty, D. E., and Bernard, N. F. (2019) The Education of NK Cells Determines Their Responsiveness to Autologous HIV-Infected CD4 T Cells, *Journal of Virology 93*, e01185-01119.
[178] Richard, J., Prévost, J., Baxter, A. E., von Bredow, B., Ding, S., Medjahed, H., Delgado, G. G., Brassard, N., Stürzel, C. M., Kirchhoff, F., Hahn, B. H., Parsons, M. S., Kaufmann, D. E., Evans, D. T., and Finzi, A. (2018) Uninfected Bystander Cells Impact the Measurement of HIV-Specific Antibody-Dependent Cellular Cytotoxicity Responses, *mBio 9*, e00358-00318.
[179] Luo, L., Wang, N., Yue, Y., Han, Y., Lv, W., Liu, Z., Qiu, Z., Lu, H., Tang, X., Zhang, T., Zhao, M., He, Y., Shenghua, H., Wang, M., Li, Y., Huang, S., Li, Y., Liu, J., Tuofu, Z., Routy, J.-P., and Li, T. (2019) The effects of antiretroviral therapy initiation time on HIV reservoir size in Chinese chronically HIV infected patients: a prospective, multi-site cohort study, *BMC Infectious Diseases 19*.
[180] Lane, H. C., Masur, H., Edgar, L. C., Whalen, G., Rook, A. H., and Fauci, A. S. (1983) Abnormalities of B-Cell Activation and Immunoregulation in Patients with the Acquired Immunodeficiency Syndrome, *New England Journal of Medicine 309*, 453-458.
[181] Schnittman, S. M., Lane, H. C., Higgins, S. E., Folks, T., and Fauci, A. S. (1986) Direct polyclonal activation of human B lymphocytes by the acquired immune deficiency syndrome virus, *Science 233*, 1084-1086.
[182] Sherwood, G. (2016) Waldenstrom's Macroglobulinemia, Medical Tests, International Waldenstrom's Macroglobulinemia Foundation.
[183] Sáez-Cirión, A., Bacchus, C., Hocqueloux, L., Avettand-Fenoel, V., Girault, I., Lecuroux, C., Potard, V., Versmisse, P., Melard, A., Prazuck, T., Descours, B., Guergnon, J., Viard, J.-P., Boufassa, F., Lambotte, O., Goujard, C., Meyer, L., Costagliola, D., Venet, A., Pancino, G., Autran, B., Rouzioux, C., and the, A. V. S. G. (2013) Post-Treatment HIV-1 Controllers with a Long-Term Virological Remission after the Interruption of Early Initiated Antiretroviral Therapy ANRS VISCONTI Study, *PLOS Pathogens 9*, e1003211.
[184] Zoubchenok, D., Veillette, M., Prévost, J., Sanders-Buell, E., Wagh, K., Korber, B., Chenine, A. L., and Finzi, A. (2017) Histidine 375 Modulates CD4 Binding in HIV-1 CRF01_AE Envelope Glycoproteins, *Journal of Virology 91*, e02151-02116.
[185] Xiang, S.-H., Kwong, P. D., Gupta, R., Rizzuto, C. D., Casper, D. J., Wyatt, R., Wang, L., Hendrickson, W. A., Doyle, M. L., and Sodroski, J. (2002) Mutagenic Stabilization and/or Disruption of a CD4-Bound State Reveals Distinct Conformations of the Human

Immunodeficiency Virus Type 1 gp120 Envelope Glycoprotein, *Journal of Virology 76*, 9888-9899.

[186] Bekker, L.-G., Moodie, Z., Grunenberg, N., Laher, F., Tomaras, G. D., Cohen, K. W., Allen, M., Malahleha, M., Mngadi, K., Daniels, B., Innes, C., Bentley, C., Frahm, N., Morris, D. E., Morris, L., Mkhize, N. N., Montefiori, D. C., Sarzotti-Kelsoe, M., Grant, S., Yu, C., Mehra, V. L., Pensiero, M. N., Phogat, S., DiazGranados, C. A., Barnett, S. W., Kanesa-thasan, N., Koutsoukos, M., Michael, N. L., Robb, M. L., Kublin, J. G., Gilbert, P. B., Corey, L., Gray, G. E., and McElrath, M. J. (2018) Subtype C ALVAC-HIV and bivalent subtype C gp120/MF59 HIV-1 vaccine in low-risk, HIV-uninfected, South African adults: a phase 1/2 trial, *The Lancet HIV 5*, e366-e378.

[187] NIAID. (2016) First New HIV Vaccine Efficacy Study in Seven Years Has Begun, In *South Africa Hosts Historic NIH-Supported Clinical Trial* (Diseases, N. I. o. A. a. I., Ed.).

[188] NIAID. (2020) Experimental HIV Vaccine Regimen Ineffective in Preventing HIV, National Institute of Allergy and Infectious Diseases.

[189] Gray, G. E., Huang, Y., Grunenberg, N., Laher, F., Roux, S., Andersen-Nissen, E., De Rosa, S. C., Flach, B., Randhawa, A. K., Jensen, R., Swann, E. M., Bekker, L.-G., Innes, C., Lazarus, E., Morris, L., Mkhize, N. N., Ferrari, G., Montefiori, D. C., Shen, X., Sawant, S., Yates, N., Hural, J., Isaacs, A., Phogat, S., DiazGranados, C. A., Lee, C., Sinangil, F., Michael, N. L., Robb, M. L., Kublin, J. G., Gilbert, P. B., McElrath, M. J., Tomaras, G. D., and Corey, L. (2019) Immune correlates of the Thai RV144 HIV vaccine regimen in South Africa, *Science Translational Medicine 11*, eaax1880.

[190] Dugast, A.-S., Stamatatos, L., Tonelli, A., Suscovich, T. J., Licht, A. F., Mikell, I., Ackerman, M. E., Streeck, H., Klasse, P. J., Moore, J. P., and Alter, G. (2014) Independent evolution of Fc- and Fab-mediated HIV-1-specific antiviral antibody activity following acute infection, *European Journal of Immunology 44*, 2925-2937.

[191] Naiman, N. E., Slyker, J., Richardson, B. A., John-Stewart, G., Nduati, R., and Overbaugh, J. M. (2019) Antibody-dependent cellular cytotoxicity targeting CD4-inducible epitopes predicts mortality in HIV-infected infants, *EBioMedicine 47*, 257-268.

[192] Dupuy, F. P., Kant, S., Barbé, A., Routy, J.-P., Bruneau, J., Lebouché, B., Tremblay, C., Pazgier, M., Finzi, A., and Bernard, N. F. (2019) Antibody-Dependent Cellular Cytotoxicity-Competent Antibodies against HIV-1-Infected Cells in Plasma from HIV-Infected Subjects, *mBio 10*, e02690-02619.

[193] Kant, S., Zhang, N., Routy, J.-P., Tremblay, C., Thomas, R., Szabo, J., Côté, P., Trottier, B., LeBlanc, R., Rouleau, D., Harris, M., Dupuy, P. F., and Bernard, F. N. (2019) Quantifying Anti-HIV Envelope-Specific Antibodies in Plasma from HIV Infected Individuals, *Viruses 11*, 487-503.

[194] Jensen, S. S., Fomsgaard, A., Borggren, M., Tingstedt, J. L., Gerstoft, J., Kronborg, G., Rasmussen, L. D., Pedersen, C., and Karlsson, I. (2015) HIV-Specific Antibody-Dependent Cellular Cytotoxicity (ADCC) -Mediating Antibodies Decline while NK Cell Function Increases during Antiretroviral Therapy (ART), *PLOS ONE 10*, e0145249.

[195] Jensen, S. S. H., H.J.; Tingstedt, J.L. ; Larsen, T.K.; Nielsen, S.D.; Pedersen, C.; Fomsgaard, A.; Karlsson, I. (2015) HIV-Specific ADCC Improves After Antiretroviral Therapy and Correlates With Normalization of the NK Cell Phenotype, *Journal of Acquired Immune Deficiency Syndromes 68*, 103-111.

[196] Michailidis, C., Giannopoulos, G., Vigklis, V., Armenis, K., Tsakris, A., and Gargalianos, P. (2012) Impaired phagocytosis among patients infected by the human immunodeficiency virus: implication for a role of highly active anti-retroviral therapy, *Clin Exp Immunol 167*, 499-504.

[197] Meri, S., and Jarva, H. (2013) Complement Regulatory Proteins and Related Diseases.

[198] Yu, Q., Yu, R., and Qin, X. (2010) The good and evil of complement activation in HIV-1 infection, *Cell Mol Immunol 7*, 334-340.

[199] Spear, G. T., Olinger, G., Sullivan, B.L., Landay, A.L., Kessler, H., Connick, E., Kuritzkes, D., St. Clair, M., Spritzler, J., Wu, H., Lederman, M.M. (1999) Letter to the Editor, *AIDS Research and Human Retroviruses 15*, 1713-1715.

[200] Jain, V., Hartogensis, W., Bacchetti, P., Hunt, P. W., Hatano, H., Sinclair, E., Epling, L., Lee, T.-H., Busch, M. P., McCune, J. M., Pilcher, C. D., Hecht, F. M., and Deeks, S. G. (2013) Antiretroviral Therapy Initiated Within 6 Months of HIV Infection Is Associated With Lower T-Cell Activation and Smaller HIV Reservoir Size, *The Journal of Infectious Diseases 208*, 1202-1211.

[201] Laanani, M., Ghosn, J., Essat, A., Melard, A., Seng, R., Gousset, M., Panjo, H., Mortier, E., Girard, P.-M., Goujard, C., Meyer, L., Rouzioux, C., and for the Agence Nationale de Recherche sur le Sida, P. C. S. G. (2015) Impact of the Timing of Initiation of Antiretroviral Therapy During Primary HIV-1 Infection on the Decay of Cell-Associated HIV-DNA, *Clinical Infectious Diseases 60*, 1715-1721.

[202] Ananworanich, J., Chomont, N., Eller, L. A., Kroon, E., Tovanabutra, S., Bose, M., Nau, M., Fletcher, J. L. K., Tipsuk, S., Vandergeeten, C., O'Connell, R. J., Pinyakorn, S., Michael, N., Phanuphak, N., Robb, M. L., Rv, and groups, R. S. s. (2016) HIV DNA Set Point is Rapidly Established in Acute HIV Infection and Dramatically Reduced by Early ART, *EBioMedicine 11*, 68-72.

[203] Bachmann, N., von Siebenthal, C., Vongrad, V., Turk, T., Neumann, K., Beerenwinkel, N., Bogojeska, J., Fellay, J., Roth, V., Kok, Y. L., Thorball, C. W., Borghesi, A., Parbhoo, S., Wieser, M., Böni, J., Perreau, M., Klimkait, T., Yerly, S., Battegay, M., Rauch, A., Hoffmann, M., Bernasconi, E., Cavassini, M., Kouyos, R. D., Günthard, H. F., Metzner, K. J., Anagnostopoulos, A., Battegay, M., Bernasconi, E., Böni, J., Braun, D. L., Bucher, H. C., Calmy, A., Cavassini, M., Ciuffi, A., Dollenmaier, G., Egger, M., Elzi, L., Fehr, J., Fellay, J., Furrer, H., Fux, C. A., Günthard, H. F., Haerry, D., Hasse, B., Hirsch, H. H., Hoffmann, M., Hösli, I., Huber, M., Kahlert, C., Kaiser, L., Keiser, O., Klimkait, T., Kouyos, R. D., Kovari, H., Ledergerber, B., Martinetti, G., Tejada, B. M. d., Marzolini, C., Metzner, K. J., Müller, N., Nicca, D., Paioni, P., Pantaleo, G., Perreau, M., Rauch, A., Rudin, C., Scherrer, A. U., Schmid, P., Speck, R., Stöckle, M., Tarr, P., Trkola, A., Vernazza, P., Wandeler, G., Weber, R., Yerly, S., and the Swiss, H. I. V. C. S. (2019) Determinants of HIV-1 reservoir size and long-term dynamics during suppressive ART, *Nature Communications 10*, 3193.

[204] Scully, E. P. (2018) Sex Differences in HIV Infection, *Current HIV/AIDS Reports 15*, 136-146.

[205] Gianella, S., Massanella, M., Wertheim, J. O., and Smith, D. M. (2015) The Sordid Affair Between Human Herpesvirus and HIV, *The Journal of Infectious Diseases 212*, 845-852.

[206] Ackerman, M. E., Mikhailova, A., Brown, E. P., Dowell, K. G., Walker, B. D., Bailey-Kellogg, C., Suscovich, T. J., and Alter, G. (2016) Polyfunctional HIV-Specific Antibody Responses Are Associated with Spontaneous HIV Control, *PLOS Pathogens 12*, e1005315.

[207] Finzi, D., Hermankova, M., Pierson, T., Carruth, L. M., Buck, C., Chaisson, R. E., Quinn, T. C., Chadwick, K., Margolick, J., Brookmeyer, R., Gallant, J., Markowitz, M., Ho, D. D., Richman, D. D., and Siliciano, R. F. (1997) Identification of a Reservoir for HIV-1 in Patients on Highly Active Antiretroviral Therapy, *Science 278*, 1295-1300.

[208] Vanhamel, J., Bruggemans, A., and Debyser, Z. (2019) Establishment of latent HIV-1 reservoirs: what do we really know?, *J Virus Erad 5*, 3-9.

[209] Ko, A., Kang, G., Hattler, J. B., Galadima, H. I., Zhang, J., Li, Q., and Kim, W.-K. (2019) Macrophages but not Astrocytes Harbor HIV DNA in the Brains of HIV-1-Infected Aviremic Individuals on Suppressive Antiretroviral Therapy, *Journal of Neuroimmune Pharmacology 14*, 110-119.